Reactions of Halogenated Ethylenes on the α-Cr_2O_3 $(10\bar{1}2)$ Surface

Mary Amanda Minton

Dissertation submitted to the faculty of the Virginia Polytechnic Institute and State University in partial fulfillment of the requirements for the degree of

Doctor of Philosophy
In
Chemical Engineering

Dr. David F. Cox
Dr. S. Ted Oyama
Dr. John G. Dillard
Dr. Brian E. Hanson
Dr. John R. Morris

September 7, 2006
Blacksburg, Virginia

Keywords: vinyl, vinylidene, chlorovinyl, acetylene, ethylene, butadiene, halocarbons

Reactions of halogenated ethylenes on the α-Cr_2O_3 ($10\bar{1}2$) surface

Mary Amanda Minton

ABSTRACT

The thermally induced reaction of halogenated ethylenes on the α-Cr_2O_3 ($10\bar{1}2$) single crystal surface results in the formation of gas phase hydrocarbons including acetylene, ethylene, butadiene, and dihydrogen, and deposition of surface chlorine adatoms. No surface carbon or combustion products are observed in any reactions indicating no thermally induced C-C bond cleavage occurs and surface lattice oxygen is not incorporated into surface intermediates. Thermal desorption spectroscopy indicates that in all halogenated ethylene reactions acetylene is the major product, regardless of the reaction scheme. The surface reactions of halogenated ethylenes are proposed to proceed through C-X (X=halogen) bond cleavage to form surface halogen adatoms and surface C2 hydrocarbon fragments. Halogen adatom deposition affects reaction barriers to hydrocarbon formation, and eventually shuts down surface chemistry. Photoemission and near edge x-ray absorption fine structure spectra show that all studied reactants undergo some C-X bond cleavage upon low temperature adsorption forming adsorbed C2 fragments and halogen adatoms. Photoemission for each reaction system shows at least two C1s features (283.0-286.0 eV) and two Cl2p features ($2p_{3/2}$=198.0-201.0 eV) with higher binding energy features associated with molecularly intact halogenated ethylenes and lower binding energy features associated with dissociated surface species. Near edge x-ray absorption fine structure spectra taken, corresponding to photoemission spectra, indicate the occurrence of C1s→π* transitions, indicating intact π-systems are present. Heating the surface results in a reduction in intensity of higher energy photoemission and near edge x-ray absorption fine structure indicative of a decrease in surface C-X bonds.

Acknowledgements

I would like to thank my advisor, Dr. David F. Cox, for his support and guidance over the last five years. Thanks to his passion for research and compassion for his students I was able to grow as both a scientist and a person while working with him. I would also like to thank my committee members Dr. S. Ted Oyama, Dr. John G. Dillard, Dr. Brian E. Hanson, and Dr. John R. Morris. Thanks Qiang. I would also like to thank Dr. David Mullins of ORNL for his support in the form of experimental advice, trouble shooting, maintenance, and financial support associated with upgrading facilities at U12A. His efforts are sponsored by the Division of Chemical Sciences, Geosciences, and Biosciences, Office of Basic Energy Sciences, U.S. Department of Energy, under contract DE-AC05-00OR22725 with Oak Ridge National Laboratory, managed and operated by UT-Battelle, LLC. Use of the National Synchrotron Light Source, Brookhaven National Laboratory, was supported by the U.S. Department of Energy, Office of Science, Office of Basic Energy Sciences, under Contract No. DE-AC02-98CH10886. Special thanks are offered to NSLS staff members Steven Hulbert and Qing-Li Dong for their assistance. Financial support for this project was provided by the Chemical Sciences, Geosciences and Biosciences Division, Office of Basic Energy Sciences, Office of Science, US Department of Energy through grant DE-FG02-97ER14751.

I would like to thank the ladies in the chemical engineering office, Chris Moore, Diane Cannaday, and Jane Price. Without the three of them, graduate school wouldn't have been as much fun. Their hard work and dedication to the department make everything possible. Mike and Wendell in the Chemical Engineering shop not only made all of those valve fittings vacuum-sealed, they also always brought a smile to my face.

Thanks vacuum equipment, without you two silly chambers graduate school would have been a breeze. Seriously fellas, I love ya.

I would like to thank all of the dear friends that I made in graduate school. Without Eric, Mike (Bortner), Cory, and Beth I wouldn't have made it through those first years. The football made life even better, but only because Derek, Doug, Emmett, Som, and Carl are masters of the tailgate. Thanks to John Brooks for making my last year in the lab a little more bearable.

Thanks to my loving family who have supported me through nine years of college. Thank you grandma Pat for always making sure I knew that I 'better get that degree'. Thanks mom and dad for always having faith in me even when my own faltered. Thanks sissy and Matt Powers for coming to see me and for understanding how hard graduate school could be (I'm still waiting for my thank you for helping you meet your husband), I'm so proud of you too Matt Powers. Thanks to my grandfather and Grandma Evelyn who have always loved and supported me, in person and in spirit.

Finally, thank you Matt. I really couldn't have made it without you. I can't tell you how much it meant to have someone so close who really understood the difficulties and set-backs of graduate school, but who also understood how to have a good time. All of the memories are so good, but I know that they are nothing compared to the ones to come. I'll enjoy being Dr. Minton, but I can't wait to be Dr. McKee.

Table of Contents

List of Figures

Chapter 1
Introduction

The production of alkenes from their hydrogenated alkane counterparts is an energetically expensive process. The catalytic dehydrogenation of ethane produces ethylene and secondary reaction products resulting in low selectivity to ethylene. Surface science studies of the reactions of vinylidene and vinyl intermediates, created through C-halogen bond cleavage can provide insight into possible routes for the reaction of these surface fragments over metal oxides. Possible reactions of these fragments include forming acetylene through vinylidene isomerization [1], or vinyl group dehydrogenation [2-4], vinyl group hydrogenation to form ethylene [5-7], and coupling of vinyl species to form butadiene [8-10]. Factors affecting surface reactivity may include type of adsorbed fragment, fragment orientation, degree of fragment mobility, and availability of both surface hydrogen species and active metal centers. The goal of this study is to understand secondary reaction routes of ethylene by directing the C-ligand bond cleavage with the placement of C-Cl bonds.

1.1 Catalytic Dehydrogenation

Ethane and ethylene dehydrogenation reactions are not only endothermic but are also unselective due to equivalency of all C-H bonds [11]. The lack of selectivity in dehydrogenation reactions can lead to a variety of side reactions [11]. Dehydrogenation of alkanes may result in normal or cyclic alkenes, or higher molecular weight hydrocarbons through C-C bond formation [11]. Due to product stability, the formation of heavier alkenes is more thermodynamically favorable than the formation of lighter

alkenes [11]. When extensive dehydrogenation occurs, the substrates may be converted to hydrogen gas and surface carbon (coke) [11].

In studies from the 1920s, Pease and Stewart found that the combination of hydrogen with olefins to form the corresponding paraffin readily occurs at moderate temperatures over traditional metal catalysts such as nickel, copper, and palladium [12,13]. Frey and Huppke later reported that the reverse reaction, producing olefins from paraffins, is only thermodynamically possible with elevated temperatures at which traditional catalysts may become deactivated or trigger decomposition of the paraffin to coke [14].

Supported metal oxides are catalytically active toward oxidative dehydrogenation of alkanes. Michalakos *et al.* [15] found that supported magnesium and vanadium oxide powder catalysts in steady state oxidative dehydrogenation reactions show 20-80% selectivity for ethane conversion to ethylene with the balance comprised of combustion products [15]. Karamullaoglu *et al.* [16] found that mixed chromium, vanadium, and niobium oxide supported powder catalysts show an average overall ethane conversion of ~35% with 20-30% selectivity to ethylene in steady state reactions conducted in the presence of oxygen [16].

Frey and Huppke found that chromic oxide gels catalyze dehydrogenation of alkanes [14]. It is commonly seen that catalytic activity of supported chromia catalysts is centered on Cr cations and increases with chromia loading up to monolayer coverage [17-20]. Weckhuysen *et al.* found that above monolayer coverage the activity decreases as a result of the formation of bulk sites with no coordination vacancies [19]. The adsorption of alkanes on active chromia sites is followed by C-H bond cleavage, perhaps forming

both O-H and Cr-C bonds, shown in Figure 1, and release of alkene and hydrogen [11]. Flick and Huff have shown that supported chromia/alumina catalysts promoted by platinum exhibit ethane dehydrogenation selectivity to ethylene on the order of 60% [21]. Additionally, methyl tert-butyl ether (MTBE) plants responsible for isobutane dehydrogenation to isobutene using chromium oxide based catalysts report above 90% selectivity for the alkane dehydrogenation process [11]. These studies show that Cr_2O_3 is an effective dehydrogenation catalyst. In addition to dehydrogenation, chromium oxide based catalysts have been used for a number of different reactions including: hydrogenation, oxidation, isomerization, aromatization, and polymerization of hydrocarbons, and halogenation and dehalogenation reactions of halo-hydrocarbons [1,18,21-25].

1.2 The α-Cr_2O_3 ($10\bar{1}2$) Surface

Weller and Voltz initially reported that α-Cr_2O_3 is the most abundant species found in chromia gels [26]. Zecchina and co-workers identified the predominant crystallographic face in microcrystalline chromia to be the α-Cr_2O_3 ($10\bar{1}2$) plane, Figure 2, which has the lowest energy of all low-index surfaces of α-Cr_2O_3 [27,28]. Previous studies on the α-Cr_2O_3 ($10\bar{1}2$) single crystal surface [29] have shown that oxygenating the stoichiometric surface followed by adsorbing halo-hydrocarbons and heating results in oxygenated products, similar to what is seen during initial reduction periods for microcrystalline chromia powders during alkane dehydrogenation catalysis [11,19]. The similar reduction behavior of the α-Cr_2O_3 ($10\bar{1}2$) single crystal surface and chromium oxide microcrystalline powders indicate that the ($10\bar{1}2$) single crystal surface is a

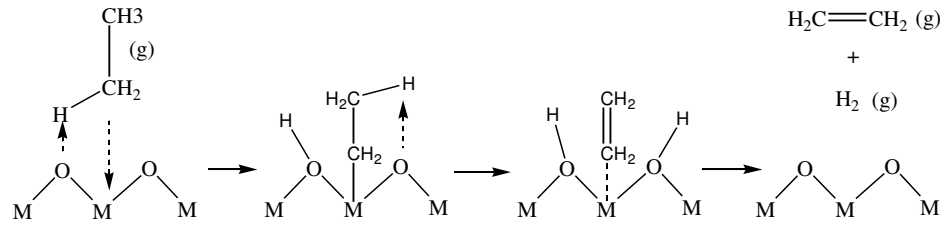

Figure 1. Metal oxide catalyzed ethane C-H bond cleavage followed by β-hydrogen elimination to form ethylene.

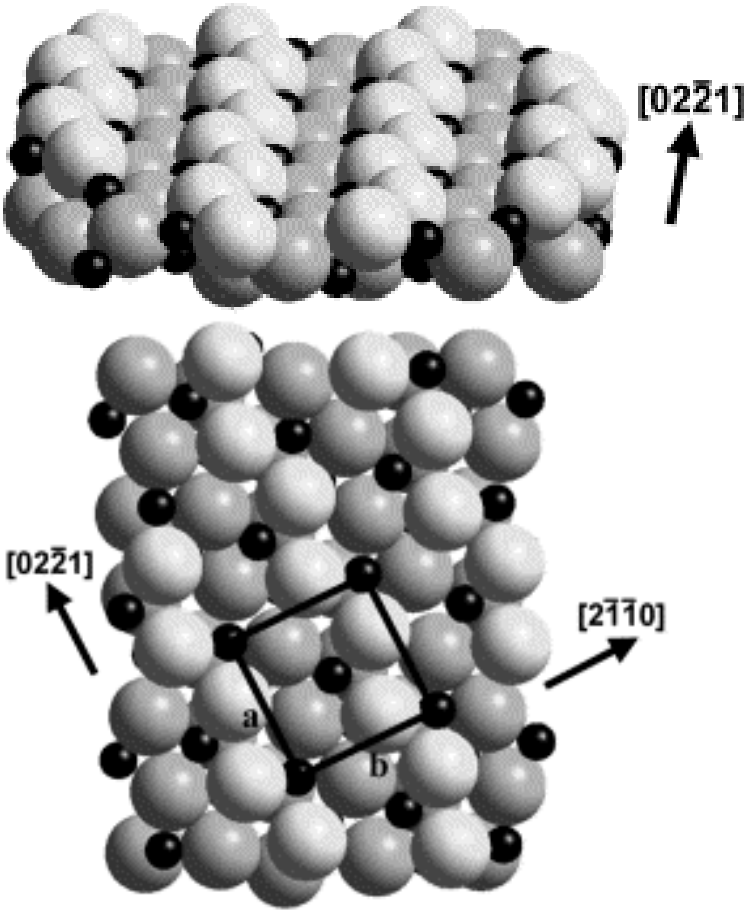

Figure 2. (a) Ideal, stoichiometric α-Cr_2O_3 (10$\bar{1}$2) surface. Large spheres represent 3-coordinate O^{2-} anions and small spheres represent 5-coordinate Cr^{3+} cations. (b) Two-dimensional surface with a side ratio a:b of 0.94.

reasonable starting model for understanding hydrocarbon reactions on chromium oxide powders. Hence, the α-Cr_2O_3 ($10\bar{1}2$) surface is the focus for this study.

α-Cr_2O_3 is an insulator with a band gap of 3.4 eV, and is resistant to corrosion even at high temperatures [30,31]. α-Cr_2O_3 has the corundum bulk structure [31] in which the metal-ligand orientations are of distorted d^3 octahedral symmetry resulting from 1/3 of all possible cation sites being vacant [27,32]. Oxygen ligands in the bulk are oriented in a distorted tetrahedral arrangement.

The ideal stoichiometric α-Cr_2O_3 ($10\bar{1}2$) surface contains both Lewis acid sites, chromium cations (small dark spheres in Figure 2), and Lewis base sites, oxygen anions (large gray spheres in Figure 2). Although the surface exposes an outermost layer of oxygen anions, the surface is non-polar because the stoichiometric repeating unit contains no net dipole moment [33]. One full repeating stoichiometric unit of α-Cr_2O_3 in the [$10\bar{1}2$] direction includes five atomic layers ordering as [O, Cr, O, Cr, O]. The two-dimensional surface periodicity is nearly square with an a:b ratio of 0.94 (Figure 2b). All surface ions on the ideal, stoichiometric, non-polar α-Cr_2O_3 ($10\bar{1}2$) surface possess one degree of coordinative unsaturation. The small degree of unsaturation provides a stable surface as evidenced by previous work on the α-Cr_2O_3 ($10\bar{1}2$) surface [29,32]. A real, nearly-stoichiometric α-Cr_2O_3 ($10\bar{1}2$) surface prepared through Ar^+ ion bombardment and annealing and characterized by low energy electron diffraction (LEED) and x-ray photoelectron spectroscopy (XPS) [34] will be used to study the reactions of chlorinated ethylenes.

The formal oxidation state of both six-coordinate (bulk) and five-coordinate (surface) chromium ions in the α-Cr_2O_3 ($10\bar{1}2$) single crystal is 3+ as is the operating

oxidation state of chromia in microcrystalline powders following an initial reduction period that produces oxygenated species in alkane dehydrogenation reactions [11,19]. Oxygen anions on the ideal, stoichiometric α-Cr_2O_3 ($10\bar{1}2$) surface are three-coordinate as opposed to the four coordinate bulk oxygen anions. Studies of metal oxide surfaces by Henrich suggest that the oxygen anions in both the bulk and surface sites in metal oxides can be considered as doubly charged (O^{2-}) having a closed shell configuration [12]. There has been no clear indication that the electronic configuration of surface anions is different than that of bulk anions. While some metal oxide surfaces may lose surface oxygen under vacuum conditions, previous work on the nearly stoichiometric α-Cr_2O_3 ($10\bar{1}2$) surface shows that 3-coordinated surface oxygen is not readily released under the UHV conditions to be used for this study [29,32,35,36].

For reactions of hydrocarbons in the absence of gas phase or adsorbed oxygen, metal oxides that are non-reducible do not produce oxygenated gas phase products, and dehydrogenation is the major reaction pathway [15]. Studies by Cox and co-workers indicate the nearly stoichiometric ($10\bar{1}2$) surface of α-Cr_2O_3 is non-reducible [29,32]. Byrd has found that redox reactions in which molecules are oxidized while the surface is reduced by oxygen loss do not occur on the nearly stoichiometric α-Cr_2O_3 ($10\bar{1}2$) surface [29]. York has found for the same surface that the dissociation of halogenated vinyl species followed by thermal desorption show no combustion products to associate with the reaction and subsequent release of surface lattice oxygen [32]. These studies indicate little to no reactivity of 3-coordinate surface lattice oxygen with respect to formation of combustion products for reactions of hydrocarbon fragments on this surface. Although combustion products are not expected to desorb from the nearly stoichiometric ($10\bar{1}2$) α-

Cr_2O_3 surface in UHV conditions, it may be expected that surface oxygen plays an important role in surface reactivity. Weckhuysen and co-workers allude that forming an oxygen-hydrogen interaction facilitates hydrogen elimination [11,16], Figure 1, favored by the strength of the O-H hydrogen bond. β-hydrogen elimination, either metal or oxygen catalyzed, is reported as a common route for surface alkyl decomposition [37]. No literature has been found that presents common routes for hydrogen elimination from vinyl surface intermediates.

1.3 C2 adsorbates and halogen adatoms

This study, conducted under ultrahigh vacuum (UHV) conditions, focuses on the products of vinyl, vinylidene, and chlorovinyl surface fragments formed on the well-ordered, model, single crystal. Reactions of surface vinyl and vinylidene fragments on the nearly-stoichiometric $(10\bar{1}2)$ surface of α-Cr_2O_3 under UHV may mimic reactions of surface intermediates that form in the dehydrogenation of ethylene over supported chromia powders. The conditions for this study do not allow the formation of vinyl and vinylidene fragments from ethylene because the energy required for ethylene desorption from this surface is lower than the energy required for C-H bond cleavage. Vinyl and vinylidene surface groups are more easily derived from halogenated substrates, in this case the chlorinated ethylenes pictured in Figure 3, due to the relative weakness of C-Cl bonds when compared to C-H bonds. Gas phase products resulting from the reactions of vinyl chloride, 1,1- dichloroethylene, cis-1,2- dichloroethylene, and trans-1,2-dichloroethylene on α-Cr_2O_3 $(10\bar{1}2)$ were examined with thermal desorption spectroscopy (TDS); surface intermediates and molecular adsorbates were probed with

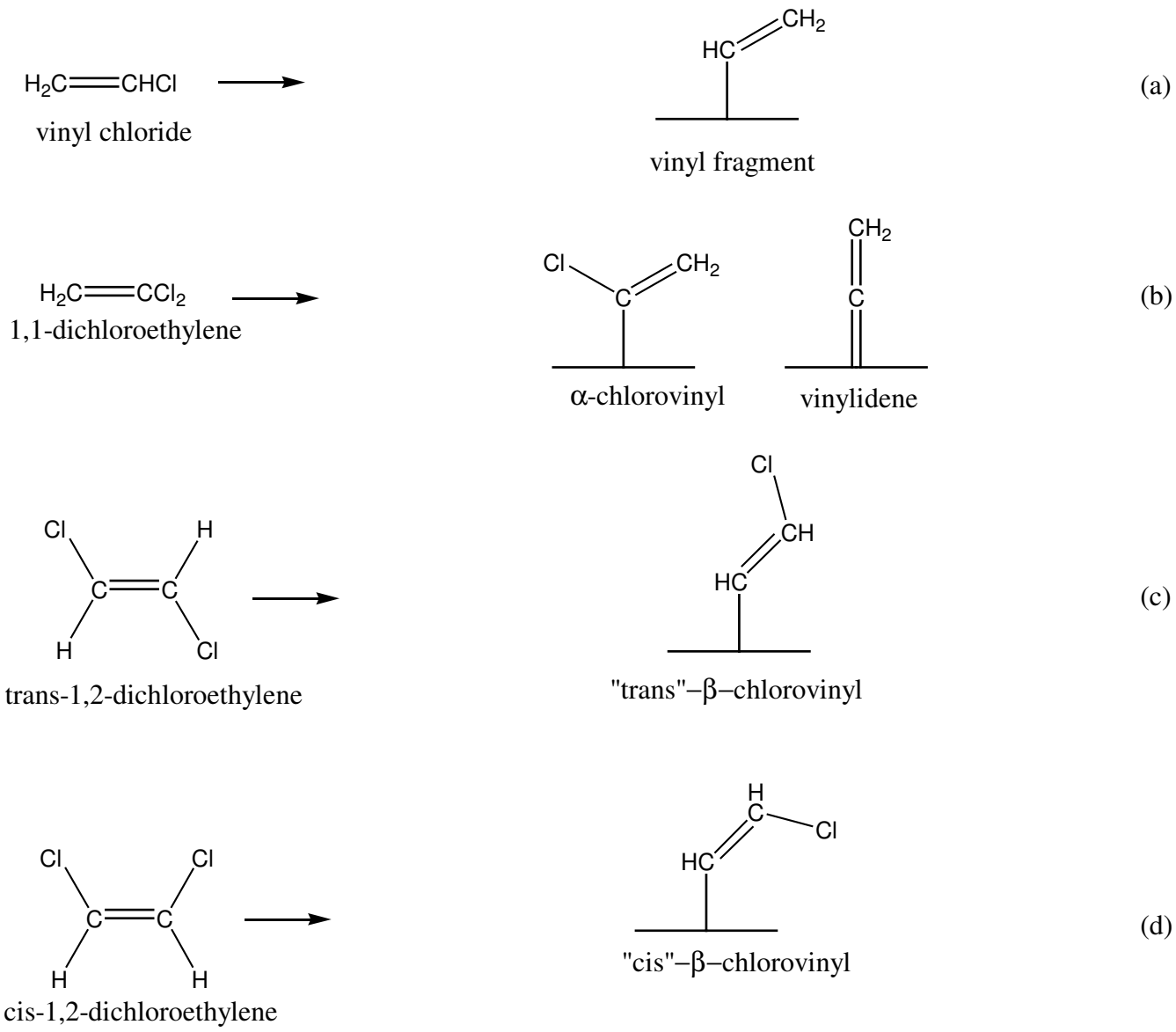

Figure 3. Possible surface fragments formed from the reactions of a) vinyl chloride, b) 1,1-dichloroethylene, c) trans-1,2-dichloroethylene, d) cis-1,2-dichlroethylene.

photoemission spectroscopy (PES) and near-edge x-ray absorption fine structure (NEXAFS). Figure 3 shows some of the possible surface fragments that may be derived by C-Cl bond cleavage from their chlorinated ethylene counterparts. Bent and co-workers have determined through near edge x-ray absorption fine structure (NEXAFS) studies that vinyl halides dissociate on Cu(100) to form surface vinyl groups which dehydrogenate to form acetylene, couple to form 1,3-butadiene, and trimerize to form benzene [8,10]. Dihalogenated ethylenes have been reported to form vinylidene, halovinyl, and adsorbed acetylene through C-X (X=halogen) bond cleavage. York et. al. showed that 1-chloro-1-flouroethylene forms acetylene on Cr_2O_3 ($10\bar{1}2$), presumably through a vinylidene intermediate [1]. Adsorbed 1,2-dichloroethylenes on well defined surfaces undergo sequential C-Cl bond cleavage to form chlorovinyl groups that subsequently react to acetylene through β-chlorine elimination [38,39]. Trans-1,2-dichloroethylene also adsorbs parallel to the Cu(110) surface at 85 K and forms adsorbed acetylene through concerted C-Cl bond cleavage[40]. These studies suggest the possibility of forming surface fragments by cleaving C-Cl bonds, Figure 3.

Dissociation of chlorinated ethylenes will deposit chlorine adatoms on active chromium centers. A nearly stoichiometric α-Cr_2O_3 single crystal ($10\bar{1}2$) surface with a Cl:Cr of 1:1 (all surface cations are chlorine capped) has an Auger electron spectroscopy (AES) Cl/Cr ratio of 0.32 [32]. Lugo and co-workers report for dehydrogenation studies with coke formation on supported chromia catalysts that deactivation occurs at a C:Cr coverage of 1:1 with selective coking at the active chromium site [22]. Site blocking by surface adatoms in which all active sites are blocked deactivates the catalyst surface,

shuts down surface chemistry, and may change barriers to surface diffusion and surface reactions.

1.4 Experimental

Experiments were conducted in two separate UHV chambers, both with a base operating pressure of ~1×10^{-10} Torr. Thermal desorption spectroscopy (TDS) was conducted in an ion pumped Physical Electronics chamber equipped with an Inficon Quadrex 200 mass spectrometer for thermal desorption measurements. This system is also equipped with a Model 15-155 single pass cylindrical mirror analyzer used in Auger electron spectroscopy (AES) measurements for clean and post-reaction surface analysis. Clean surface AES spectra were collected at 800 K. AES spectra were also collected following each thermal desorption cycle to determine the effect of depositing Cl adatoms on surface reactivity. The AES spectra taken of the chlorinated surface were obtained at a temperature of 773 K with a total beam exposure time of ~12 sec. These AES conditions were used to compensate for surface charging and reduce the effects of both thermally stimulated Cl migration into the crystal and electron stimulated desorption of Cl from the surface [1]. The signal-to-noise ratio for these AES measurement conditions leads to some variability in the measured Cl/Cr ratio reflected in the standard deviations (error bars) reported in the results sections below. The error bars represent a 10% standard deviation that was measured as a result of the experimental parameters used to collect the post reaction spectra.

Near edge X-ray absorption fine structure (NEXAFS) and photoemission spectroscopy (PES) measurements were conducted at beamline U12A at the National Synchrotron Light Source. C 1s and Cl 2p photoemission spectra were collected using a

350 eV photon energy, and F 1s spectra were collected at a photon energy of 700 eV. All spectra were collected at an instrumental resolution of 0.5 eV, and referenced to a Cr $2p_{3/2}$ binding energy of 576.9 eV [34,41]. FitXPS2 software was used to curve fit the photoemission spectral features [42]. NEXAFS data were collected in the excitation range of 275-320 eV using electron partial yield detection with a -150.0 V retarding grid bias. The polarization vector of the incident light was parallel to the Cr_2O_3 $(10\bar{1}2)$ surface when the wave vector of the light was normal to the surface. The NEXAFS photon energy scale is referenced to the absorbance of adventitious carbon, 284.7 eV, in the total electron yield spectrum of the gold reference grid in the beamline [43,44]. The adsorbate NEXAFS spectra presented in this study are normalized using spectra collected from a clean surface. Compensation for surface charging during NEXAFS and PES was achieved with a Gammadata Scienta FG-300 flood gun using 0.5 eV electrons. Only limited polarization dependence was possible using NEXAFS spectra collected with grazing angle (75° off surface normal) and normal incidence light for reasons described in detail in Section 2.2.3.

Vinyl chloride (99.5%) from Sigma Aldrich and PCR 1-chloro-1-fluoroethylene ($CFCl=CH_2$, 97%) gas reactants were used as received; Sigma Aldrich 1,1-dichloroethylene ($CCl_2=CH_2$, ≥99.5%), cis-1,2-dichloroethylene (HClC=CHCl) 97%, and trans-1,2-dichloroethylene (HClC=CHCl) 99.7% liquid reactants were purified by flash distillation and multiple freeze-pump-thaw cycles prior to use. The liquid reactants were kept in stainless steel tubes attached to the pump manifold using VCR fittings and sealed with copper (Cu) VCR gaskets. Hydrocarbon standards Sigma Aldrich 1,3-butadiene

(C_4H_6, 99+%), Special Gas Systems grade 3.0 ethylene (C_2H_4), and Matheson acetylene (C_2H_2, 99.6%) were used as received for this study.

For thermal desorption, gas exposures were performed by back filling the chamber through a variable leak valve; reported doses have been corrected for ion gauge sensitivity [45,46]. The mass spectrometer was equipped with a glass skimmer to minimize the sampling of desorption products from the sample support hardware, and a linear temperature ramp of 2.5 K/sec was used to minimize the possibility of thermal fracture of the ceramic sample. A product check including all mass numbers (m/z) in the range of 2-200 was conducted to identify possible desorbing gas phase species. The desorbing gas species were positively identified through comparison of thermal desorption peak intensities with mass spectrometer cracking patterns of hydrocarbon standards. The intensities of reported thermal desorption traces have been corrected with relative mass spectrometer sensitivity factors [47]. The mass fragmentation patterns for the two 1,2-dichloroethylene isomers cannot be distinguished from one another with mass spectrometry. For all experiments conducted, the initially clean surface was prepared by Ar^+ ion bombardment followed by annealing to 900 K resulting in a nearly-stoichiometric, non-polar, (1x1) α-Cr_2O_3 $(10\bar{1}2)$ surface [34].

The crystal was oriented to within 1° of the $(10\bar{1}2)$ surface using Laue backreflection and polished to a mirror finish. The sample was mechanically clamped, using tantalum (Ta) foil, onto a Ta stage fastened to LN_2-copper conductors for heating and cooling. Direct sample temperature measurement was achieved with a Type K thermocouple attached through a hole in the Ta stage to the back of the single crystal using Aremco # 569 ceramic cement.

Chapter 2

Vinyl Chloride

2.1 Introduction

The production of ethylene is important because of its high demand as a feedstock in the manufacture of various plastics and synthetic materials [48-51]. Currently, the majority of ethylene is produced through steam cracking of ethane, a process requiring high pressures and temperatures on the order of 1000-2000 °C [48]. Catalytic oxidative dehydrogenation (ODH) of ethane to ethylene, while requiring a larger initial capital investment, could provide a low temperature (~700-900 °C) route to supplement current ethylene production [48]. While there has been much research regarding the development of catalytic processes for ethane ODH there is not yet a commercially viable process [52]. Understanding factors affecting the selectivity for catalytic oxidative ethane dehydrogenation to ethylene may reveal options for future development of practical dehydrogenation processes. Secondary reactions such as ethylene dehydrogenation to acetylene or decomposition to coke are important in determining the factors that influence selectivity in ethane ODH.

Metal catalyzed hydrocarbon hydrogenation and dehydrogenation reactions have been extensively studied [2,4,7,10,53]; however, the high temperatures required for dehydrogenation reactions often lead to deactivation of traditional metal catalysts. Alternatives to traditional metal catalysts that allow reasonable reaction conditions include mixed metal catalysts, such as the Mo/V/Nb/Sb catalyst used in the Union

Carbide ethane ODH process [48], and metal oxide catalysts, such as chromium oxides, which promote dehydrogenation reactions [11,14].

This work focuses on the reaction of vinyl chloride on the well-defined α-Cr_2O_3 $(10\bar{1}2)$ single crystal surface to mimic chromia catalyzed ethylene dehydrogenation through a surface vinyl intermediate. The use of halogenated reactants to simulate the formation of surface intermediates occurring in hydrocarbon surface reactions has found increasing application in surface science experiments [8,39], and vinyl chloride is expected to provide a low temperature route to the formation of surface vinyl groups in UHV on α-Cr_2O_3 $(10\bar{1}2)$. Thermal desorption spectroscopy (TDS), Auger electron spectroscopy (AES), x-ray photoelectron spectroscopy (XPS), and near-edge x-ray absorption fine structure (NEXAFS) experiments were conducted to identify reaction products and surface intermediates formed in the thermally induced reaction of adsorbed vinyl chloride.

2.2 Results

2.2.1 gas phase and surface products

Thermal desorption of adsorbed vinyl chloride results in four gas-phase reaction products: acetylene (HC≡CH), ethylene (CH_2=CH_2), 1,3-butadiene (CH_2=CH–CH=CH_2), and dihydrogen (Section 4.1.1). No water, CO, CO_2 or chlorinated gas phase products are observed. Relative intensities of multiple m/z signals were used to positively identify all hydrocarbon products. Overlap of mass signals from vinyl chloride, butadiene, ethylene, and acetylene was accounted for by subtracting overlapping contributions out of the raw mass spectrometer signal. Following these subtractions, the relative intensities of

m/z fragments for all hydrocarbon products formed were found to be in good agreement with mass spectrometer cracking patterns of hydrocarbon standards. A primary m/z signal of 54 was followed for 1,3-butadiene, and positive identification was achieved through comparison of m/z=54, 53, and 39 for a 1,3-butadiene standard. For ethylene, m/z=27 was followed in TDS experiments, and positive identification of ethylene was achieved through comparing relative intensities of m/z=27, 26, and 25. The primary mass signal followed for acetylene identification was m/z=25, and relative intensities of m/z=26, 25, and 24 were used to positively identify acetylene. Comparison of pre- and post-reaction AES, section 4.1.2, indicates that chlorine adatoms are the only surface product resulting from the thermally-induced reaction of vinyl chloride. No surface carbon resulting from the reaction of vinyl chloride is observed with AES.

2.2.1.1 thermal desorption spectroscopy

Figure 4 shows a typical set of thermal desorption traces for a 0.1 L dose of vinyl chloride on a partially chlorinated surface. Vinyl chloride desorption occurs near 280 K, 1,3-butadiene production peaks at 515 K, while the reaction products acetylene, ethylene and dihydrogen desorb in the range from about 450-750 K. Dosed and molecularly adsorbed acetylene and ethylene desorb without reaction at 325 K and 220 K (not shown), respectively, indicating that the kinetics for the production of both molecules from vinyl chloride are surface reaction limited. The maximum in the butadiene product feature near 515 K is more than 65 K higher in temperature than that observed for the desorption of chemisorbed (dosed) 1,3-butadiene (not shown), indicating that the

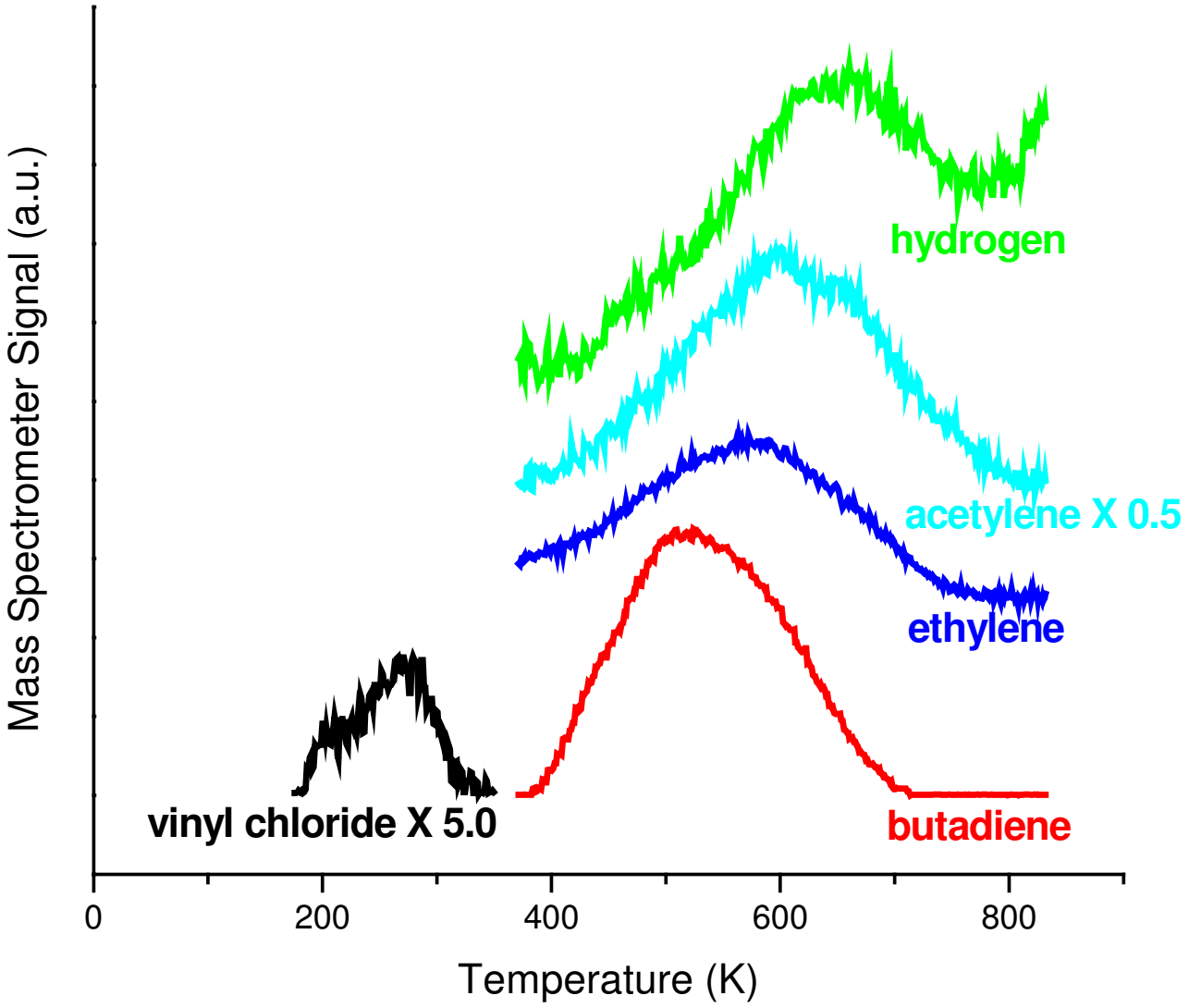

Figure 4. **Typical TDS trace of a corrected 0.1 L dose of vinyl chloride on a partially chlorinated surface. The vinyl chloride peak desorption temperature is 275 K. The temperature range for acetylene, ethylene, and butadiene desorption is 400-800 K. Desorption limited acetylene and ethylene (not shown) evolves from the surface at 300 K and 200 K, respectively. Desorption limited butadiene evolves from the surface at ~400 K and appears as a shoulder on the butadiene desorption curve.**

butadiene product from vinyl chloride also shows predominantly surface reaction limited kinetics.

Acetylene is the predominant gas phase product (note the scale factor in Fig. 4 and evolves in a desorption feature centered at 605 K. As seen also in Figure 4, ethylene formation peaks near 575 K, and H_2 reaches a maximum near 645 K. While the temperature maxima for these three product desorption signals are different, it is clear that desorption signals for ethylene and dihydrogen fall within the same temperature "envelope" encompassed by the acetylene desorption signal. The similarities in desorption temperatures suggest that these three products likely arise from the reaction a common surface reaction intermediate.

The surface chemistry giving rise to acetylene, ethylene, and H_2 is readily explained as originating from the surface vinyl fragment expected to form following the thermal dissociation of the weakest bond, the C-Cl bond, in vinyl chloride. The expected rate-limiting step for acetylene production is vinyl dehydrogenation which also produces surface hydrogen atoms. Ethylene and H_2 formation then follows by H addition to surface vinyl groups or other H atoms, respectively. The chemistry is described by the following simple reaction sequence:

$$CH_2{=}CHCl \rightarrow CH_2{=}CH{-}_{(ads)} + Cl_{(ads)} \qquad (1)$$

$$CH_2{=}CH{-}_{(ads)} \rightarrow CH{\equiv}CH + H_{(ads)} \qquad (2)$$

$$CH_2{=}CH{-}_{(ads)} + H_{(ads)} \rightarrow CH_2{=}CH_2 \qquad (3)$$

$$H_{(ads)} + H_{(ads)} \rightarrow H_2 \qquad (4)$$

Even though ethylene and dihydrogen appear at different temperatures, a first order rate-limiting step of vinyl dehydrogenation is sufficient to explain their kinetics

because they both appear within the temperature range observed for acetylene production via vinyl dehydrogenation. The elementary steps producing ethylene and dihydrogen (3 and 4) compete for the H atoms released by vinyl dehydrogenation (2), with rates for the two reaction channels being dependent on surface coverage of vinyl. At low reaction temperatures (below 600 K) where the coverage of surface vinyl groups is higher, H atoms released by vinyl dehydrogenation to acetylene (2) are scavenged primarily by the remaining surface vinyl groups to form ethylene (3). At higher temperatures (above 600 K) where the coverage of surface vinyl groups is lower, the reaction channel to H_2 (4) becomes important.

1,3-butadiene production in Figure 4 is centered around 535 K, with a maximum in the desorption trace at 515 K. The surface chemistry that gives rise to 1,3-butadiene is readily explained by coupling of the vinyl species (5) proposed above as the primary

$$2\ CH_2{=}CH{-}_{(ads)} \rightarrow CH_2{=}CH{-}CH{=}CH_2 \qquad (5)$$

surface reaction intermediate. The lower temperature for butadiene production compared to that for acetylene production suggests a barrier to the vinyl coupling reaction that is lower than that for vinyl decomposition.

A series of consecutive 0.1L doses of vinyl chloride starting on an initially clean, nearly-stoichiometric Cr_2O_3 $(10\bar{1}2)$ surface is depicted in Figure 5. Acetylene desorption, Figure 5a, initially appears as a rather misshapen peak centered at 550 K. The initial peak shape likely results from the multiple subtractions required to extract the acetylene desorption signal. Sequential exposures to vinyl chloride results in an increase in the acetylene peak desorption temperature, suggesting a change in surface reactivity with consecutive dose. The acetylene trace corresponding to 0.5L total exposure of vinyl

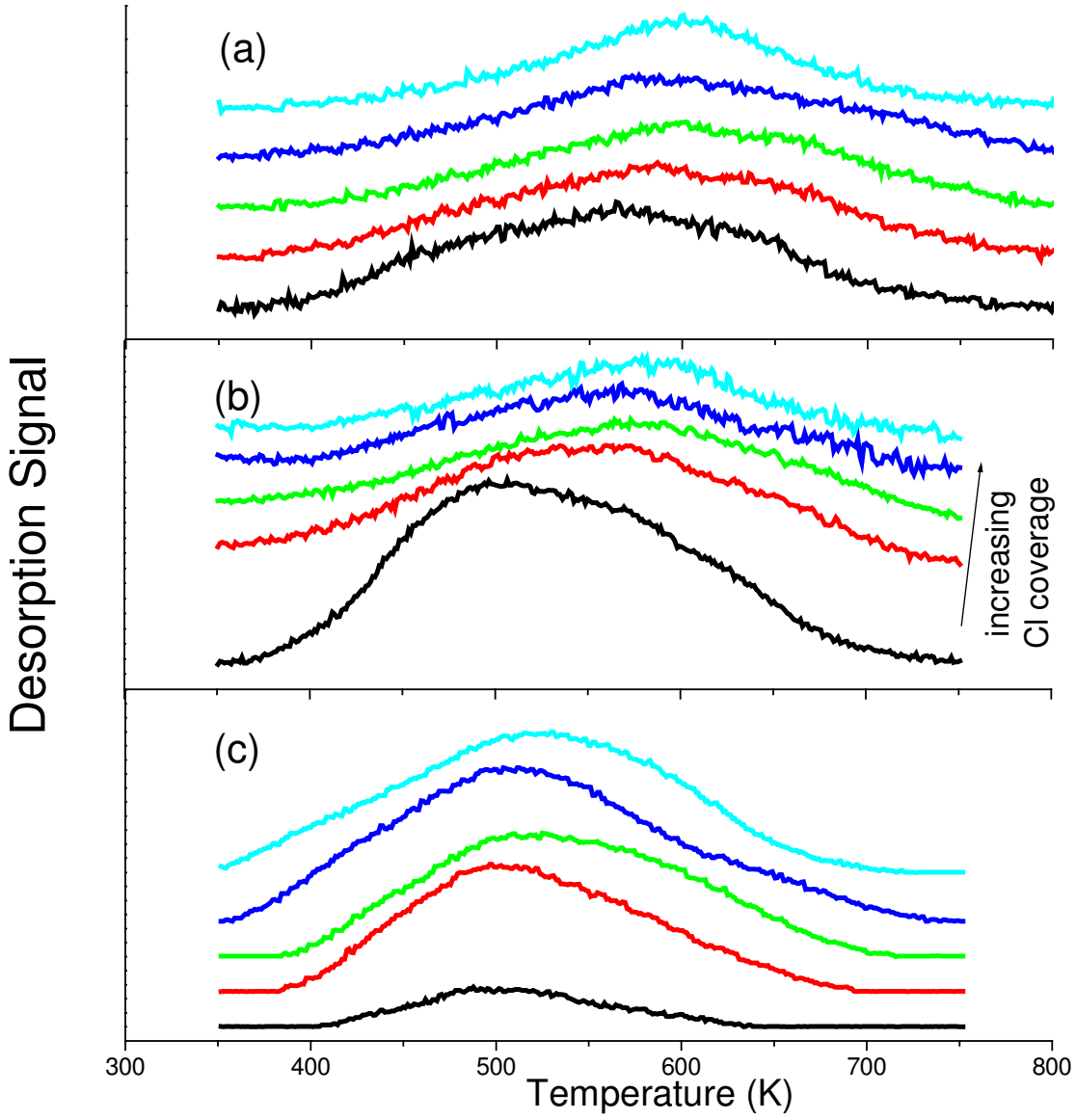

Figure 5. Series of corrected 0.1L vinyl chloride doses on an initially clean, nearly-stoichiometric α-Cr_2O_3 (10 $\bar{1}$ 2) surface: a) acetylene, b) ethylene, c) butadiene. Acetylene and ethylene product traces have had contributions from overlapping mass signals (i.e. m/z= 25 and 27) subtracted out. The increasing peak desorption temperature indicates that with increased exposure to vinyl chloride there is an increased barrier to the production of acetylene, ethylene, and butadiene.

chloride appears at 600 K, and has the usual asymmetric shape expected for a first order process. Using the Redhead method [54] and assuming a normal first order pre-exponential factor of 10^{13} s^{-1}, the activation barrier to vinyl decomposition (acetylene formation) is estimated to vary between about 145 and 160 kJ/mol for the consecutive doses shown in Figure 5a.

Ethylene desorption, Figure 5b, follows trends similar to acetylene desorption. The shape of the initial trace, centered at 500 K, likely results from multiple subtractions applied to the raw data. Similar to acetylene, the ethylene peak desorption temperature increases with each successive exposure to vinyl chloride, indicating a change in surface reactivity with sequential dose. Finally, the ethylene trace resulting from 0.5L total exposure to vinyl chloride shows a typical first order peak shape. The similarities in desorption features in Figures 5a and 5b further substantiate the assumption that acetylene and ethylene share a common first order rate-limiting step: surface vinyl group dehydrogenation (reaction 2).

Butadiene production is shown in Figure 5c. The butadiene desorption temperature appears to increase with successive exposure to vinyl chloride. Also, the amount of butadiene production per thermal desorption run increases with consecutive 0.1 L dose, most notably between the first and second runs.

The increasing desorption temperatures for acetylene, ethylene, and butadiene as a function of consecutive 0.1 L dose indicates that the surface reactivity changes as a result of the consecutive exposures to vinyl chloride. Since no chlorinated gas phase reaction products are observed, the likely cause of the variations is the deposition of surface Cl adatoms as a result of the reaction of vinyl chloride to form hydrocarbons. The

increasing desorption temperatures is a sign that Cl adatoms tend to stabilize the surface fragments that are intermediates in surface reactions to form the hydrocarbon products.

Figure 6 shows the integrated desorption signals (left hand axis) for carbon containing molecules from consecutive 0.1L doses of vinyl chloride on an initially clean Cr_2O_3 $(10\bar{1}2)$ surface. The right hand axis in Figure 6 also shows the variation in surface Cl coverage as measured by AES as a function of consecutive 0.1 L thermal desorption runs. As the total vinyl chloride exposure increases, the Cl adatom coverage increases up about 1 ML, where 1 ML is defined as one Cl adatom per surface Cr cation. Details of the Cl adatom coverage determinations are described in Section 4.2.

Figure 6 shows that acetylene and ethylene production is at a maximum for the first 0.1L vinyl chloride dose. Continued exposure to vinyl chloride results in a steady decrease in the amounts of both products as the surface becomes chlorinated. Conversely, butadiene production makes up only 5% (on a C2 basis) of the total gas desorption for the first 0.1L dose of vinyl chloride. The production of butadiene increases up to a total vinyl chloride exposure of 0.4L, corresponding to a pre-dose Cl coverage of 2/3 to 3/4 ML. After 0.4L total exposure, butadiene production decreases steadily with each successive exposure to vinyl chloride. It should also be noted that until approximately 0.4L total exposure, nearly all the vinyl chloride reacts to form nonchlorinated hydrocarbons, and almost no vinyl chloride desorbs from the surface. For higher total doses, as the surface coverage of Cl increases, the vinyl chloride reaction probability decreases and molecular vinyl chloride, CH_2=CHCl, desorption becomes dominant. Hence, Cl adatoms act as modifiers which change both the selectivity and

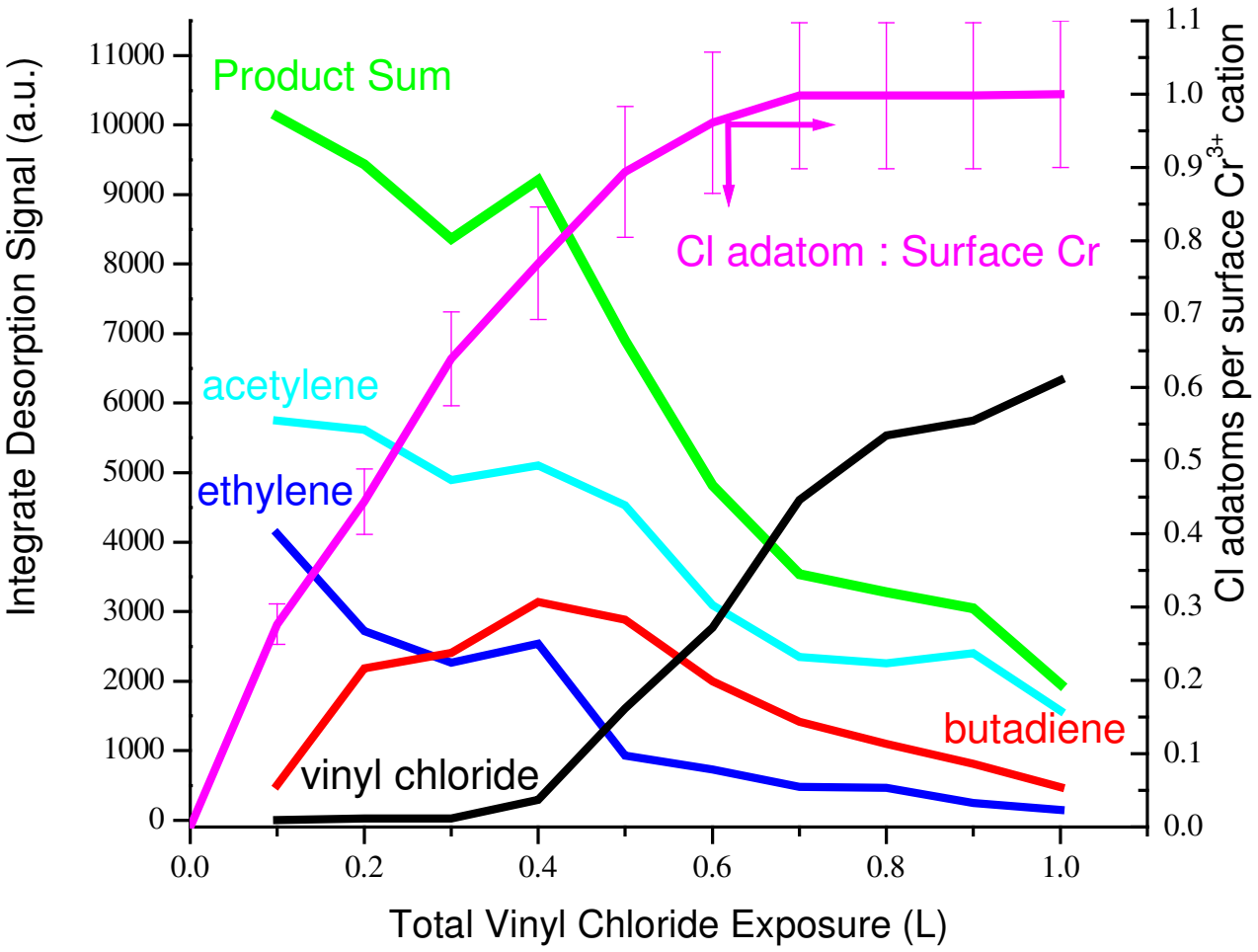

Figure 6. Integrated, corrected consecutive TDS product traces show that acetylene is the major hydrocarbon produced in the reaction of vinyl chloride on the α-Cr_2O_3 $(10\bar{1}2)$ surface. The plot of surface Cr coverage by Cl adatoms vs. total vinyl chloride exposure shows that surface Cl coverage increases with increasing vinyl chloride exposure up to the point at which all surface Cr cations have been capped by Cl adatoms. Butadiene, which proceeds through a production maximum, appears to be stabilized by a partial surface coverage of Cl adatoms. Acetylene and ethylene desorption is immediately affected by increasing surface Cl adatom coverage. The overall effect of Cl adatom coverage is to shut down surface reactivity towards hydrocarbon production.

activity of the surface reactions. The decreased surface reactivity for vinyl chloride exposures above 0.4 L indicates that Cl adatoms block the active sites for the reaction.

2.2.1.2 Auger electron spectroscopy

An AES spectrum of a nearly-stoichiometric Cr_2O_3 $(10\bar{1}2)$ surface is shown in Figure 7a. The Cr and O features in the range of 470-550 eV are a characteristic fingerprint of the Cr_2O_3 $(10\bar{1}2)$ clean, nearly-stoichiometric surface [34]. Due to the overlap of the main Cr $L_3M_{2,3}M_{4,5}$ peak (529 eV) with the O KLL peak (508 eV), as seen in Figure 7a, the Cr $L_{2,3}M_{2,3}M_{2,3}$ peak (near 490 eV) makes a more reasonable point of reference for the calculation of surface concentrations. To estimate an AES sensitivity factor for the Cr $L_{2,3}M_{2,3}M_{2,3}$ peak, an assumption is made that the peak-to-peak height ratios for all Cr LMM features are the same in both chromium metal and Cr_2O_3. The Cr $L_3M_{2,3}M_{4,5}$ /Cr $L_{2,3}M_{2,3}M_{2,3}$ peak ratio from a standard chromium metal spectrum [55] is then applied to the sensitivity factor for the Cr $L_3M_{2,3}M_{4,5}$ peak to determine a sensitivity factor for the Cr $L_{2,3}M_{2,3}M_{2,3}$ feature [34]. All surface Cl adatom coverages are calculated using the estimated Cr $L_{2,3}M_{2,3}M_{2,3}$ sensitivity factor.

Figure 7b is an AES spectrum taken after a set of 10 consecutive TDS runs of 0.1L doses vinyl chloride starting with a clean Cr_2O_3 $(10\bar{1}2)$ surface. The characteristic fingerprint of stoichiometric α-Cr_2O_3 $(10\bar{1}2)$ is intact, and the only observed change in the spectrum is the presence of a feature at 180 eV due to Cl. The Cl/Cr ratio for the spectrum in Figure 7b is 0.33, and is characteristic of a Cl coverage equivalent to one Cl per surface Cr cation based on a previous analysis utilizing layer-by-layer summations

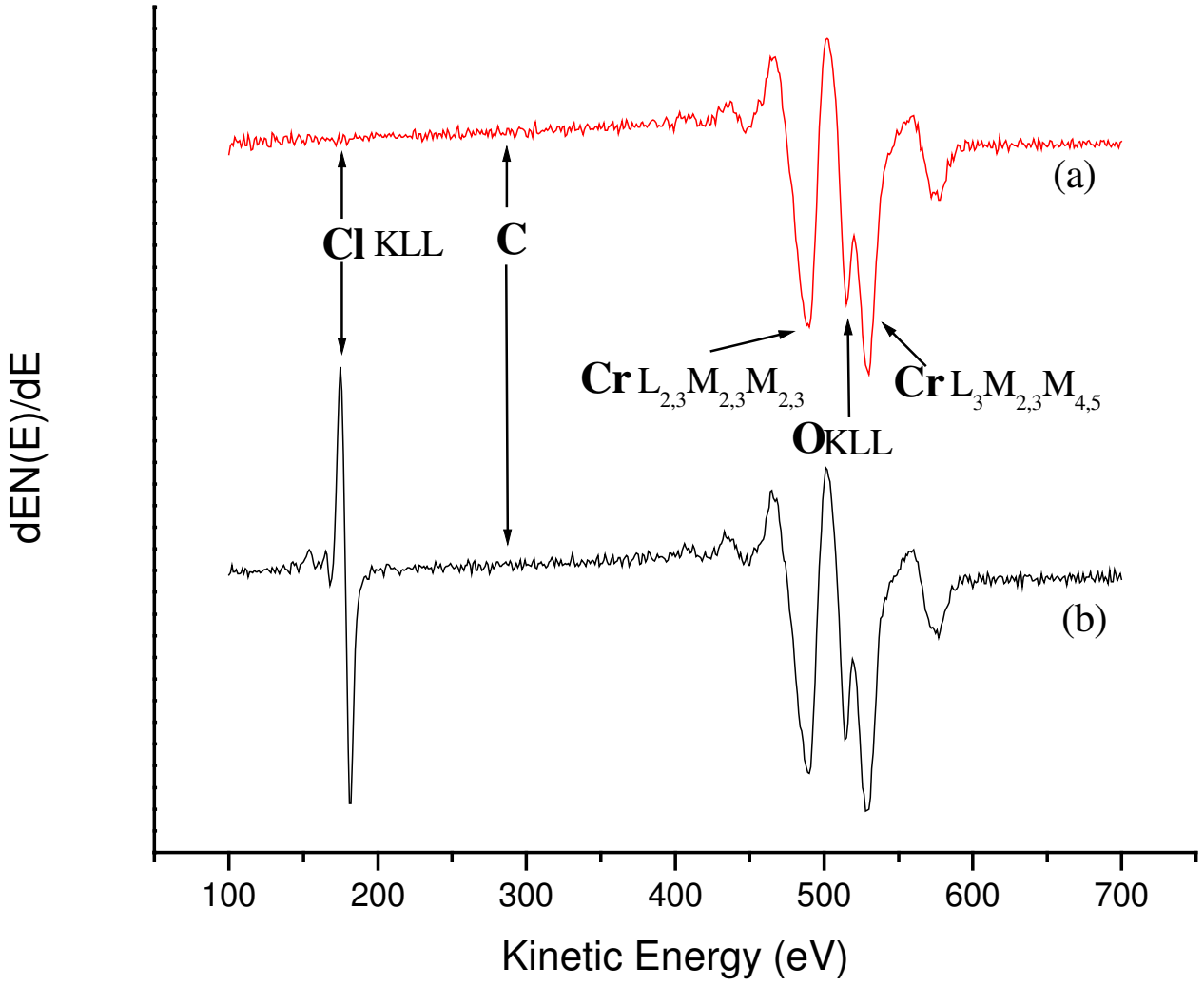

Figure 7. (a) Auger Electron Spectrum collected from a clean, nearly-stoichiometric α-Cr_2O_3 ($10\bar{1}2$) surface. The fingerprint between 450-550 eV is characteristic of the α-Cr_2O_3 ($10\bar{1}2$) surface. There is no observable surface carbon of chlorine present on the surface prior to exposure to vinyl chloride. (b) Auger Electron Spectrum of a deactivated α-Cr_2O_3 ($10\bar{1}2$) surface collected after ten consecutive TDS cycles of 0.1 L doses of vinyl chloride. The thermally induced surface reaction of vinyl chloride deposits no surface carbon (285 eV) but leaves Cl adatoms (181 eV). The deactivated surface has a Cl:Cr ratio of 0.32.

and the mean-free-path dependence of the Auger emission [25]. This coverage has been interpreted previously as an indication of a 1:1 capping of all surface Cr^{3+} ions with Cl adatoms, and hence a 1 ML coverage of Cl [25]. Additional support for this interpretation is offered in Section 4.2.

It is important to note that no surface carbon (285 eV) is observed with AES following a complete set of consecutive thermal desorption runs of vinyl chloride. The lack of surface carbon indicates that complete dehydrogenation and/or cleavage of the C-C bond to surface carbon does not occur under the conditions of this study.

2.2.2 photoelectron spectroscopy

For the synchrotron-based photoemission study, the sample was cooled to 130 K and exposed to a 20L dose of vinyl chloride. Following the 20L dose, photoemission spectra were collected at 130 K then the sample was heated to consecutively higher temperatures. Following each heating treatment, the sample was cooled again to near 130 K and photoemission spectra were collected in an attempt to isolate any surface intermediates formed during the thermally induced surface reaction of vinyl chloride.

Figure 8a shows the series of XPS C 1s spectra, and Figure 8b shows the corresponding data for Cl 2p. The C 1s spectrum collected at the dosing temperature, 130 K, shows unresolved multiple carbon features ranging from ~283-286 eV. For molecular vinyl chloride, two C 1s contributions are expected, one at higher binding energies due near 285.5 eV attributable to the chlorinated carbon (CHCl=), and a second at lower binding energies near 283.4 eV associated with the methylene carbon ($=CH_2$) [41]. Heating to temperatures up to 300 K results in a decrease and eventual loss of the feature associated with chlorinated carbon, and leaves one broad (FWHM=2.1 eV) C 1s

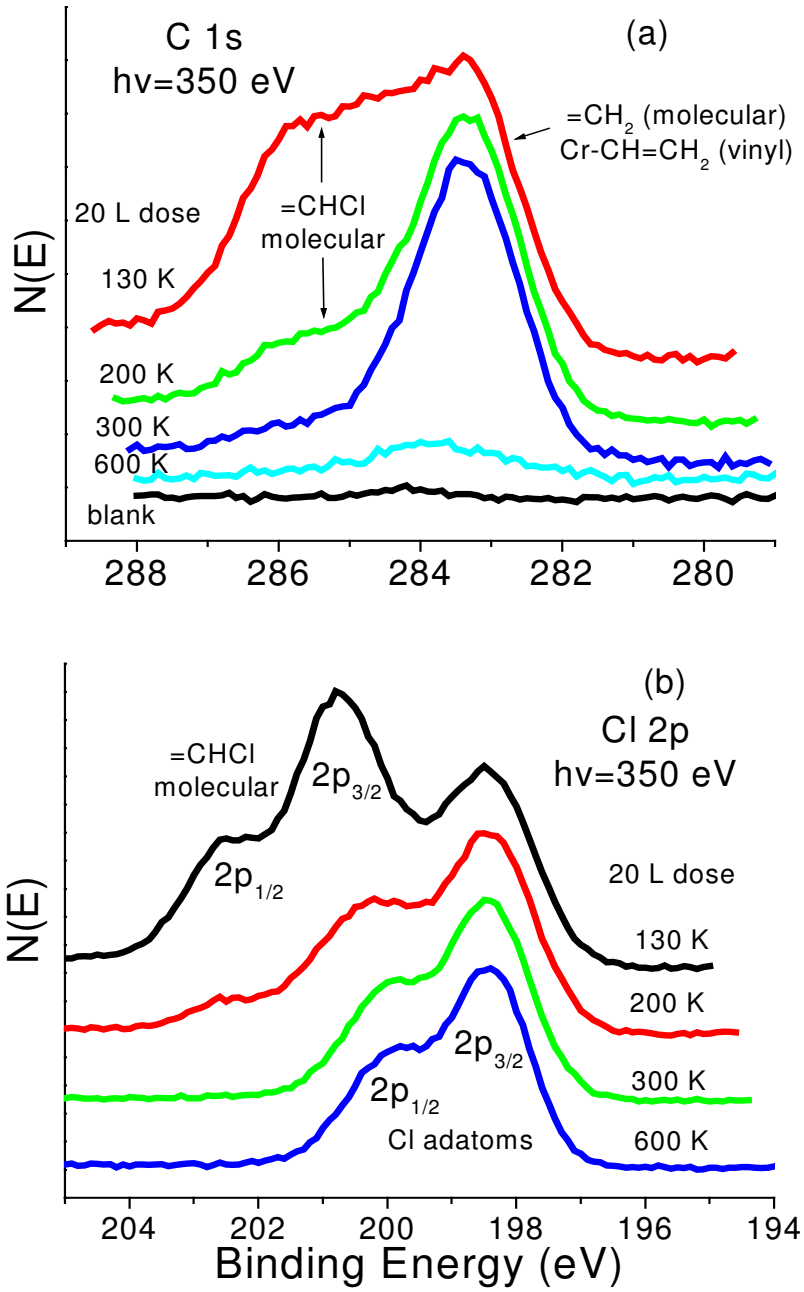

Figure 8. PES for a) C1s and b) Cl2p spectra collected following a 20L vinyl chloride dose at a series of sample temperatures. C1s and Cl2p spectra collected at the dosing temperature, 130 K, both exhibit multiple features indicating the presence of a mixed monolayer of intact molecular vinyl chloride and dissociated species are adsorbed on the surface. Spectra collected after heating to 200 K, after molecular vinyl chloride has begun to desorb, exhibit a decrease in the higher binding energy features for C1s (~286.0 eV) and Cl2p$_{3/2}$ (200.5 eV). Further heating to 300 K, above the vinyl chloride peak desorption temperature, leaves the Cl2p$_{3/2}$ (198.0 eV) lower binding energy feature associated with Cl adatoms and the C1s (283.0 eV) lower binding energy feature is associated with a carbon containing surface intermediate [41].

feature at 283.3 eV. The remaining C 1s feature at 300 K, above the vinyl chloride desorption temperature observed in thermal desorption, is characteristic of the surface intermediate responsible for the observed reaction chemistry. The loss of the high binding energy feature can be attributed to both desorption of molecular vinyl chloride and C-Cl bond cleavage to form the reaction intermediate presumed to be a surface vinyl group. The C 1s binding energy of 283.3 eV for the surface reaction intermediate indicates that it is bound to surface Cr cations rather than O anions following C-Cl bond cleavage since C 1s binding energies for oxygenated carbons (ex., alkoxides, carboxylates, carbonates) typically fall at binding energies of 286 eV or greater [41,56]. Heating to 600 K removes the majority of the surface carbon, consistent with the evolution of carbon-containing reaction products in this temperature range in thermal desorption. In contrast to the post reaction AES results, a small amount of surface C remains after heating to 600 K. This difference is thought to be due to some minor amount of decomposition associated with exposure to the high flux of synchrotron radiation (350 eV) and the low energy electrons (0.5 eV) from the flood gun used for charge neutralization.

The Cl 2p spectra shown in Figure 8b exhibit a similar trend to the C 1s data. Multiple Cl species are observed following the dose, and high binding energy features are lost as a result of heating. The Cl 2p spectrum collected at the dosing temperature, 130 K, shows three distinct peaks characteristic of a minimum of two sets of overlapping and partially resolved doublets with Cl $2p_{3/2}$ features at about 200.7 eV and 198.5 eV. Heating to temperatures up to 300 K results in a decrease and eventual loss of the high binding energy features, and leaves a single Cl 2p doublet with a Cl $2p_{3/2}$ feature at 198.4

eV. Similar to the assignment for C 1s, the high binding energy features are attributed to Cl in molecular vinyl chloride, with the low binding energy features attributed to Cl surface reaction products. This low binding energy Cl 2p doublet (Cl $2p_{3/2}$ at 198.4 eV) is characteristic of metal chlorides [41,57], and is assigned to Cl adatoms bound at surface Cr sites. Heating to 600 K does not remove the Cl adatoms, consistent with the lack of Cl containing reaction products in thermal desorption. These XPS observations support earlier suggestions that halogen adatoms cap the coordinately unsaturated Cr sites on the stoichiometric surface [1,25], and indicate that the loss of surface reactivity with the build up of surface Cl shown in Figure 6 is due to site blocking of active Cr^{3+} sites by Cl.

The observation of C 1s and Cl 2p features associated Cl adatoms and intact C-Cl bonds in molecular vinyl chloride following the dose indicates a mixed monolayer of molecularly intact vinyl chloride, hydrocarbon surface fragments, and Cl adatoms upon dosing at 130 K. Areas of the two Cl 2p doublets determined from curve fits (not shown) using FitXPS software [42], suggest that approximately half of the vinyl chloride that adsorbs at 130 K dissociates via C-Cl bond cleavage. The activation barrier (if any) to C-Cl bond cleavage is therefore thought to be small.

2.2.3 near edge x-ray absorption fine structure

C 1s NEXAFS spectra were obtained at normal and grazing incidences, 0° and 75° off the surface normal, respectively. For normal incidence the polarization vector of the light is parallel to the surface, and for grazing incidence the polarization vector is 75° off the surface normal such that the largest component is parallel to the surface normal. C 1s$\rightarrow\pi^*$ transitions are expected in the photon energy range from about 284.0-288.0 eV

[8,39,43] when there is a species containing an intact π-system on the surface and the polarization vector of the light has a non-zero projection on p-orbitals in the π-system. Resonances for C 1s transitions corresponding to carbon sigma bonds, such as C $1s \rightarrow \sigma^*_{(C-C)}$ and C $1s \rightarrow \sigma^*_{(C-H)}$, should appear at higher photon energies in the range of about 288.0-305.0 eV [8,39].

Raw spectra of the clean surface over the range of 275-320 eV were obtained to use for background removal from the spectra for adsorbed vinyl chloride. An example background spectrum for the clean surface for normal incidence light is shown in Figure 9a. The two large features observed at 288.6 and 292.6 are Cr 2p resonances arising from second order light off the monochromator at two times the indicated photon energies. For comparison, the raw spectrum collected following a 20 L vinyl chloride dose at 130 K is also shown in Figure 9a. The small features at 284.6 and 285.5 eV are assigned to C $1s \rightarrow \pi^*$ transitions. Because of the high concentration of Cr in the sample, the signal from the small fraction of second order light is much larger than the C 1s NEXAFS. In principle, these contributions can be removed by taking the ratio ($I_{signal}/I_{background}$) with a background spectrum, but in practice we have found that the details of the resulting spectrum in the range of photon energies from 288-296 eV are strongly dependent on small details of the alignment and relative intensities of the spectra. Hence, while the sharp C $1s \rightarrow \pi^*$ transitions can be readily observed and used to provide an indication of the presence of a π system in the adsorbate, most of information from the σ* transitions is lost. Note that the overlap of the Cr 2p resonances with the carbon π* resonances is minimized because of the higher binding energy of Cr^{3+} in Cr_2O_3 relative to chromium metal.

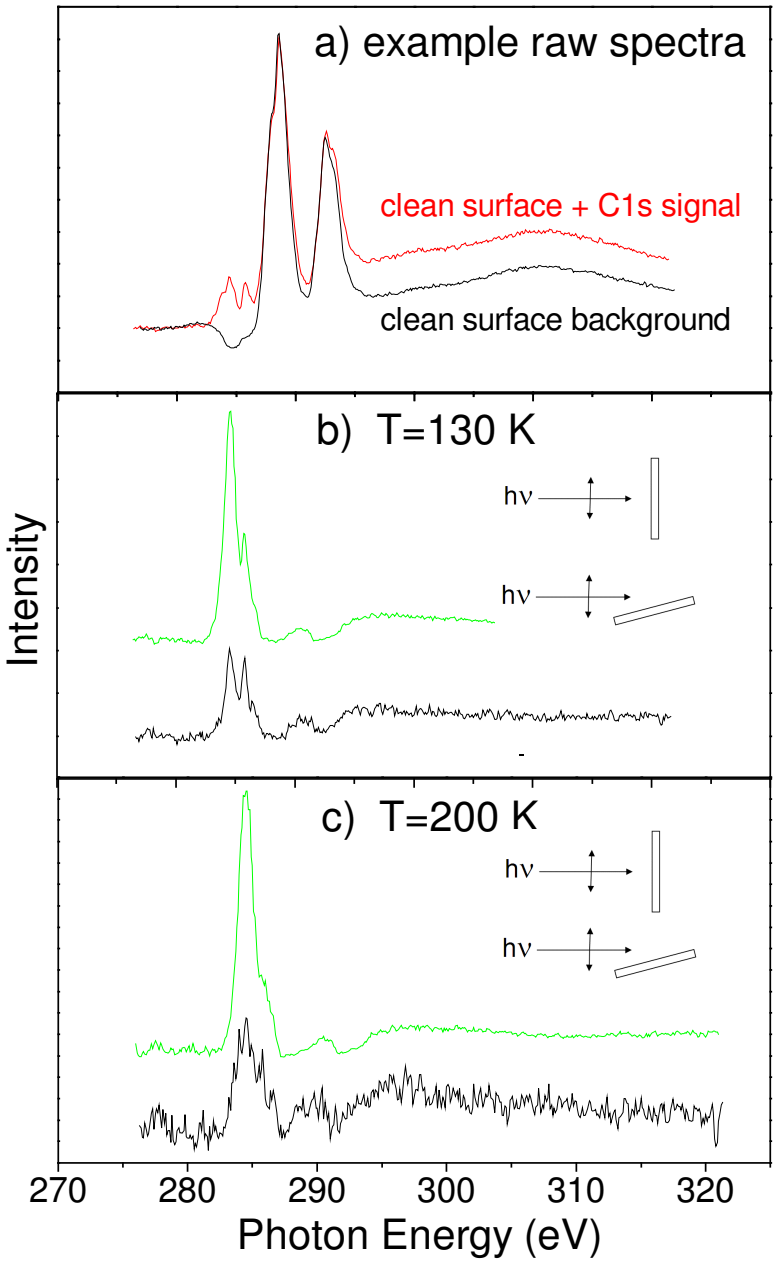

Figure 9. a) Background spectrum (black) and C1s spectrum (red) collected at 130 K with normal incidence light. The features at 288.6 and 292.6 eV are a result of Cr2p absorption of second order light, and these features have some overlap with C1s transitions (~274.5 – 293 eV). b) C1s NEXAFS spectra collected at 130 K after a ~20L dose of vinyl chloride taken at normal, upper plot, and grazing, lower plot, incidences. The two transitions are assigned to C1s→π* transitions characteristic of adsorbed vinyl chloride [8]. c) C1s NEXAFS spectra collected after dosing ~20 L of vinyl chloride and heating the sample to 200 K. The upper spectrum, collected at normal incidence, shows predominantly one peak at 284.7 eV associated with surface vinyl groups [8]. Comparison of the upper and lower, collected at grazing incidence, spectra indicates that the species remaining on the surface are predominantly surface vinyl groups oriented with their molecular plane perpendicular to the surface.

Figure 9b shows NEXAFS spectra for both grazing and normal incidence following a 20 L dose at 130 K. The Cr resonances have been removed from the raw data by division with corresponding background spectra. Two sharp C 1s→π* resonances are seen at photon energies of 284.5 and 285.7 eV. The π* feature at higher photon energies is associated with the chlorinated carbon in molecular vinyl chloride, consistent with the higher binding energy C 1s feature seen in photoemission and similar to NEXAFS spectra reported for multilayer vinyl chloride on Cu (100) [39]. In the mixed monolayer following adsorption at 130 K, spectra most characteristic of molecular vinyl chloride (i.e., two π* resonances of nearly equal intensity) are seen for grazing incidence light, while the dominant contribution for normal incidence is the lower photon energy π* resonance for non chlorinated carbon [39]. These data suggest the molecular species are bound nominally parallel to the surface since the π* resonances should be largest for a polarization vector perpendicular to the molecular plane [43].

Heating the sample to 200 K yields the spectra shown in Figure 9c. For both polarizations the C 1s→π* transition at 285.5 eV decreases, indicating the loss of intact C-Cl bonds by C-Cl bond cleavage or desorption of molecularly intact vinyl chloride. This interpretation is consistent with the photoemission data which indicates that most of the C-Cl bonds are broken after heating to 200 K. The remaining C 1s→π* transition at 284.6 eV is similar to the reported spectrum for surface vinyl on Cu (100) [8], and serves as a fingerprint for surface vinyl groups while unambiguously demonstrating the presence of an intact π system in the surface intermediate responsible for observed reaction chemistry. Additionally, since the intensity of the C1s→π* transition is largest for normal incidence and smallest at grazing incidence, the polarization dependence of the

spectrum indicates the vinyl groups are orientated with the molecular plane nominally perpendicular to the surface. Taken together, the NEXAFS and XPS data clearly indicate that surface vinyl groups are formed from vinyl chloride by C-Cl bond cleavage, in agreement with the proposed vinyl-mediated reaction mechanism suggested from the thermal desorption data.

2.3 Discussion

The thermally induced reaction of vinyl chloride on α-Cr_2O_3 $(10\bar{1}2)$ proceeds through C-Cl bond cleavage resulting in surface Cl adatoms and surface vinyl groups. Thermal desorption and spectroscopic data are consistent with a vinyl mediated reaction pathway involving vinyl coupling to 1,3-butadiene, and a rate limiting hydride elimination for the production of acetylene, ethylene and dihydrogen. The lack of combustion products (CO, CO_2, H_2O) indicates that the stoichiometric surface is nonreducible, and that 3-coordinated surface lattice oxygen is not consumed in the reaction.

Surprisingly, post reaction AES analysis indicates vinyl groups react cleanly with no significant decomposition to surface C (coke) over α-Cr_2O_3 $(10\bar{1}2)$ under the conditions of this study. Hence, it appears that surface vinyl groups are not a major intermediate in coke production, at least not on this simple chromia surface where the available cation and anions sites expose a single coordination vacancy.

Surface Cl adatoms have a measurable impact on the kinetics, activity, and selectivity of the reaction. The temperature for acetylene production increases by 50 K for successive 0.1 L doses, indicating stabilization of vinyl fragments and an increase in the activation barrier to vinyl dehydrogenation of about 15 kJ/mol due to the presence of

Cl adatom modifiers. The dominant effect of surface Cl on activity is to decrease the overall surface reactivity by simple site blocking of the coordinately unsaturated Cr^{3+} reaction sites available on the clean, stoichiometric surface. The production of acetylene and ethylene decreases monotonically with increasing Cl adatom coverage due to site blocking. However, for successive 0.1 L doses the yield of the coupling product 1,3-butadiene goes through a maximum for a pre-dose Cl coverage between 2/3 and 3/4 ML.

The variations in selectivity to 1,3-butadiene are likely the result of several competing factors. Since the primary reaction sites are isolated cations with a single coordination vacancy, butadiene production is thought to involve an activated vinyl migration (surface diffusion) between adjacent cation sites for coupling in parallel with the vinyl dehydrogenation pathway. Since vinyl groups are stabilized by Cl adatoms, the initial increase in butadiene production may be the result of enhanced surface diffusion as the activation barrier to the vinyl dehydrogenation increases. For higher Cl coverages, butadiene production rolls over presumably because the deposited halogen impacts the mobility of vinyl groups by cation site blocking.

2.4 Conclusions

α-Cr_2O_3 $(10\bar{1}2)$ readily cleaves the C-Cl bond in vinyl chloride at 130 K to deposit Cl adatoms and surface vinyl groups. Acetylene, ethylene, butadiene, and dihydrogen are the only gas phase reaction products, and originate from a common surface vinyl intermediate. All gas phase products can be attributed to simple set of elementary reactions including vinyl dehydrogenation to acetylene, hydrogenation to ethylene, and coupling to 1,3-butadiene. Cl adatoms affect selectivity as evidenced by a

maximum in butadiene production at an intermediate surface Cl coverage. Cl deposition affects the surface reactivity by stabilizing vinyl groups, increasing surface diffusion barriers, and by capping active Cr sites which eventually shuts down the surface reactions.

Chapter 3

Thermal Desorption and Spectroscopic Characterization of Acetylene on Nearly Stoichiometric α-Cr_2O_3 ($10\bar{1}2$)

3.1 Introduction

Acetylene is the major product in the reaction of vinyl groups on the α-Cr_2O_3 ($10\bar{1}2$) surface. Due to the abundance of acetylene from vinyl dehydrogenation, it is important to understand the behavior of adsorbed acetylene, including any possible reactions and its desorption kinetics, on this surface. The adsorption of acetylene on well-defined metal surfaces has been extensively studied. On most metal surfaces, vibrational and x-ray absorption spectroscopies show that adsorbed acetylene rehybridizes from an sp configuration to an sp^2 or sp^3 configuration [58-63]. Acetylene rehybridizes to an sp^3 configuration on Co(0001) by forming a tetra-σ-bond with the surface [58]. It has been reported that acetylene adsorbed on Si(001) undergoes rehybridization to form a di-σ-bonded species (sp^2-hybridized) with the molecular plane nearly perpendicular to the surface [60,61]. Ormerod *et al.* found that acetylene undergoes a hydrogen shift upon room temperature adsorption on Pd(111) to form sp^2-hybridized vinylidene [63]. Photoelectron diffraction was used by Woodruff *et. al.* to show that the acetylene C-C bond elongates upon adsorption on Ni(111) indicating rehybridization, however no suggestions regarding C-surface bonds were made [64]. Molecular orbital theoretical studies show that for acetylene adsorption on Cu (110) [65] and Pt(111) [66] there is C-C bond lengthening and C-H bond bending; these results imply di-σ-bonding and formation of an ethylene-like adsorbate with the molecular plane

near perpendicular to the surface. However, NEXAFS spectra collected following acetylene adsorption on Cu(100) and Ag(100) show that there is only a weak surface/acetylene interaction and little or no rehybridization occurs, leaving acetylene in a weakly π-bonded (sp-hybridized) state [67].

There is not much literature regarding adsorption of acetylene on metal oxides. Photoemission and nuclear magnetic resonance measurements on rough and nano-sized MgO shows that acetylene forms acetylides [68,69]. Vohs and Barteau also examined the adsorption of acetylene on the (0001)-Zn polar surface of ZnO with ultraviolet photoelectron spectroscopy and found that acetylene adsorbs dissociatively at 300 K to form acetylide [70]. Infrared spectroscopy of adsorbed acetylene on several metal oxide powders show that physisorbed acetylene and acetylides are the predominant species at 293 K [71].

A non-reducible metal oxide surface, nearly stoichiometric α-Cr_2O_3 ($10\bar{1}2$), has been shown, under ultrahigh vacuum (UHV) conditions, to decompose vinyl, vinyl halide, and vinylidene surface fragments to acetylene [1]. Acetylene is the major product in the vinylic reactions on this surface, and surprisingly, no surface carbon is observed following dehydrogenation or dehalogenation reactions, Chapter 2. It has also been seen that acetylene adsorbs and desorbs without reaction from nearly stoichiometric α-Cr_2O_3 ($10\bar{1}2$), leaving no surface carbon, and creating no oxygenated (CO_x) products [1]. It has been proposed that acetylene binds to surface Cr cations in a simple π-bound molecular configuration on this surface in UHV [1], however no spectroscopic evidence to support this proposal has been offered.

Possible acetylene binding configurations on this surface are shown in Figure 10. Given the isolated nature of the surface cations on α-Cr_2O_3 $(10\bar{1}2)$ with cation nearest neighbor separations of ~3.5 Å, π-bonded, di-σ-bonded, or vinylidene species involving single Cr^{3+} surface cations appear to be the most likely possibilities for molecular acetylene adsorption.

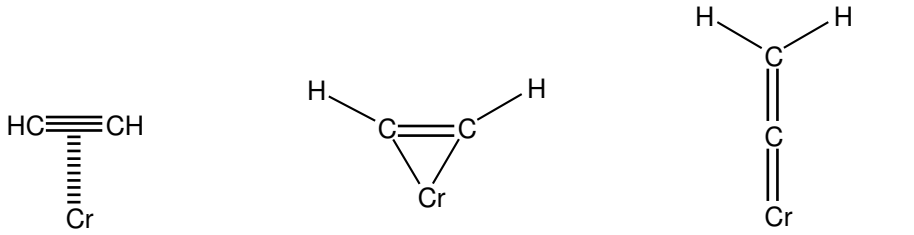

π-bonding –
molecularly intact

di-σ-bonding –
molecularly intact

vinylidene –
acetylene isomer

Figure 10. Possible acetylene binding modes to a single Cr site

3.2 Results

3.2.1 thermal desorption of C_2H_2

The thermal desorption traces following exposures of acetylene to the clean, nearly stoichiometric α-Cr_2O_3 ($10\bar{1}2$) surface at 120 K are shown in Figure 11. The inset in Figure 11 shows a magnification of the thermal desorption data for small exposures (0.01-0.04 L) of acetylene. Acetylene is the only desorbing species observed following adsorption of acetylene at 120 K regardless of the dose size, no dihydrogen was detected above the background level in the UHV chamber. Desorbing acetylene was positively identified through comparison of thermal desorption peak intensities with the mass spectrometer cracking pattern of gas phase acetylene. No surface reaction products, including carbon, are observed with AES or XPS (laboratory Mg anode).

A thermal desorption feature, initially centered at 420 K for a 0.01 L dose, shifts to 320 K for a 0.1 L dose, and remains at 320 K for increasing acetylene exposures up to 0.1 L. This temperature range corresponds to an apparent first-order activation energy for desorption which decreases from 109 kJ/mol (420 K) to 83 kJ/mol (320 K), as estimated by the Redhead method [54] assuming a normal pre-exponential factor of 10^{13} s^{-1}. An acetylene exposure of 0.3 L results in saturation of the high temperature feature (320 K), and the formation of a second desorption peak centered at 250 K. The two sets of features above 200 K are associated with more strongly bound acetylene, and will be referred to as a "chemisorbed" species. For all dose sizes, features below 200 K are also observed, and increase in intensity and shift down in temperature with increasing dose size. The features below 200 K are associated with desorption of more weakly bound

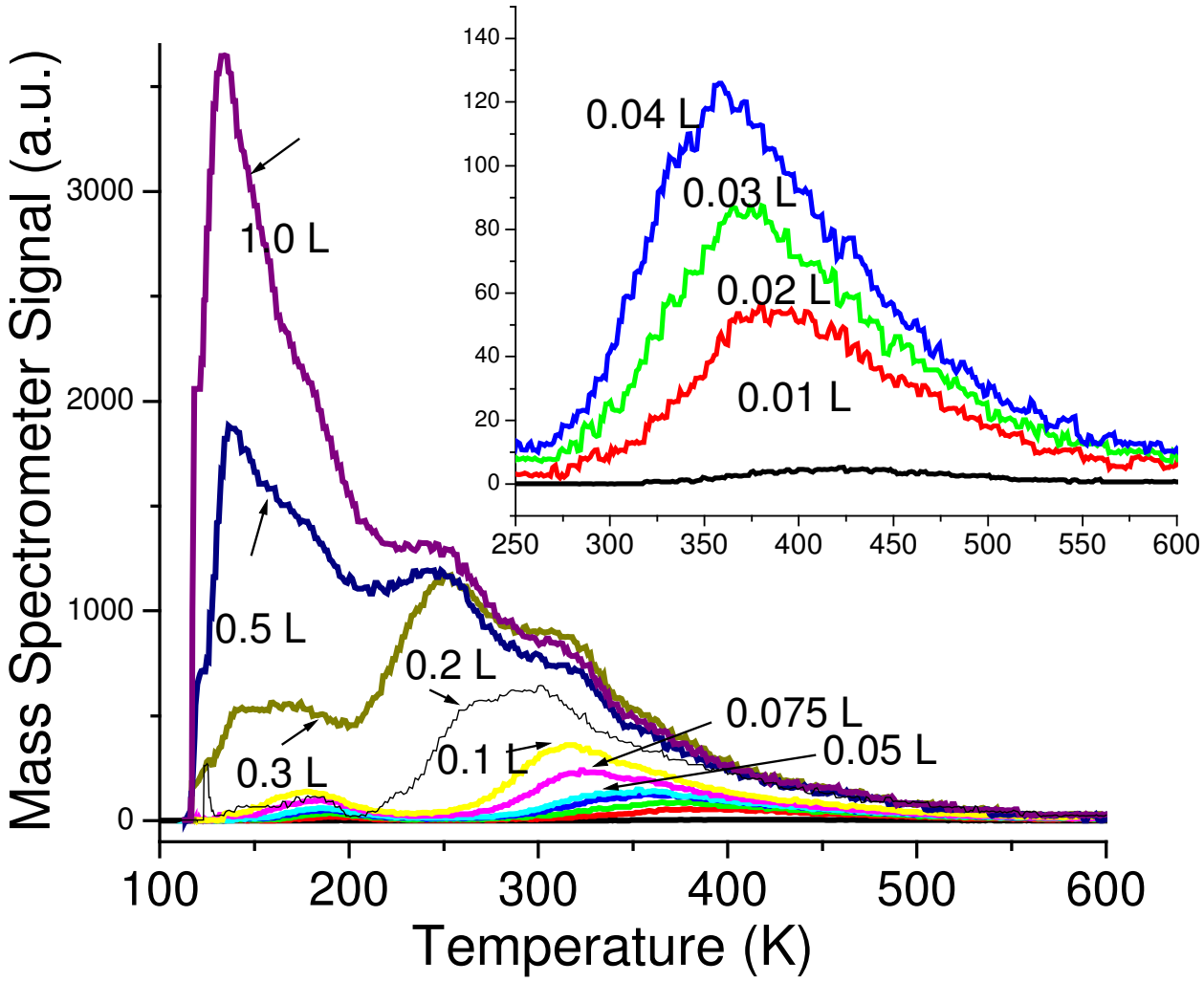

Figure 11. Thermal desorption traces ranging from 0.01 to 1.0 L adsorption on a clean surface show acetylene desorption trends. The inset shows magnified desorption traces of low dose sizes (0.01-0.04 L).

acetylene, and will be referred to as a "physisorbed" species. The physisorbed acetylene features become pronounced for acetylene exposures greater than 0.5 L, and give a peak desorption temperature of 135 K for a 1.0 L dose. The apparent first-order activation barrier for the 135 K acetylene desorption feature is 34 kJ/mol [54]. The integrated area of the desorption features associated with physisorbed acetylene (in the range of 120-200 K) for a 1.0 L dose accounts for approximately ~50% of the total acetylene coverage.

3.2.2 photoemission and NEXAFS characterization of adsorbed acetylene

Figure 12 shows the C 1s photoemission spectrum (hν=350 eV) collected following a ~200 L dose on clean surface at 115 K. The lack of attenuation of the Cr 3p signal following adsorption (not shown) indicates a saturation (rather than multilayer) coverage of acetylene at this temperature. The sample was heated to the temperatures designated in Figure 12, held for ~30 seconds, and allowed to cool. The C 1s spectrum collected following the dose at 115 K is fit well with two peaks centered at 285.5 and 283.8 eV with a full width at half maximum (FWHM) of 1.9 eV [42]. Heating to 250 K results in a decrease in the amount of carbon on the surface seen mostly as a decrease in the high binding energy feature.

The C 1s high binding energy feature (285.5 eV) observed at 115 K is associated with the physisorbed acetylene seen in thermal desorption at temperatures below 200 K. The assignment of the high binding energy feature is made partly due to the decrease in intensity of this feature above the 135 K desorption temperature (associated with weakly bound acetylene in thermal desorption) and partly due to the assignment of NEXAFS

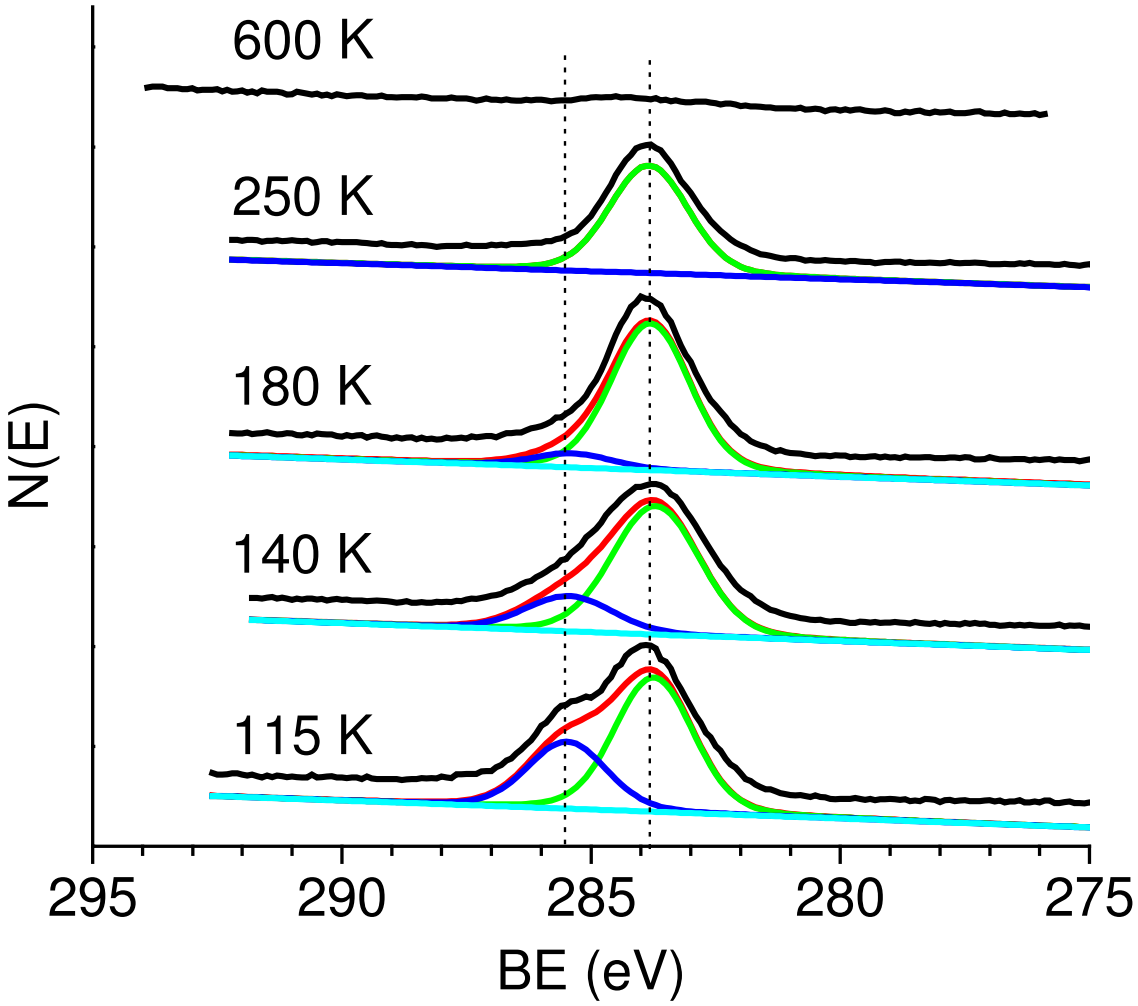

Figure 12. C 1s photoemission spectra were collected with using hν=350 eV, and referenced to a Cr2p$_{3/2}$ peak at 576.9 eV. Peak fits shown were calculated using FitXPS, all fits retain a FWHM=1.9 eV [42]. The first spectrum collected at 115 K following a ~200 L dose of acetylene shows two features at 285.5 eV (multilayer and π-bonded acetylene) and 283.8 eV (di-σ-bonded acetylene). At 250 K there is a single C 1s feature attributed to di-σ-bonded acetylene remaining on the surface after multilayer desorption.

features described below. The low binding energy feature at 283.8 eV is associated with chemisorbed acetylene that is present on the surface until at least 250 K. The low binding energy C 1s feature at 283.8 eV is consistent with acetylene bound to metal centers; carbon atoms associated with surface oxygen, in the form of alkoxides, carboxylates, or carbonates would exhibit C 1s binding energies in excess of 286 eV [41,56]. Heating to 250 K results in the removal of ~47% of the carbon observed in the C 1s spectrum collected at 115 K, as determined from C 1s peak areas. After heating to 600 K, ~4% of the initial amount of carbon seen at 115 K remains on the surface. Since no surface carbon was observed by AES or XPS (with Mg anode) following thermal desorption experiments, the residual carbon observed in the photoemission experiment is attributed to irradiation of adsorbed acetylene by synchrotron light and/or bombardment with low energy electrons.

NEXAFS spectra collected at grazing incidence, 75° from the surface normal, are shown in Figure 13. Following the initial ~200 L dose at 115 K, the primary features observed between ~284-288 eV fall in the range for C1s$\rightarrow\pi^*$ transitions [43]. Following acetylene adsorption at 115 K, a sharp peak is observed at 285.9 eV with broadening toward lower photon energy and a shoulder at ~285 eV. The peak at 285.9 eV is consistent with carbon atoms present in an sp-hybridization [72], and is attributed to the physisorbed acetylene that desorbs at low temperatures in TDS. Heating the surface to 250 K results in a decrease in the overall intensity of the transitions (consistent with desorption of physisorbed acetylene), and a broadening of the feature with the shoulder emerging as a second peak at 284.9 eV. The poorly resolved C1s$\rightarrow\pi^*$ features (FWHM=2.6 eV) are representative of having both sp (285.9 eV) [72] and sp^2 (284.9 eV)

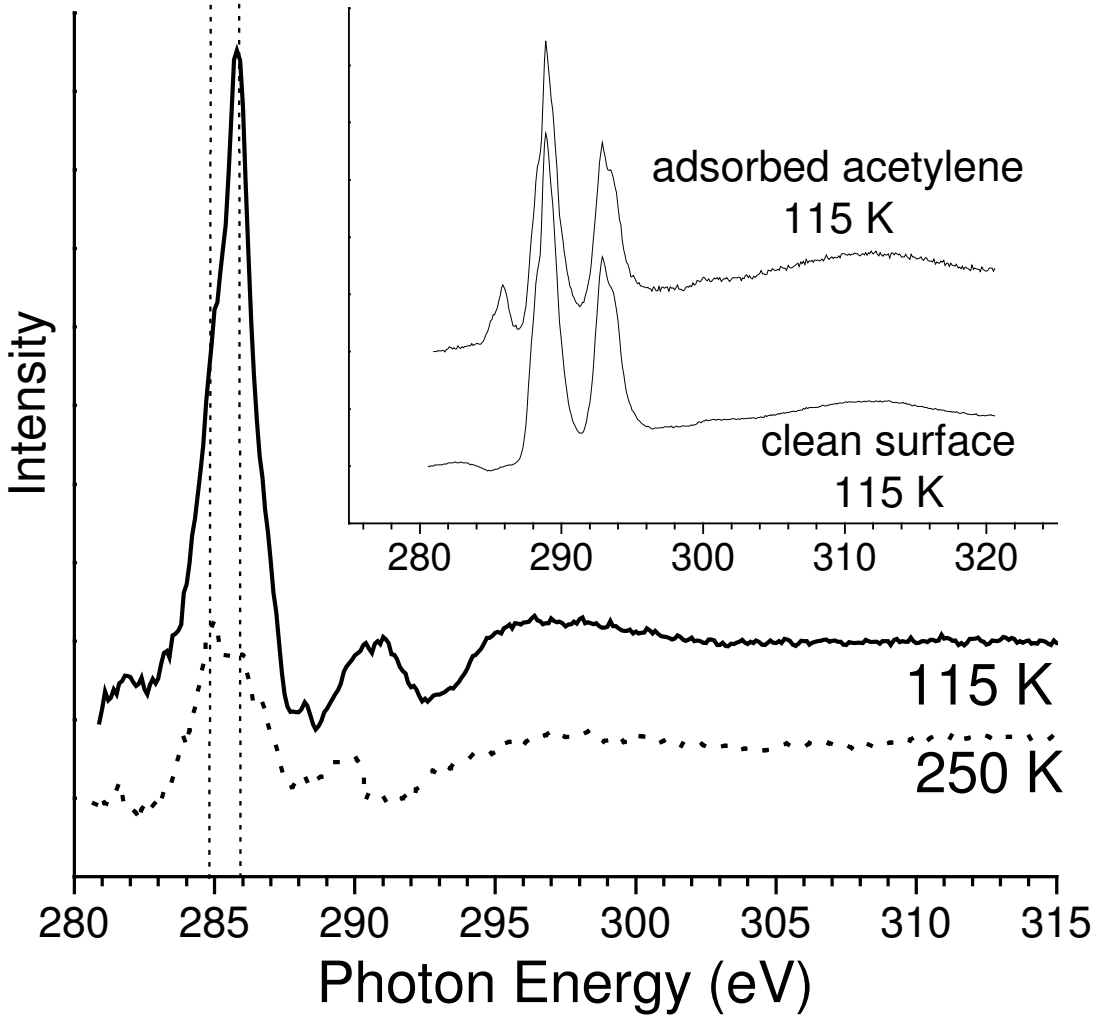

Figure 13. **NEXAFS spectra in the inset depict the Cr 2p spectral features arising from 2nd order synchrotron light in both raw data and data collected following ~200L dose of acetylene. The figure itself shows the C K-edge spectra collected at grazing incidence following the ~200L exposure to acetylene, the clean surface background has been divided out of the raw data. The sharp feature collected at 115 K is slightly skewed toward higher photon energy with a peak at 285.9 eV. Heating the surface to 250 K desorbs some acetylene and resolution of a peak at 284.9 eV.**

[73] hybridized carbon attributed to π-bonded and di-σ-bonded acetylene, respectively. Using this same experimental set-up, well separated, sharp C1s→π* transitions for adsorbates on this surface have been reported as having FWHM=0.7 eV (Section 5.2.2.2), which are significantly narrower than the peak observed after heating to 250 K. The sp^2-hybridized carbon is believed to be di-σ-bonded acetylene and not vinylidene because acetylene desorbs at a temperature (420 K) below that required for acetylene formation from the rate-limiting isomerization of vinylidene to acetylene (460 K) observed in other experiments with 1,1-dihaloethylenes, discussed in Chapter 4 [1]. For π-bonded acetylene (sp-hybridization) with the molecular plane parallel to the surface, no significant dependence of the intensity on the polar angle of the incident light is expected due to the cylindrical symmetry of the π system. For di-σ-bonded acetylene (sp^2-hybridization) with the molecular plane perpendicular (or nearly so) to the surface (Figure 10) and the π system nominally parallel to the surface [59], it is expected that C1s→π* transitions would give a greater intensity for normal incident light. Acetylides are not considered to be likely adsorbates because they tend to decompose [70] and should, therefore, produce surface carbon and dihydrogen; neither of these products are observed in significant amounts.

The inset in Figure 13 shows raw data collected from both a clean α-Cr_2O_3 $(10\bar{1}2)$ surface, and following a ~200 L dose of acetylene at 115 K. The two large features at 288.9 and 289.4 eV are Cr 2p background resonances resulting from absorbance of second order synchrotron light, and these features must be divided out of the raw data for interpretation of C1s transitions. Corrections for the Cr 2p resonances are strongly

dependent on small details of alignment and relative intensities of the background spectrum, and impact the shape of the spectrum in the range of ~288-296 eV. As a result, no assignments or interpretations are offered for features in this range of photon energies. Spectra were also collected with normal (0° from surface normal) and off angle (45° from surface normal) incidence light, however, the interference from the Cr 2p resonances is larger in comparison to carbon K-edge transitions at these angles, and at low acetylene coverages (250 K annealing temperatures), resulting in poor signal-to-noise following background removal.

3.3 Discussion

For low acetylene coverages, the decreasing desorption temperature with increasing acetylene coverage could be an indication of either repulsive interactions between adsorbed acetylene molecules or surface heterogeneity (steps, edges, point defects) which gives rise to a small number of sites that bind acetylene more strongly than terraces. The small (~4%) carbon on the surface following the synchrotron photoemission experiments is attributed to the activation of a minor amount of adsorbed acetylene by synchrotron radiation, likely arising at a small fraction of defect sites. For higher coverages of acetylene (doses greater than 0.2 L), the presence of two features (250 K and 320 K) is well-modeled by a first order desorption of acetylene (2.5 K/s heating rate) experiencing repulsive pairwise interactions of approximately –4 kJ/mol [74] with an activation energy of ~83 kJ/mol. The absence of any observable surface reactions in the thermal desorption experiments to deposit surface carbon or generate other gas phase products is an indication that even in the chemisorbed state the acetylene-surface interaction is not strong enough to activate C-H or C-C bond cleavage to any significant extent. It is

apparent in NEXAFS spectra that chemisorbed acetylene, remaining on the surface at 250 K, consists of a mixture of both strongly bound π- and di-σ-bonded acetylene at Cr^{3+} sites on the surface.

The physisorbed acetylene desorbs at 200 K and below, and accounts for approximately half the coverage for a ~1.0 L dose. The large sp contribution observed in NEXAFS for the physisorbed species suggests a nominally unperturbed adsorbate. The different (higher) binding energy observed for the physisorbed species suggests a significantly different binding configuration than that attributed to the π-bonded chemisorbed species. Infrared studies of acetylene on oxide powders suggest that physisorbed species can be bound via hydrogen bonding to basic O^{2-} surface oxygen anion sites [71]. Given the equivalent number of exposed, coordinately unsaturated cation and anion sites on the ideal, stoichiometric α-Cr_2O_3 $(10\bar{1}2)$ surface, a similar binding configuration may be associated with the physisorbed species observed in this study.

3.4 Conclusions

Acetylene adsorbs in both "physisorbed" and "chemisorbed" states at 115 K on the clean, nearly stoichiometric α-Cr_2O_3 $(10\bar{1}2)$ surface. Physisorbed acetylene is characterized as having a low desorption temperature (~140 K) and sp-hybridization. For higher temperatures and/or smaller exposures, chemisorbed acetylene is the predominant surface species. Chemisorbed acetylene is adsorbed on the surface as a mixture of both sp- and sp^2-hybridized configurations (as seen in NEXAFS) corresponding to π- and di-σ-bonded acetylene, respectively.

Chapter 4

A comparative study on the reactions of 1,1-dichloroethylene and 1-chloro-1-fluoroethylene on stoichiometric α-Cr_2O_3 ($10\bar{1}2$)

4.1 Introduction

Understanding how acetylene is formed from surface vinyl groups, Chapter 2, is the next step in this work due to the high selectivity to acetylene from vinyl groups. The second tier of experiments, discussed here and in Chapter 5, were conducted to consider the effects of cleaving C-substituent bonds on acetylene formation. This study was carried out to examine the reactivity of surface vinylidene, by cleaving C-substituent bonds on the same carbon atom, on the well-ordered.α-Cr_2O_3 ($10\bar{1}2$) single crystal surface.

Since C-H bonds in alkanes and alkenes are not activated readily at low temperatures in ultrahigh vacuum (UHV) over α-Cr_2O_3 ($10\bar{1}2$), previous work has made use of halogenated compounds to produce hydrocarbon fragments [1,25,29,32]. Thermal desorption studies of the reaction of 1-chloro-1-fluoroethylene on this surface show that acetylene is the only gas phase reaction product [1]. Two acetylene desorption features are observed, and attributed to two separate kinetic pathways which produce desorption and reaction limited acetylene. The reaction is thought to proceed through the following sequence [1]: (1) C-Cl bond cleavage to surface α-fluorovinyl, (2) α-fluorine elimination to vinylidene, and (3) vinylidene isomerization to acetylene as shown in Figure 14. The rate-limiting step for the production of reaction-limited acetylene was

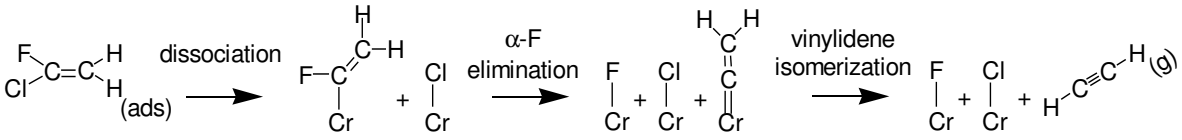

Figure 14. Proposed reaction pathway for acetylene production from 1-chloro-1-fluoroethene [1].

proposed to be vinylidene isomerization [1]. However, no spectroscopic evidence was available to justify this proposal, and the kinetic data were insufficient to distinguish between α-fluorine elimination and vinylidene isomerization in the rate limiting step.

This study focuses on a kinetic and spectroscopic comparison of the reactions of 1,1-dichloroethylene (CCl_2=CH_2) and 1-chloro-1-fluoroethylene (CFCl=CH_2) to identify the most likely rate-limiting step in the formation of reaction-limited acetylene from 1,1-dihalogenated ethylenes. Since the C-Cl bonds are the weakest in these molecules, sequential C-X bond breaking should yield differently-substituted α-halovinyl groups: α-chlorovinyl from CCl_2=CH_2 and α-fluorovinyl from CFCl=CH_2 (as shown in scheme 1). As the strength of C-F bonds are generally greater than those of C-Cl bonds, a rate limiting step involving α-halogen elimination from α-halovinyl species should occur at higher temperatures in thermal desorption for an α-fluorovinyl intermediate than for an α-chlorovinyl intermediate.

4.2 Results

4.2.1 reactions of 1,1-dihaloethylenes

Thermal desorption traces are shown in Figure 15 for the adsorption at 110 K and thermal activation of a series of consecutive 0.05 L exposures of 1,1-dichloroethylene on an initially clean, nearly stoichiometric α-Cr_2O_3 ($10\bar{1}2$) surface. Desorption of the 1,1-dichloroethylene reactant, Figure 15 (top), occurs at 340 K. The fragmentation patterns for 1,1- and 1,2-dichloroethylene can be distinguished by the contributions of the m/z 14

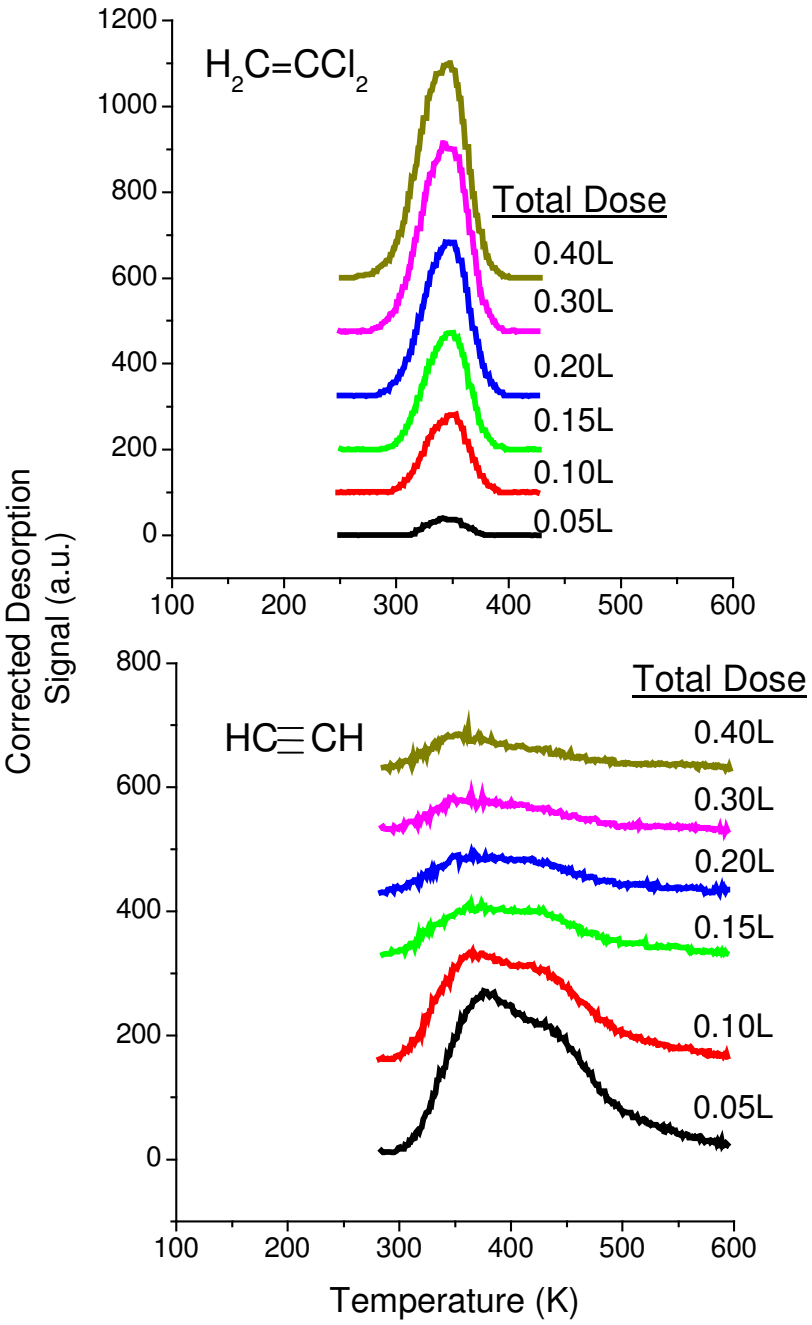

Figure 15. Thermal desorption spectra collected following a series of 0.05 L exposures of 1,1-dichloroethylene to a clean α-Cr_2O_3 ($10\bar{1}2$) surface are shown. The top panel shows desorption of consecutive 0.05 L doses of 1,1-dichloroethylene; the bottom panel shows variation in acetylene (HC≡CH) desorption following consecutive 0.05 L doses of 1,1-dichloroethylene. Desorption signals have been corrected with mass spectrometer sensitivity signals.

(CH_2^+) and m/z 48 ($CHCl^+$) signals, respectively. The mass fragmentation pattern of the desorbing species in Figure 15 (top) (m/z=61,48,14) match that for 1,1-dichloroethylene, indicating that no isomerization of the reactant occurs. While the desorption temperature remains constant with each successive 0.05 L exposure of 1,1-dichloroethylene, the intensity of the CCl_2=CH_2 desorption feature increases.

Acetylene is the only gas phase product formed in the surface reaction of 1,1-dichloroethylene. The acetylene desorption trace for the first 0.05 L dose in Figure 15 (bottom) has two features, a peak at 380 K and a shoulder at ~420 K. Consecutive thermal desorption cycles result in a decrease of acetylene production, and the 380 K feature shifts slightly to lower temperatures with each cycle, down to about 350 K following the sixth 0.05 L dose. There is no apparent change in desorption temperature for the shoulder near 420 K, suggesting a first-order rate limiting process. Comparison of the relative intensities of the two thermal desorption features suggests that ratio of low temperature to high temperature acetylene decreases for the first few doses (up to about 0.15 L total exposure), then increases slightly for subsequent doses.

The integrated desorption peak areas, Figure 16, show an increase in the amount of 1,1-dichloroethylene desorption and decrease in acetylene production with each successive small dose indicating that the consecutive exposures and thermal desorption cycles result in an alteration of the surface which shuts down the chemistry and causes the conversion of 1,1-dichloroethylene to decrease with each successive dose. Post reaction AES analysis indicates that Cl adatoms build up on the surface as a result of the reaction of1,1-dichloroethylene, but AES gives no indication of a build up of residual surface carbon associated with coke formation.

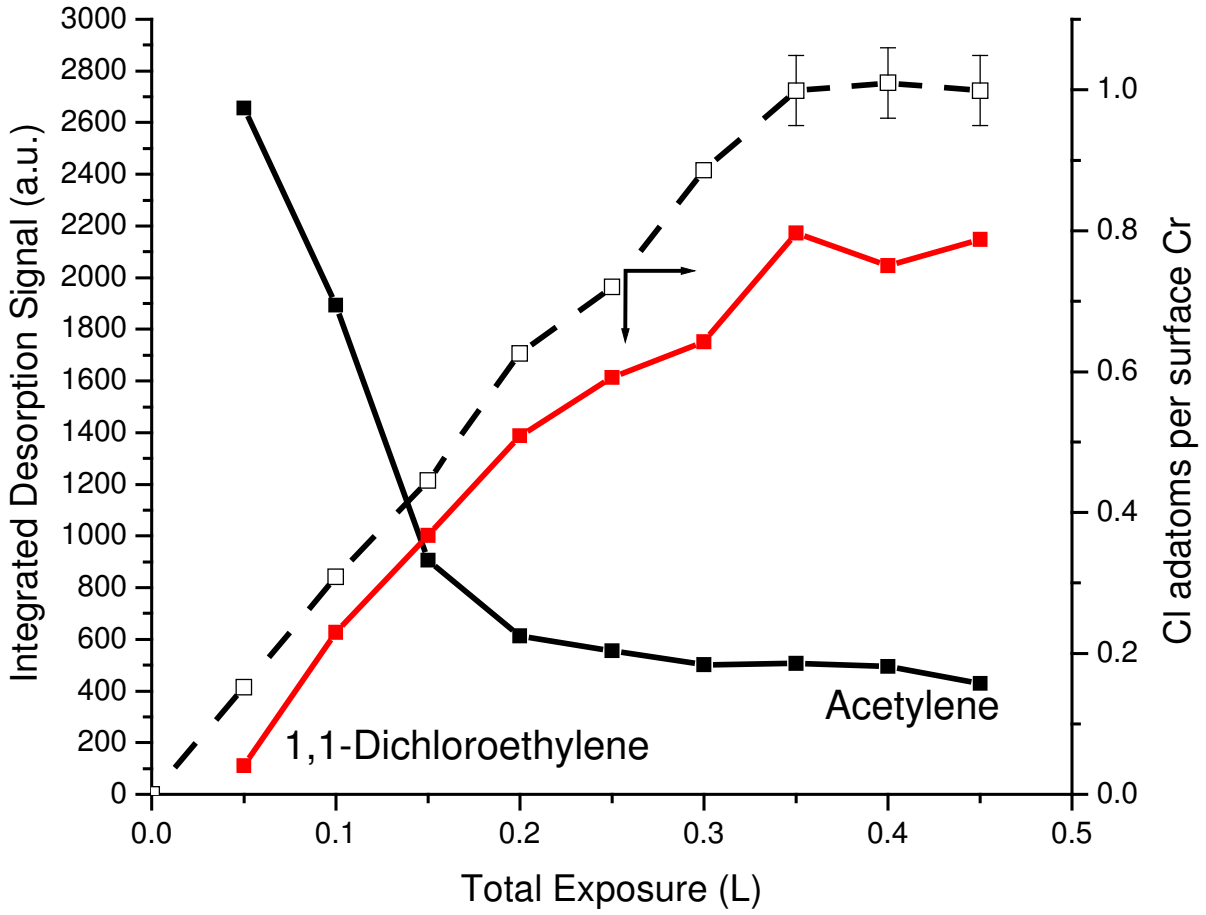

Figure 16. Changes in relative amounts of 1,1-dichloroethylene and acetylene in thermal desorption for consecutive 0.05 L exposures of 1,1-dichloroethylene (left axis), compared to the change in the Cl coverage in adatoms per surface Cr cation (dashed line, right axis). The error bars (± 0.5) on the Cl coverage indicate the variability in the measurements due to the small signal-to-noise ratio associated with the short electron beam exposures (see experimental section for details).

Figure 16 provides a comparison of the build up of surface Cl to the changes in the amounts of desorbing acetylene product and 1,1-dichloroethylene reactant. Post reaction AES analysis was performed following each successive 0.05 L dose and thermal desorption cycle. Previous work suggests that Cl (halogen) adatoms bind at the coordinately unsaturated Cr^{3+} surface sites, and that an AES Cl/Cr ratio of 0.32 corresponds to a Cl coverage equivalent to about one Cl adatom per surface Cr cation [1,36]. Figure 16 indicates that the increase in the amount of desorbing 1,1-dichloroethylene (i.e., the decreased conversion and the loss of activity) is directly related to the build up of Cl adatoms (right hand axis). The production of acetylene decreases from the initial value by about 85% as the Cl coverage approaches one adatom per surface cation. Hence, the shut down in the surface chemistry is attributed to site blocking of the surface cations by Cl adatoms which cap the single coordination vacancy of the five coordinate Cr cations present on the clean, stoichiometric surface [1,25].

The acetylene desorption traces shown in Figure 15 (bottom) give evidence of acetylene desorption at two different temperatures, indicating that at least two different kinetic pathways exist for the formation of acetylene from 1,1-dichloroethylene. Figure 17 shows a comparison of acetylene desorption from a clean or partially halogenated surface from three separate sources: (1) a 0.05 L dose of 1,1-dichloroethylene, (2) a 0.05 L dose of and 1-chloro-1-fluoroethylene, and (3) desorption of a 0.02 L dose of molecularly adsorbed acetylene on an initially clean surface. It is clear from Figure 17 that the low temperature (380 K) acetylene desorption feature from both 1,1-dichloroethylene and 1-chloro-1-fluoroethylene results from the desorption of molecularly bound acetylene (i.e., a desorption limited feature). By comparison, the

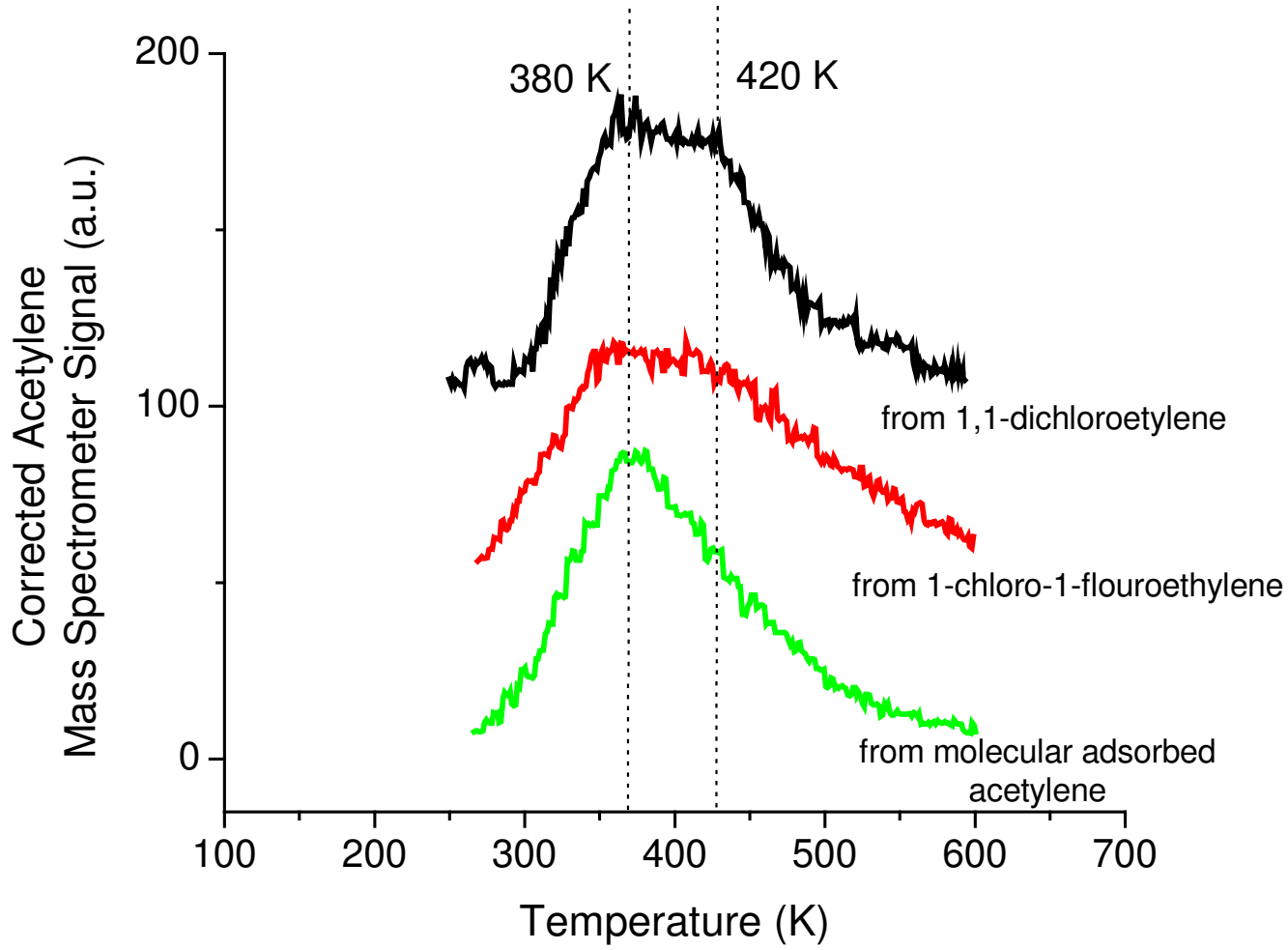

Figure 17. The acetylene desorption signals resulting from the reaction of 1,1-dichloroethylene, 1-chloro-1-fluoroethylene and from desorption of molecularly adsorbed acetylene show that the low temperature feature for acetylene from the reactants is due to desorption of molecularly adsorbed acetylene.

higher-temperature acetylene feature at 420 K is associated with the rate-limiting reaction of a surface species to form acetylene.

For the low temperature, desorption limited acetylene product feature in Figure 15 (bottom), the desorption temperature decreases continuously with successive dose, decreasing by about 30 K following the sixth consecutive dose. The decrease in the desorption temperature corresponds to a decrease in the activation energy for desorption of ~8 kJ/mol, as calculated by the Redhead method assuming a normal first order pre-exponential factor of 10^{13} s^{-1} [54]. The decreased binding of molecular acetylene is attributed to surface modification by chlorine adatoms deposited as a result of the reaction of 1,1-dichloroethylene.

For the higher temperature reaction limited acetylene desorption features, the similarity in temperature in Figure 17 for the two different 1,1-dihaloethylene reactants argues in favor of a rate limiting step involving vinylidene isomerization. For a reaction sequence involving consecutive halogen bond breaking, the two reactants should give rise to α-chlorovinyl and α-fluorovinyl from 1,1-dichloroethylene and 1-chloro-1-fluoroethylene, respectively. Since C-F bonds are expected to be stronger than C-Cl bonds [1,25], a difference in the activation barrier to reaction (and hence the temperature in thermal desorption) would be expected for a rate limiting step involving α-halogen elimination from an α-halovinyl species. Deposited halogen has no apparent impact on the activation barrier of the reaction-limited process.

It is noted that there are small deviations in the desorption temperatures reported here for 1-chloro-1-fluoroethylene and those in an earlier report [1]. The temperature discrepancies are attributed to small variations in the quality of the thermocouple contact

and variations in the uniformity of heating of the large sample in contact with the metallic holder.

4.2.2 surface intermediate characterization

4.2.2.1 photoemission of adsorbed 1,1-dichloroethylene

Figure 18 shows the photoemission spectra (hν = 350 eV) collected following a ~200 L dose of 1,1-dichloroethylene at 115 K on a clean surface, along with the effects of heating to consecutively higher temperatures. For the temperatures listed in Figure 18, the sample was heated then allowed to cool before the spectra were collected. The attenuation of the Cr 3p feature following adsorption (not shown) suggests a multilayer thickness of ~7 Å based on a mean-free-path for the dichloroethylene layer estimated from the NIST Electron Inelastic-Mean-Free-Path Database [75].

The C 1s spectrum, Figure 18 (top), collected following adsorption at 115 K shows two well-resolved features at binding energies of 287.1 and 284.3 eV. Each of the two features are fit well by peaks with a full-width at half maximum (FWHM) of 1.9 eV [42], consistent with the FWHM of a single carbon species by comparison to photoemission spectra for molecularly adsorbed acetylene on this surface, Section 4.2. At 115 K, a primary contribution from the molecular 1,1-dichloroethylene layer is expected, suggesting an assignment for the low binding energy feature (284.3 eV) to the nonchlorinated methylene carbon in 1,1-dichloroethylene, and the high binding energy feature (287.1 eV) to the doubly chlorinated carbon (ΔBE=2.8 eV). The assignment of binding energies is consistent with findings for nonchlorinated and dichlorinated carbon atoms in carbon black [76]. Heating to 150 K, above the 1,1-dichloroethylene multilayer

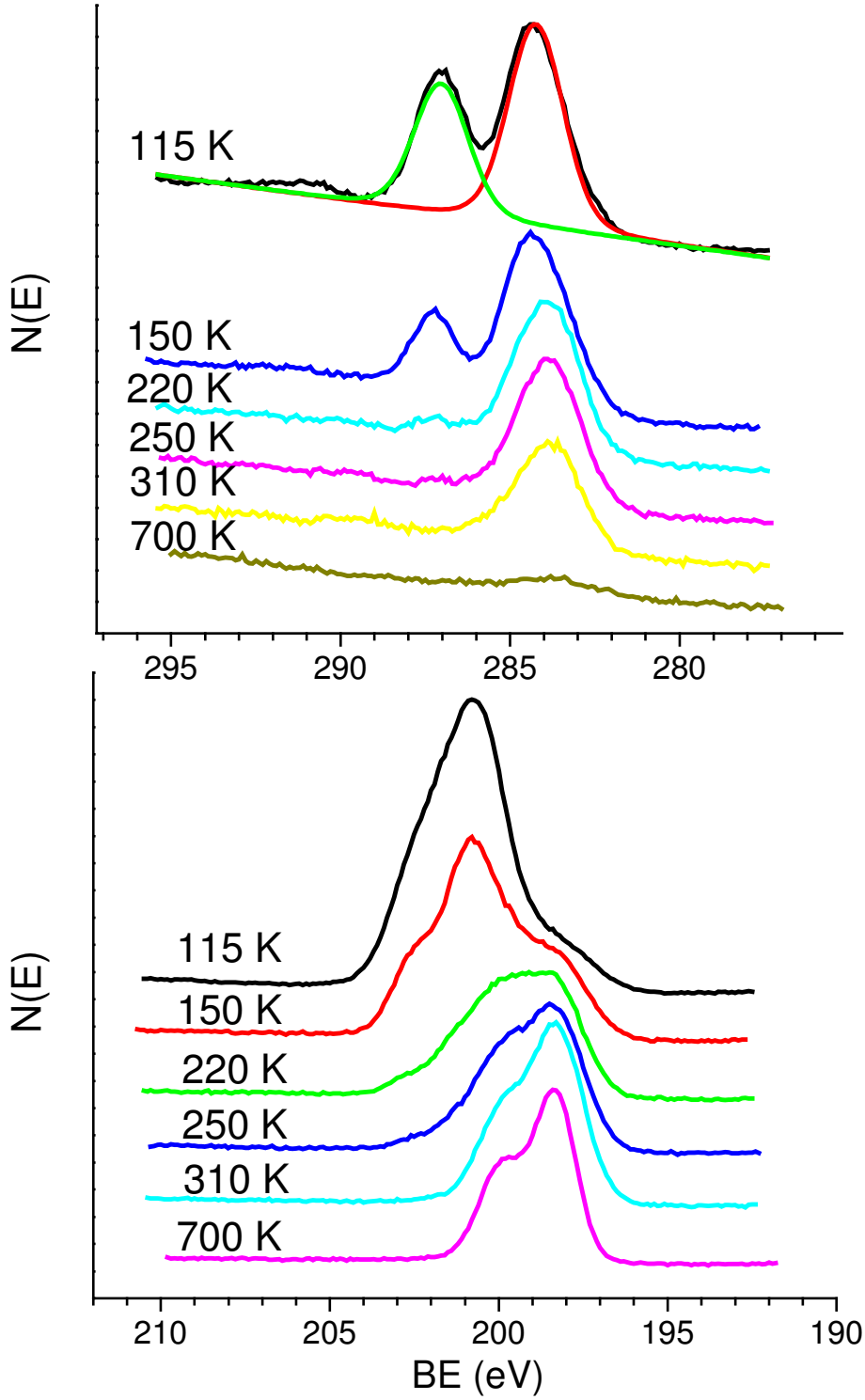

Figure 18. C 1s (top) and Cl 2p (bottom) spectra were collected using 350 eV excitation following a ~200 L exposure of 1,1-dichloroethylene to an initially clean α-Cr_2O_3 ($10\bar{1}2$) surface. The temperatures indicate the annealing temperature following the dose.

desorption temperature, results in a decrease in both C 1s features. By 220 K, only a low binding energy feature remains at 283.9 eV with a FWHM of 2.3 eV. This single feature remains following heating to 250 and 310 K, below the temperature for acetylene and 1,1-dichloroethylene evolution observed in thermal desorption. While this feature is broadened somewhat compared to the 1.9 eV FWHM expected for a single carbon species, for the temperatures investigated there is no clear indication of a feature near 285.9 eV characteristic of singly-chlorinated carbon, discussed in Chapter 5. Hence, the low binding energy feature at 283.9 eV is characteristic of completely dechlorinated carbon species. Since C 1s binding energies for alkoxides and carbonates species are expected at 286.4 eV or higher [56], it is clear that the surface intermediates do not include C-O σ bonds. The 283.9 eV binding energy is similar to that observed for chemisorbed acetylene (Section 4.2), and is likely associated with a combination of molecularly adsorbed acetylene (consistent with the desorption limited product observed in thermal desorption) and a vinylidene reaction intermediate bound to Cr sites and associated with the formation of reaction-limited acetylene. If consecutive C-Cl bond cleavage does occurs, it likely happens between 150 K and 220 K.

The C 1s spectrum collected for 700 K shows a small amount of carbonaceous species remaining on the surface. Since no carbon is observed with AES following thermal desorption, the small amount of residual carbon seen in photoemission is attributed to the exposure to high-intensity synchrotron radiation and the low energy electrons used for charge compensation.

The Cl 2p spectra, Figure 18 (bottom), provide complimentary information to the C 1s data. At the resolution of the photoemission measurements, the Cl 2p doublet can be

partially resolved. Upon adsorption at 115 K, an asymmetric feature is observed with a maximum at a binding energy of 200.8 eV and shoulders apparent to higher (~202.5 eV) and lower (~198.3 eV) binding energies. While there is clearly a minimum of two separate chemical states for surface Cl, the spectrum is dominated by a high binding energy contribution consistent with intact C-Cl bonds (Cl $2p_{3/2}$ BE near 201 eV [41,57]) in molecular 1,1-dichloroethylene, and a lower binding energy contribution associated with Cl adatoms formed by C-Cl bond cleavage. Heating to 150 K, above the 1,1-dichloroethylene multilayer desorption temperature, causes a decrease in the intensity of the high binding energy contribution, and an increase in the relative intensity of the low binding energy contribution. By 250 K, the low binding energy features predominate. The Cl $2p_{3/2}$ binding energy of 198.3 eV observed for the partially resolved doublet at temperatures of 250 K and above is characteristic of metal chlorides [41,57], and indicates that the Cl adatom reaction products bind at surface Cr cations sites, consistent with earlier assertions [1,36].

4.2.2.2 NEXAFS of adsorbed 1,1-dichloroethylene

C 1s NEXAFS spectra collected following the same 200 L dose of 1,1-dichloroethylene at 115 K used for photoemission is shown in Figure 19. All spectra are for grazing incidence light 70° off the surface normal. Following adsorption at 115 K, two sharp resonances are observed at 284.5 and 287.0 eV, both with a FWHM of ~0.7 eV. These peaks fall in an energy range consistent with C1s$\rightarrow \pi^*$ transitions. The low photon energy feature is assigned to the methylene carbon and the high photon energy feature is assigned to the doubly-chlorinated carbon in molecularly adsorbed 1,1-

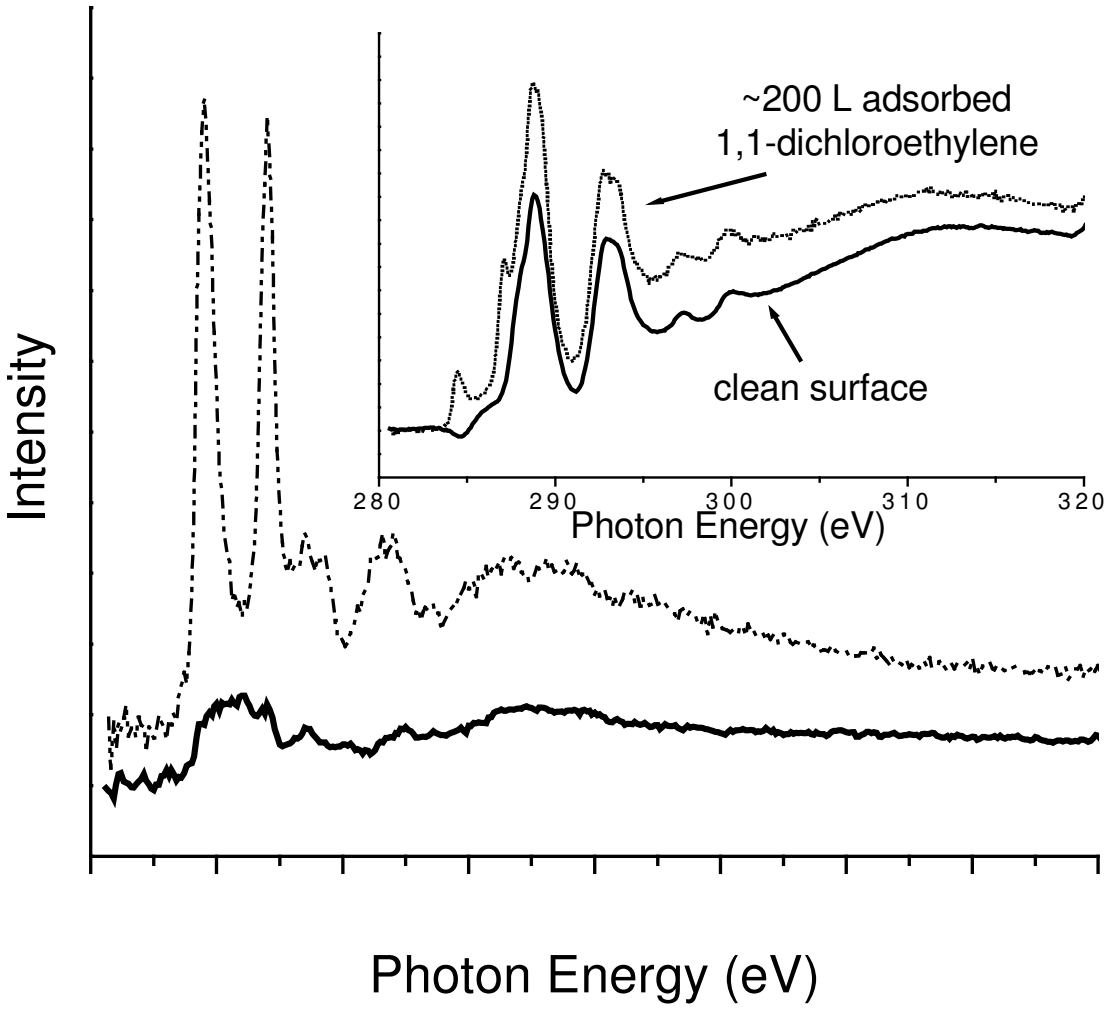

Figure 19. NEXAFS spectra collected at grazing incidence at the C K-edge show that upon adsorption of 1,1-dichloroethylene at 115 K there are two clear peaks in the C1s→π* transition range. Heating to 250 K results in a sharp decrease in transition intensity and a broadening of the features. The inset shows C K-edge spectra collected from a clean surface and a surface following ~200 L exposure to 1,1-dichloroethylene (adsorbed 1,1-dichloroethylene). The two large features present in both spectra are Cr 2p resonances associated with 2nd order light from the monochrometer.

dichloroethylene by comparison to NEXAFS results for molecular chloroethylenes on Pt (111) [77] and Cu (100) [39]. The energy difference in these features is consistent with the binding energy differences observed in photoemission.

Upon heating to 250 K (Figure 19) with removal of the multilayer, a broad (FWHM=3.0 eV) resonance centered at 285.9 eV is observed. The broad feature at 285.9 eV overlaps a range of photon energies associated primarily with C1s$\rightarrow \pi^*$ transitions, and indicate surface species with intact π systems. The broad feature observed at 250 K is much lower in intensity indicating a majority of the surface species desorb between 115 K and 250 K. C1s$\rightarrow\pi^*$ transitions for sp^2-hybridized carbon are expected near 284.8 eV, and transitions for sp-hybridized carbon occur at 285.9 eV [72,73]. Unfortunately, the broad feature observed in NEXAFS at 250 K does not allow clear distinction between adsorbed acetylene (sp-hybridized) and surface vinylidene (sp^2-hybridized), but the FWHM of the feature is such that the signal is consistent, though not definitive, with the presence of both vinylidene and molecular acetylene.

As described elsewhere [78], spectral features in the range of photon energies from 288 to 296 eV typically associated with C1s$\rightarrow\sigma^*$ transitions overlap with strong Cr 2p resonances due to second order light from the monochrometer (see inset in Figure 19). Corrections for the Cr 2p resonances are strongly dependent on small details of alignment and relative intensities of the background spectrum. Because of the inherent variability of the features in this range, no assignments or interpretations are offered. Spectra were also collected with normal (0° from surface normal) and off angle (45° from surface normal) incidence light, however, the interference from the Cr 2p resonances is larger at these angles.

4.2.2.3 photoemission of adsorbed 1-chloro-1-fluoroethylene

While the reaction of 1-chloro-1-fluoroethylene was examined previously [1], no spectroscopic characterization of the surface species was provided. Photoemission results for the adsorption and reaction of $CFCl=CH_2$ are shown in Figure 20 for a saturation dose at 120 K on a clean, stoichiometric surface. The sample was dosed with $CFCl=CH_2$, then heated to sequentially higher temperatures and allowed to cool prior to photoemission measurements. C 1s (top) and Cl 2p (center) spectra were collected using a photon energy of 350 eV, while those for F 1s (bottom) use 750 eV photons. For all three core levels, there is evidence of both high and low binding energy features. Heating the sample eventually removes the high binding energy feature in all spectra indicating that these features are associated with molecularly intact 1-chloro-1-fluoroethylene. This behavior is similar to that observed in the C 1s and Cl 2p photoemission features observed for 1,1-dichloroethylene.

Following adsorption at 120 K, the C1s spectrum, Figure 20 (top), shows two broad, asymmetric peaks: one near 289 eV associated with halogenated carbon, and one near 285 eV associated with nonhalogenated carbon. Heating to 180 K [1] removes nearly all of the high binding energy feature associated with molecularly intact 1-chloro-1-fluoroethylene, as seen with 1,1-dichloroethylene (above). The asymmetry of the broad, low binding energy feature increases and, given the 3.1 eV FWHM, is characteristic of carbon atoms in two different chemical environments, with binding energies of approximately 285.9 and 284.1 eV. The contribution at 285.9 eV is near that expected for a singly halogenated carbon, shown in Chapter 5, and is consistent with

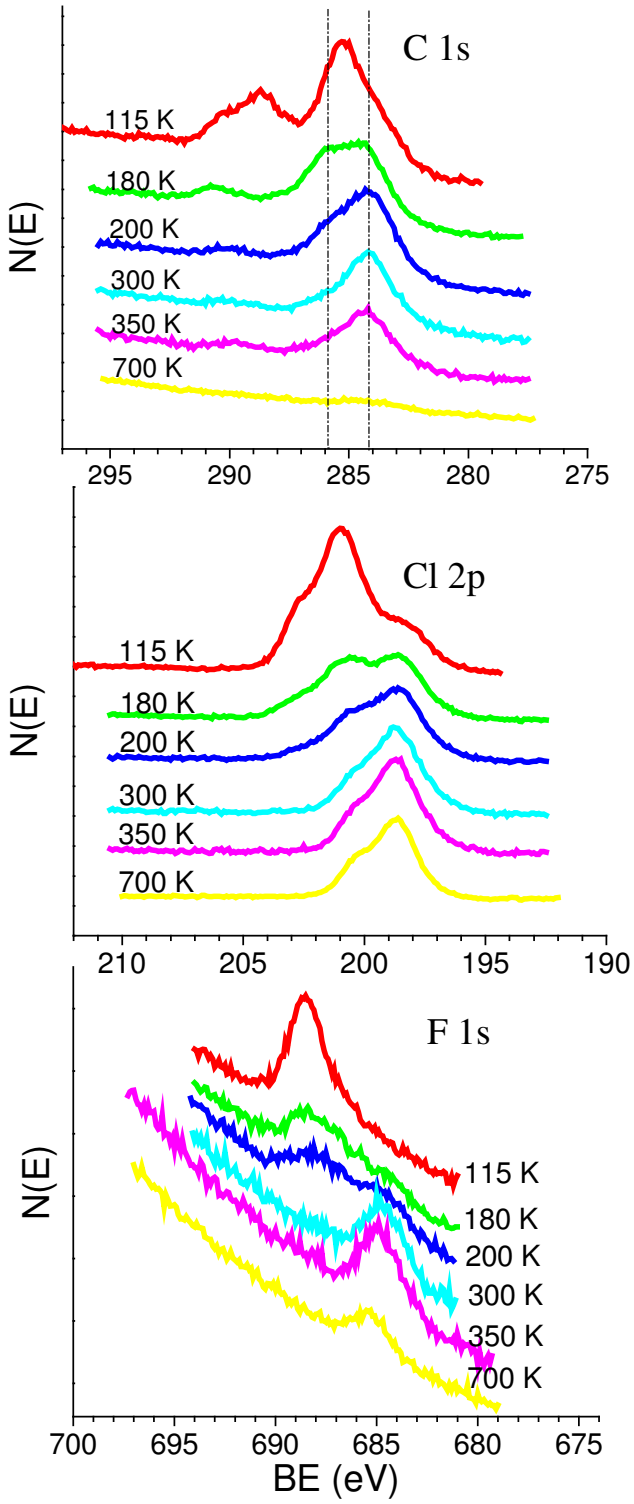

Figure 20. C 1s, Cl 2p, and F 1s spectra were collected following a saturation exposure of 1-chloro-1-fluoroethylene an initially clean surface to at 115 K. The C 1s (top) and Cl 2p (middle) spectra were collected using a 350 eV photon energy, and the F 1s (bottom) spectra were collected using a 750 eV photon energy. The temperatures indicate the annealing temperature following the dose.

some degree of sequential C-X bond breaking. The contribution at 284.1 is consistent with the binding energy attributed to methylene carbon for 1,1-dichloroethylene (above). Continued heating to 300 K reduces the contribution at 285.9 eV, leaving a feature at 284.1 eV with a FWHM of 2.8 eV. Similar to the observations above for 1,1-dichloroethylene, this feature is likely associated with a combination of molecularly adsorbed acetylene (consistent with the desorption limited product in thermal desorption) and a vinylidene reaction intermediate associated with the formation of reaction-limited acetylene and formed by dehalogenation of 1-chloro-1-fluoroethylene.

The Cl 2p spectra for 1-chloro-1-fluoroethylene, Figure 20 (center), show similar trends to the Cl 2p spectra for 1,1-dichloroethylene. The Cl 2p spectra collected following adsorption of 1-chloro-1-fluoroethylene at 120 K suggest two Cl species are present on the surface. As with 1,1-dichloroethylene, the high binding energy Cl $2p_{3/2}$ peak at 201.0 eV is assigned to intact C-Cl bonds in molecularly adsorbed 1-chloro-1-fluoroethylene, and Cl $2p_{3/2}$ at 198.7 eV assigned to Cl adatoms bound to surface Cr cations [1,36,41,57]. Heating to 200 K gives a dominant contribution due to Cl adatoms, and after heating to 300 K there is no real evidence of intact C-Cl bonds.

Figure 20 (bottom) depicts the F 1s spectra. Upon adsorption of 1-chloro-1-fluoroethylene at 120 K, a single feature is seen centered at 688.5 eV and is associated with intact C-F [79] bonds in molecularly adsorbed 1-chloro-1-fluoroethylene. Hence, it appears that some C-Cl bonds are broken at 120 K on adsorption (above), but the C-F bonds remain intact. Spectra collected after heating to 180 K and 200 K show a decrease in the feature at 688.5 eV and appearance of a lower binding energy feature at 684.8 eV. The lower binding energy feature appears at temperatures analogous to the temperatures

at which C 1s spectra are dominated by a single feature and has a binding energy consistent with metal fluorides [41,57], indicating that F adatom reaction products bind at surface Cr cations, as suggested previously [1]. Since the halogen photoemission spectra show primarily Cl adatoms after heating to 200 K, but with nearly equal contributions of C-F and F adatoms, the spectra suggest some degree of consecutive dehalogenation and the formation of surface α-fluorovinyl enroute to acetylene. Spectra collected after heating the surface to 300 K and above indicate that most of the C-F bonds have broken. It is noted that the earlier identification of surface fluorine reaction products by AES was hampered by the electron stimulated desorption of fluorine [1]. XPS provides an unequivocal identification of the halogen adatom reaction products.

4.3 Discussion

As observed previously for 1-chloro-1-fluoroethylene [1], the reaction of 1,1-dichloroethylene to form acetylene as the only gas phase product occurs via two kinetic pathways, resulting in desorption and reaction limited acetylene. For the reaction limited (420 K) acetylene, the apparent first order activation energy is estimated to be 110 kJ/mol assuming a first order pre-exponential factor of 10^{13} s^{-1} [54]. The activation barrier for the evolution of desorption limited acetylene occurs at the same temperature for both reactants, but for both the activation barrier for desorption decreases as the surface is increasingly halogenated [1]. These trends are consistent with data for the desorption of dosed acetylene on clean, Section 3.2.1, and partially chlorinated surfaces, not shown. Overall for both reactants, the production of acetylene decreases with consecutive small dose and the build up of surface halogen, demonstrating that the drop in activity is associated with the buildup of halogen adatoms. Given that halogen adatoms bind at

surface cation sites, the deactivation is attributed to simple site blocking of the active Cr^{3+} sites by halogen.

The observation that reaction limited acetylene evolves at the same temperature from both reactants indicates the involvement of the same surface reaction intermediate from both reactants. For 1,1-dichloroethylene, photoemission indicates complete dechlorination above 250 K, with no indication of sequential C-Cl bond breaking. NEXAFS indicates the presence of multiple π-bonding environments consistent with vinylidene and molecularly adsorbed acetylene. For 1-chloro-1-fluoroethylene, photoemission suggests a fraction of the adsorbate undergoes sequential C-Cl and C-F bond breaking, characteristic of an α-fluorovinyl intermediate enroute to vinylidene. However, given that heating to 300 K gives photoemission spectra characteristic of complete dehalogenation, it is clear that the α-fluorovinyl intermediate is kinetically unimportant and decomposes to vinylidene prior to the evolution of reaction limited acetylene at 420 K. The data are consistent with a rate limiting step of vinylidene isomerization in the production of reaction limited acetylene.

The origin of the two different kinetic pathways to acetylene is unclear. Changes in surface reactivity arising from halogenation have been shown to have a number of effects besides simple deactivation due to site blocking. In the earlier study of the reaction of 1-chloro-1-fluoroethylene, it was seen that the deposition of chlorine and fluorine adatoms increased the contribution of desorption limited acetylene relative to reaction limited acetylene, suggesting that surface halogen can decrease the overall activation barrier to acetylene formation [1]. For vinyl fragments, increased surface chlorine coverage appears to increase the activation barrier to vinyl dehydrogenation to acetylene, and

maximizes the selectivity for C-C bond formation (coupling to 1,3-butadiene) for Cl coverages near about ¾ ML, Section 2.2.1. In these two cases, one can imagine a modification of the electronic properties of the surface ensemble (and consequently a change in the activation barrier to reaction) by increasing coverages of halogen on neighboring cation sites. In the present case for 1,1-dichloroethylene, the relative contributions of desorption limited to reaction limited acetylene appears to first decrease, then increases with Cl coverage, suggesting no simple relationship between the two kinetic channels and Cl coverage. It is possible that surface heterogeneity in the form of step edges or terraces could account for the different reaction pathways, with more reactive step edges contributing to the formation of low temperature desorption limited acetylene production. It is clear, however, that regardless of the full details of the reaction pathway enroute to desorption limited acetylene, complete dehalogenation must occur, suggesting the likelihood of a process involving vinylidene isomerization even for the desorption limited acetylene reaction channel.

Finally, thermal desorption shows that 1,1-dichloroethylene is the only chlorinated species desorbing species and no 1,2-dichloroethylenes desorb. The photoemission and thermal desorption data for 1,1-dichloroethylene clearly show that desorption of the reactant is a result of vinylidene recombination with surface chlorine adatoms.

4.4 Conclusion

The reactions of 1, 1-dichloroethylene and 1-chloro-1-fluoroethylene over α-Cr_2O_3 $(10\bar{1}2)$ give acetylene as the only gas phase product. Acetylene production from both reactants is comprised of desorption limited (molecularly adsorbed) acetylene and reaction limited acetylene. Similarities in reaction-limited acetylene adsorption energies

for both 1,1-dichloroethylene and 1-chloro-1-fluoroethylene, in conjunction with XPS data, indicate that the rate-limiting step for evolution of reaction limited acetylene is vinylidene isomerization. XPS gives no clear indication of sequential C-Cl bond cleavage for 1,1-dichloroethylene, however it is clear that sequential C-X bond cleavage occurs to some degree for the reaction of 1-chloro-1-fluoroethylene, giving an α-fluorovinyl intermediate enroute to surface vinylidene. Regardless, for both reactants it is apparent that all C-X bonds are broken below the acetylene desorption temperature indicating that vinylidene isomerization is the rate limiting step in both cases. Furthermore, it was validated with F 1s photoemission spectra that F adatoms are deposited on the surface in the reaction of 1-chloro-1-fluoroethylene.

Chapter 5

Comparing Cis- and Trans-1,2-Dichloroethylene: Effects of Different Isomers on Reactivity

5.1 Introduction

Many studies focusing on the reactions of surface intermediates derived from halohydrocarbons have been conducted on metal surfaces [8,10,39,80]; however, not much research involving hydrocarbon fragments on metal-oxide single crystals has been reported. It has been shown previously that adsorbing halogenated hydrocarbons on the α-Cr_2O_3 $(10\bar{1}2)$ single crystal surface in UHV results in the formation of halogen adatoms and hydrocarbon fragments that participate in surface reactions [25]. Adsorbing vinyl chloride on the α-Cr_2O_3 $(10\bar{1}2)$ single crystal surface results in the formation of vinyl fragments (-CH=CH_2) that participate in several thermally activated surface reactions. Acetylene is the major product from the reaction of vinyl groups on this surface, Chapter 2.

The production of acetylene from surface vinyl groups may proceed through two general reaction pathways: α-hydrogen elimination to form vinylidene which can isomerize to acetylene (Chapter 4), or β-hydrogen elimination to directly produce adsorbed acetylene. Chlorine labeling of vinyl groups is used to study the effect of the placement of C-Cl bond on selectivity and reactivity toward acetylene formation from chlorovinyl groups. Acetylene is produced at 460 K through a vinylidene intermediate in the reaction of 1,1-dichloroethylene, possibly through the formation of an α-chlorovinyl group, Chapter 4. Using 1,2-dichloroethylenes should allow the formation of β-

chlorovinyl groups if sequential C-Cl bond cleavage occurs. It is possible that different isomers of β-chlorovinyl, that is "cis"-β-chlorovinyl and "trans"-β-chlorovinyl (Figure 21), could form depending on whether cis-1,2- dichloroethylene (cis-DCE) or trans-1,2-dichloroethylene (trans-DCE) is used as a reactant. The cis- and trans-β-chlorovinyl group geometries (cis and trans with respect to the surface) have been reported for dissociative adsorption of the respective 1,2-dichloroethylenes on many well defined surfaces [38,39,81]. Zhou and co-workers found that adsorbing the cis- and trans-isomers of 1,2-dichloroethylene on Si(100)2×1 resulted in nearly identical photoemission spectra, density functional calculations indicated that cis- and trans-β-chlorovinyl have nearly the same thermodynamic stability on the surface, and thermal desorption shows that both chlorovinyl intermediates form acetylene with nearly identical kinetics [38]. Reactivity and x-ray absorption spectroscopy studies conducted with cis- and trans-1,2-dichloroethylene on Cu(100) by Yang and co-workers also show that the two isomers form adsorbates consistent with chlorovinyl groups and these groups react with similar kinetics [39]. This study focuses on the reactions of 1,2-dichloroethylenes and the effect, if any, that placement of the β-C-Cl bond in the two possible chlorovinyl isomers has on surface reactivity. The position of the β-chlorine with respect to the metal oxide surface might impact the reaction kinetics for β-chlorine elimination as a result of different transition states.

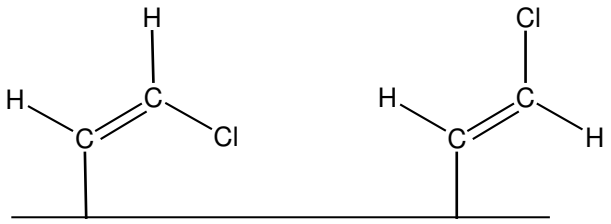

"cis"-β-chlorovinyl "trans"-β-chlorovinyl

Figure 21. Cis- and Trans-β-chlorovinyl groups that are likely formed in the reactions of cis- and trans-1,2-dichloroethylene.

5.2 Results

5.2.1 cis-1,2-dichloroethylene

5.2.1.1 gas phase and surface reaction products

Thermal desorption traces are shown in Figure 22 for consecutive thermal desorption cycles following 0.05 L doses of cis-DCE at 120 K. 1,2-dichloroethylene (1,2-DCE) desorption from consecutive doses of cis-DCE, Figure 22 (top), occurs at 380 K. The mass fragmentation pattern for the desorbing species (m/z=61,14,48) match that for 1,2-DCE, indicating that no isomerization to 1,1-dichloroethylene occurs. However, cis- to trans- isomerization cannot be ruled out by mass spectrometry. The amount of 1,2-DCE that desorbs increases with each consecutive dose of cis-DCE, indicating the surface changes with each consecutive exposure. The desorption feature for 1,2-DCE shifts down slightly in temperature to 370 K with increasing exposure. Multilayer desorption for cis-DCE (not shown) occurs at ~140 K.

Acetylene is the only gas phase product, and desorption traces shown in Figure 22 (bottom) from each consecutive thermal desorption cycle have been corrected for overlapping mass fragments of 1,2-DCE. One broad feature is observed for the first 0.05 L and it becomes apparent that there are actually two features, at 385 K and 460 K, when compared to desorption limited acetylene from an acetylene dose [23]. The desorption temperatures indicate two kinetic pathways for acetylene evolution: desorption limited (385 K) (Chapter 3) and reaction limited (460 K). With each consecutive thermal desorption cycle the desorption limited feature grows in and shifts down in temperature.

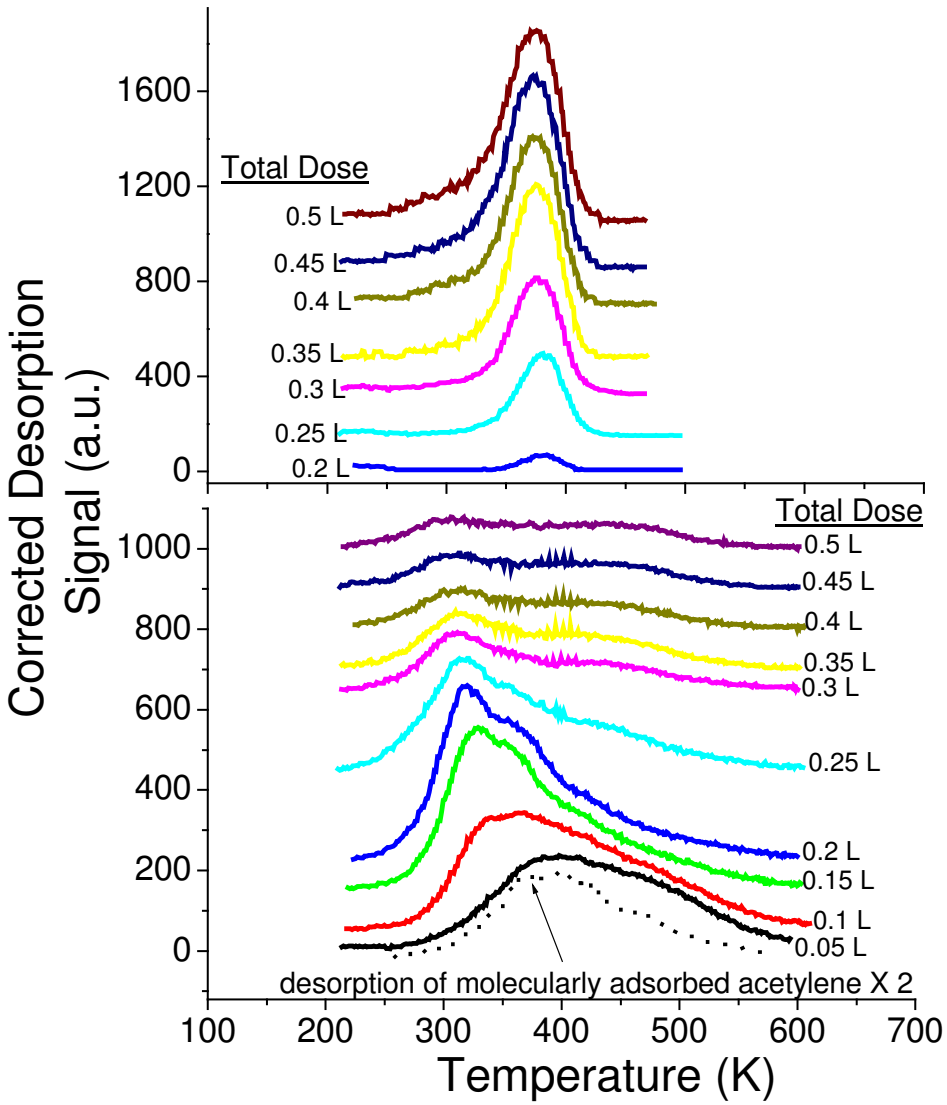

Figure 22. Corrected thermal desorption traces resulting from the reaction of cis-1,2-dichloroethylene. The top panel shows that 1,2-dichloroethylene desorbs at 375 K after the fifth consecutive 0.05 L dose, and that the desorption temperature remains constant with increasing exposure. Acetylene desorption (bottom) occurs at two temperatures (385 and 470 K) for the first dose and the desorption temperature decreases with increasing exposure to cis-1,2-dichloroethylene. Acetylene desorption resulting from adsorbing acetylene on a clean surface is shown with the dotted line.

Following the fifth dose (0.25 L total exposure) of cis-DCE, acetylene evolution is dominated by the desorption limited product. By the 10^{th} consecutive thermal desorption cycle, 0.5 L total exposure to cis-DCE, the desorption limited feature has shifted to 315 K and decreased in intensity.

Auger electron spectra taken following each consecutive thermal desorption cycle indicate that the thermal activation of cis-DCE results in Cl adatom deposition on the surface. Figure 23 shows the relationship between surface chlorine coverage with the changes in surface reactivity as a function of exposure to cis-DCE. The Cl adatom to surface Cr cation ratio reported in the graph is related to previous calculations in which it was determined that an AES Cl/Cr ratio of 0.32 is analogous to a 1:1 capping of Cl adatoms to surface Cr cation [1]. The error bars represent a 10% standard deviation that was measured as a result of the experimental parameters used to collect the post reaction spectra. The total acetylene production remains approximately constant and little 1,2-DCE desorbs up to ~0.6 Cl adatoms per surface Cr atom. After a 0.6 Cl/Cr ratio has been reached, acetylene production drops off and 1,2-dichloroethylene desorption increases. When the surface appears to be completely chlorinated, acetylene production has dropped to ~30% of its initial value. Figure 23 shows that the change in surface reactivity with increased exposure to cis-DCE (described above) is a result of depositing Cl adatoms that block sites responsible for acetylene production. No surface carbon is observed with AES as a result of the thermally activated reaction of cis-DCE in thermal desorption cycles.

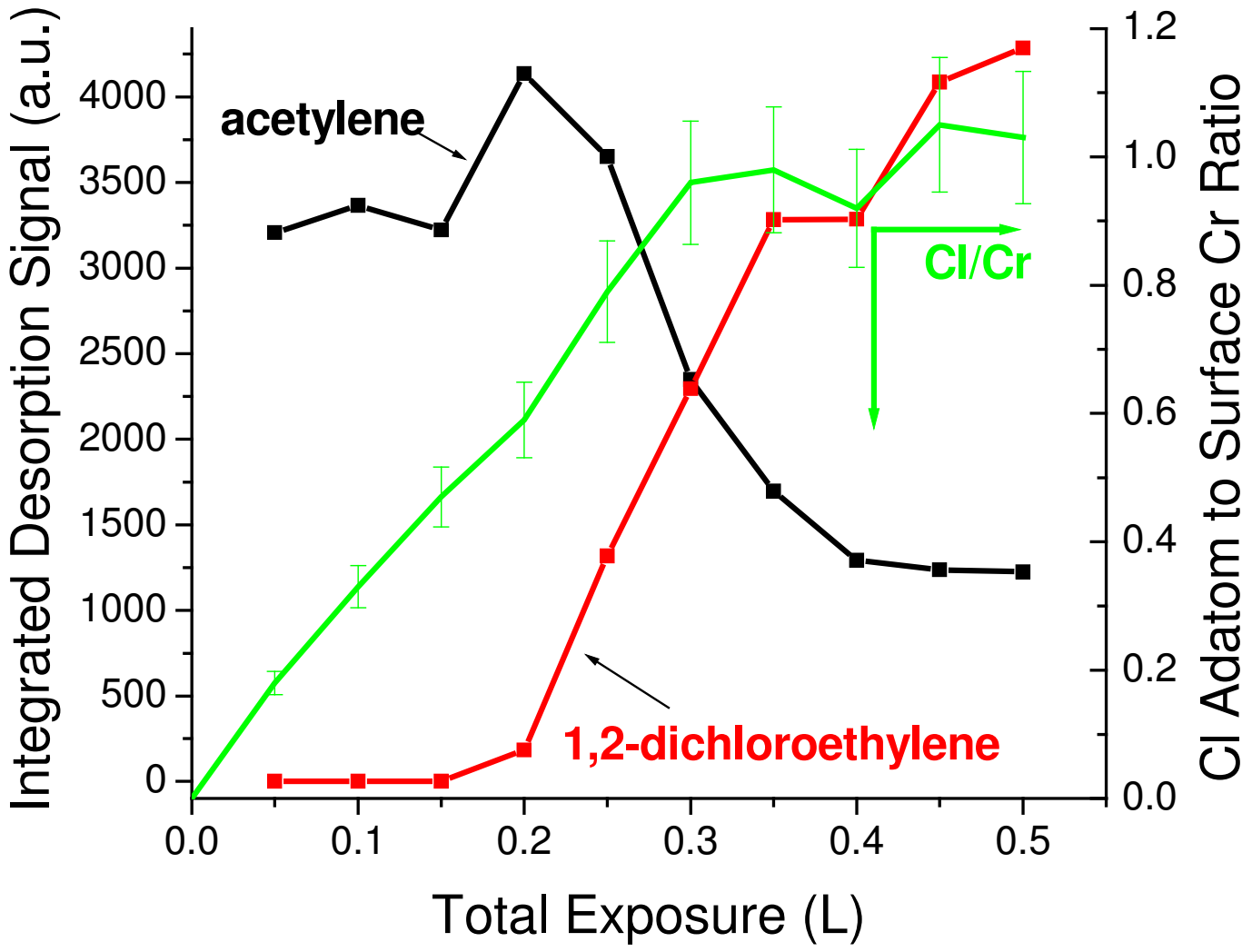

Figure 23. The effect of increasing the total surface exposure to cis-1,2-dichloroethylene is to chlorinate the surface with each dose. Chlorine adatom coverage per surface Cr atom is shown on the right-hand scale. Integrated desorption signals for acetylene and 1,2-dichloroethylene are shown on the left-hand scale. Increasing surface Cl coverage results in a decrease in acetylene desorption and evolution of 1,2-dichloroethylene.

5.2.1.2 spectroscopic characterization

The photoemission (Figure 24) and NEXAFS (Figure 25) spectra shown in this section were collected following a ~200 L dose of cis-DCE at 115 K. Each spectrum represents the species remaining on the surface after the sample was heated to the temperatures labeled in the figures and allowed to cool. The attenuation of the Cr 3p photoemission feature following adsorption (not shown) suggests a multilayer thickness of ~8 Å based on a mean free path for the dichloroethylene layer estimated from the NIST Electron Inelastic-Mean-Free-Path Database [75].

The spectra in Figure 24a,b show the photoemission resulting from the carbon and chlorine containing species on the surface, respectively. The C 1s spectra in Figure 24a show that at 115 K there is one clear feature at 286.0 eV that is assigned to the similar, singly chlorinated carbon atoms on both ends (=CHCl) of the molecular cis-DCE in the multilayer present on the surface at this temperature. The Cl 2p spectrum collected at 115 K also shows one predominant unresolved doublet. The Cl 2p doublet (Cl $2p_{3/2}$=200.6 eV) is assigned to chlorine in molecularly intact cis-DCE in the multilayer. The 115 K spectrum also has a small shoulder at ~198 eV. Heating to 160 K results in multilayer desorption, and both C 1s and Cl 2p spectra show an overall decrease in intensity and a decrease in the high binding energy feature associated with the molecularly intact cis-DCE. Additionally, the spectra collected at 160 K show that a low binding energy peak emerges that is consistent with C-Cl bond scission to form Cl adatoms bound to Cr cations (Cl $2p_{3/2}$=198.5 eV) [41,76] and non-chlorinated

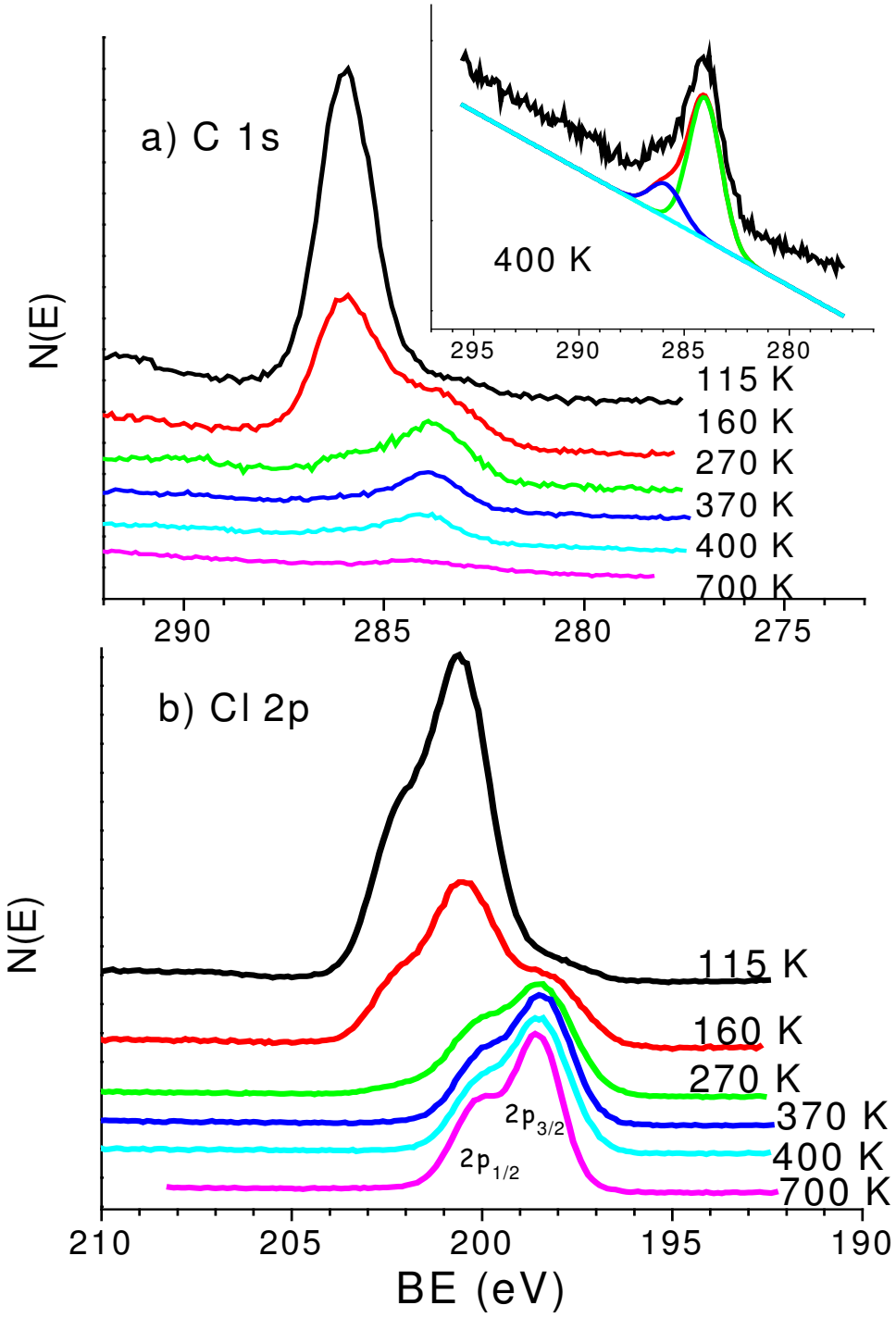

Figure 24. Photoemission spectra resulting from a ~200 L dose of cis-DCE at 115 K on an initially clean surface; the C 1s (a) and Cl 2p (b) spectra were collected using 350 eV photon energy. The C 1s spectra show that above the multilayer desorption temperature (140 K), there are two chemical states for carbon adsorbed on the surface. The C 1s inset shows that at 400 K there are still two states for adsorbed carbon.

carbon (C 1s=283.8 eV), Section 3.2.2. Heating to successively higher temperatures results in an overall decrease in the intensity of both the C 1s and Cl 2p spectra, and the C 1s high binding energy feature shifts from 286.0 to 285.8 eV. Following heating to 400 K, above the temperature for 1,2-dichloroethylene evolution and removal of most of the desorption limited acetylene (Chapter 3), the Cl 2p spectrum shows predominantly Cl adatoms (a single doublet at 198.5 eV characteristic of metal chlorides [41,57]). The C 1s spectrum at 400 K is, however, fit well [42] with two peaks with a full width at half maximum (FWHM) of 1.8 eV and a separation of 1.8 eV as shown in the inset in Figure 24a. The C 1s spectrum collected at 400 K is consistent with a mixture of non- and singly-chlorinated carbon (284.0 and 285.8 eV, respectively) in chlorovinyl groups and adsorbed acetylene (C 1s binding energy of 283.8 eV, Chapter 3) on the surface. These binding energies are consistent with other reports for chlorovinyl groups on Si(100)2×1, which were reported to have C 1s binding energies of 283.9 (nonchlorinated) and 285.6 eV (singly-chlorinated) . The relative areas of the two C 1s features suggest that approximately 20% of the carbon on the surface is chlorinated, indicating that ~40% of the carbon on the surface is contained in chlorovinyl groups. The remainder (~60%) of surface carbon is most likely contained in adsorbed acetylene, discussed in Chapter 3. The chlorine adatoms bound to Cr cations are stable on the surface up to 700 K. The small amount of carbon on the surface at 700 K (~2% of the carbon signal following adsorption at 115 K) is assigned to carbon resulting from the irradiation or low energy electron bombardment of adsorbed cis-DCE, because no carbon was seen in post-reaction AES.

The carbon K-edge NEXAFS spectra collected at grazing incidence are shown in Figure 25. The features observed upon adsorption are characteristic of a multilayer of adsorbed 1,2-dichloroethylene on the surface [39]. Upon adsorption of cis-DCE (grazing, 115 K), two primary features are visible: a sharp peak assigned as a C1s→$\pi^*_{(C\text{-}Cl)}$ transition at 285.9 eV (FWHM=0.8 eV), and a shoulder assigned to a C1s→$\sigma^*_{(C\text{-}Cl)}$ transitions at 287.2 eV [39]. Heating to 160 K, above the multilayer desorption temperature, results in a decrease in intensity for the C1s resonances for both grazing and normal incident light angles indicating either desorption of cis-DCE or C-Cl bond cleavage. The normal incidence spectra collected after heating to 160 K, Figure 25, show the same characteristics as that collected at grazing incidence, however, there is an extra shoulder centered at 284.4 eV. The shoulder around 284.4 eV corresponds to non-chlorinated carbon as was seen in vinyl groups, Section 2.2.3, and indicates formation of a non-chlorinated vinylic carbon in a surface fragment oriented with its molecular plane close to perpendicular to the surface. After heating to 270 K the C1s→$\sigma^*_{(C\text{-}Cl)}$ transition is no longer visible, indicating that most carbon remaining on the surface is non-chlorinated. Heating to 270 K leaves an intact π-system on the surface as demonstrated by the remaining C1s→π^* transition at 285.9 eV (FWHM=1.1 eV). Contributions from adsorbed acetylene (C1s→π^* transitions appear at 284.9-285.9 eV), Section 3.2.2, and chlorovinyl groups that are likely on the surface at this temperature account for the extra width of this feature collected with grazing incidence (FWHM=1.1 eV) in comparison to the C1s→$\pi^*_{(C\text{-}Cl)}$ transition for singly chlorinated carbon seen upon adsorption (FWHM=0.8 eV). Heating the surface above 270 K removes most of the carbon from the surface and the intensity of C1s transitions are too small to analyze.

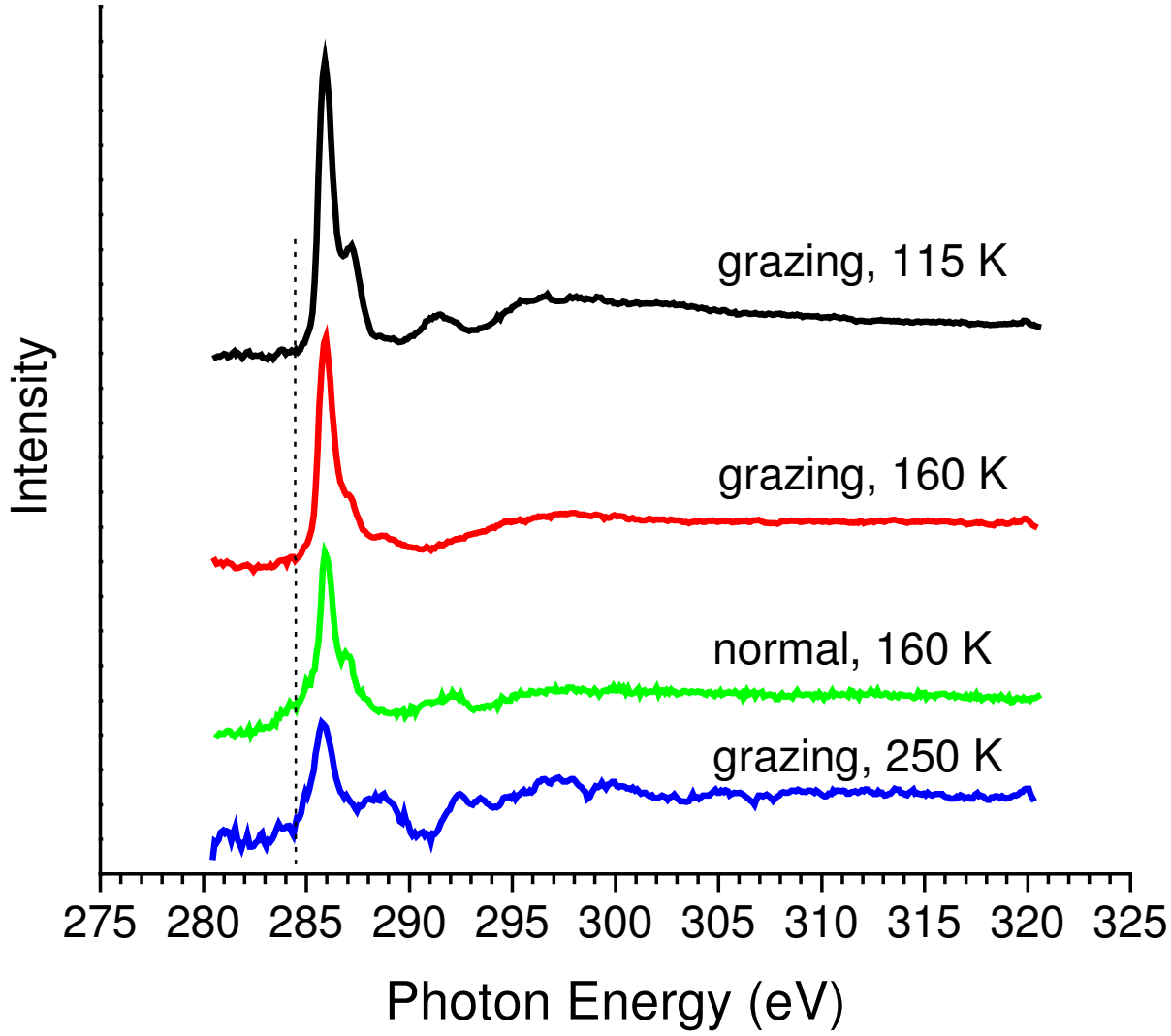

Figure 25. NEXAFS C K-edge spectra collected following photoemission show, upon adsorption at 115 K, two features associated with molecularly intact cis-DCE in a multilayer. The spectra collected at 250 K shows that intact π-systems remain on the surface after many of the C-Cl bonds have been broken.

5.2.2 trans-1,2-dichloroethylene

5.2.2.1 gas phase and surface reaction products

The product and reactant desorption traces resulting from consecutive thermal desorption cycles following 0.05 L exposures to trans-1,2-dichloroethylene (trans-DCE) are shown in Figure 26. The desorption of 1,2-DCE, Figure 26 (top), occurs at 320 K following the fifth (0.25 L total) consecutive dose. The desorbing 1,2-dichloroethylene cannot be uniquely identified as the trans-DCE from mass spectrometry, as was seen with the reaction of cis-DCE in Section 5.2.1.1. Increased exposure to trans-DCE results in an increase in intensity and temperature (320 K to 345 K) for 1,2-DCE desorption. The change in desorption trends indicates that the surface is changed with each consecutive dose, as was discussed in Section 5.2.1.1 for cis-DCE. Multilayer desorption of trans-DCE occurs at 140 K (not shown).

As with the reaction of cis-DCE, acetylene is the only identified gas phase product, and acetylene desorption is shown in Figure 26 (bottom). The acetylene traces have been corrected for overlapping mass fragments from 1,2-DCE. The first 0.05 L dose of trans-DCE results in a broad acetylene desorption feature with a shoulder at 385 K and a peak at 420 K. As with acetylene from cis-DCE, it appears that two kinetic pathways are available for acetylene evolution with the low temperature (385 K) and high temperature (420 K) features associated with desorption, Section 3.2.1, [1] and reaction limited acetylene, respectively. Figure 26 (bottom) shows an increase in desorption temperature from 420 K to 460 K indicating an increased activation barrier to acetylene formation, plus a new reaction limited feature at 550 K associated with a second, higher

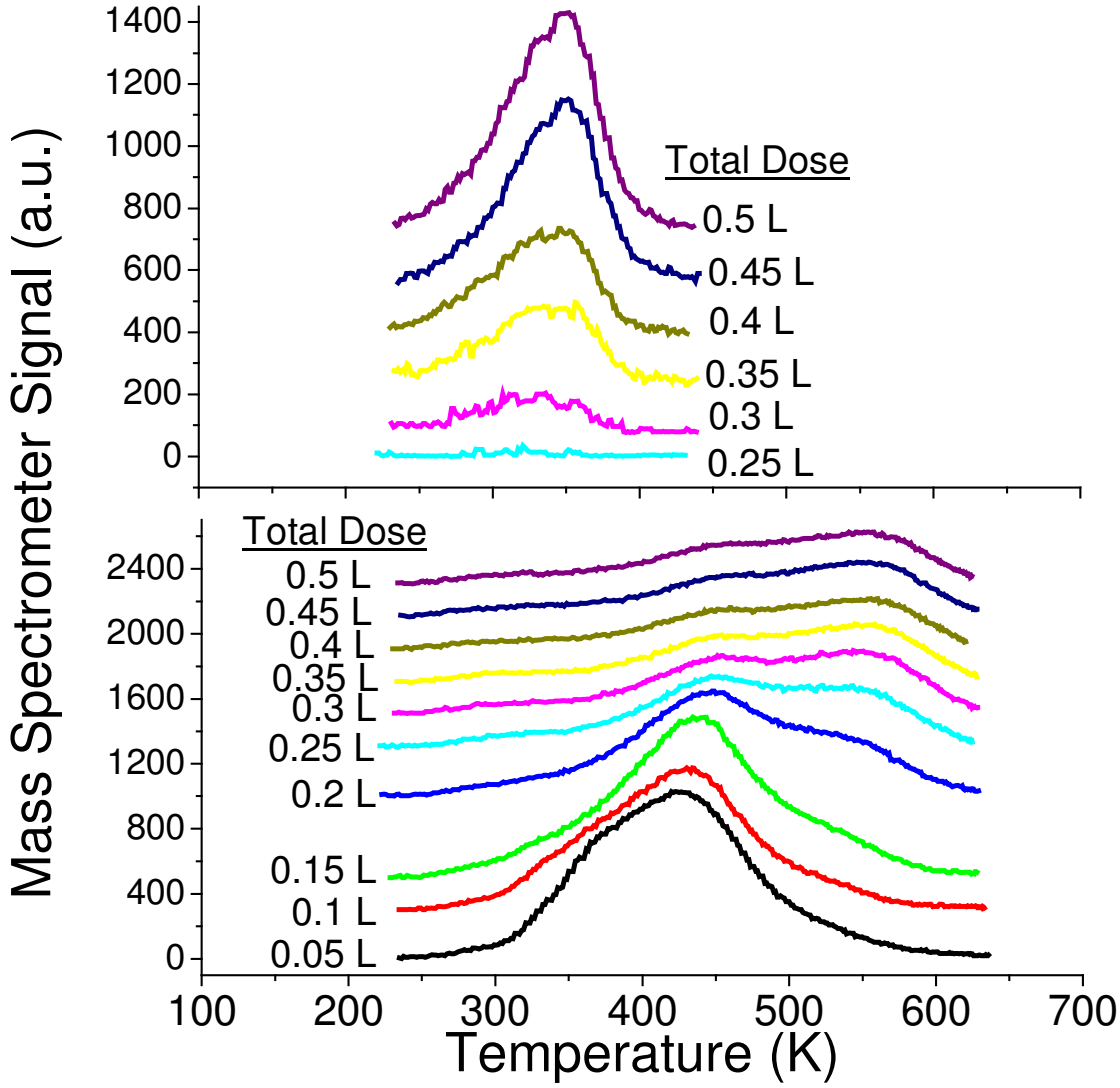

Figure 26. Thermal desorption of 1,2-dichloroethylene (top) and acetylene (bottom) resulting from the consecutive thermal desorption cycles following adsorption of 0.05 L doses of trans-DCE on an initially clean surface. 1,2-dichloroehtylene begins to desorb at ~320 K and the amount desorbing as well as the temperature increase with increased exposure to trans-DCE. Acetylene initially evolves at two temperatures (385 and 420 K), however continued exposure to trans-DCE shifts the feature at 420 K→460 K and a second high temperature feature grows in at 550 K.

energy transition state with increased exposure to trans-DCE. After the sixth consecutive 0.05 L dose of trans-DCE, the relative intensities of the two reaction limited features and temperatures remain constant. After a surface Cl coverage of ~70% has been reached, the reaction limited desorption temperature remains constant (for both reaction limited features) whether a 0.05 or 0.1 L dose of trans-DCE is used indicating a first order rate limiting step for reaction. The changes in acetylene and 1,2-dichloroethylene desorption are likely due to chlorine deposition resulting from exposure to trans-DCE, as discussed in Section 5.2.1.1.

AES spectra show that Cl is deposited following each consecutive dose of trans-DCE and thermal desorption cycle. Changes in surface reactivity in relation to Cl coverage per surface Cr cation (as a function of dose) are shown in Figure 27. The error bars represent a 10% standard deviation that was measured as a result of the experimental parameters used to collect the post reaction spectra. Depositing Cl adatoms on Cr surface sites does not appear to greatly affect the production of acetylene until there are ~0.6 Cl adatoms per surface Cr atom. For ~60 % Cl coverage, acetylene production drops off and 1,2-DCE desorption is observed. The decrease in the surface's ability to decompose trans-DCE to acetylene with chlorine coverage indicates the chromium atoms are the active sites for acetylene formation. Although Auger spectra indicate that all of the active chromium sites are capped after a total trans-DCE exposure of 0.4 L, the acetylene desorption drops by 77% from the maximum. Acetylene is still evolved even when the surface is chlorinated; however, the amount of desorbing acetylene and 1,2-DCE have begun to plateau indicating that the surface reactivity is changing less with each

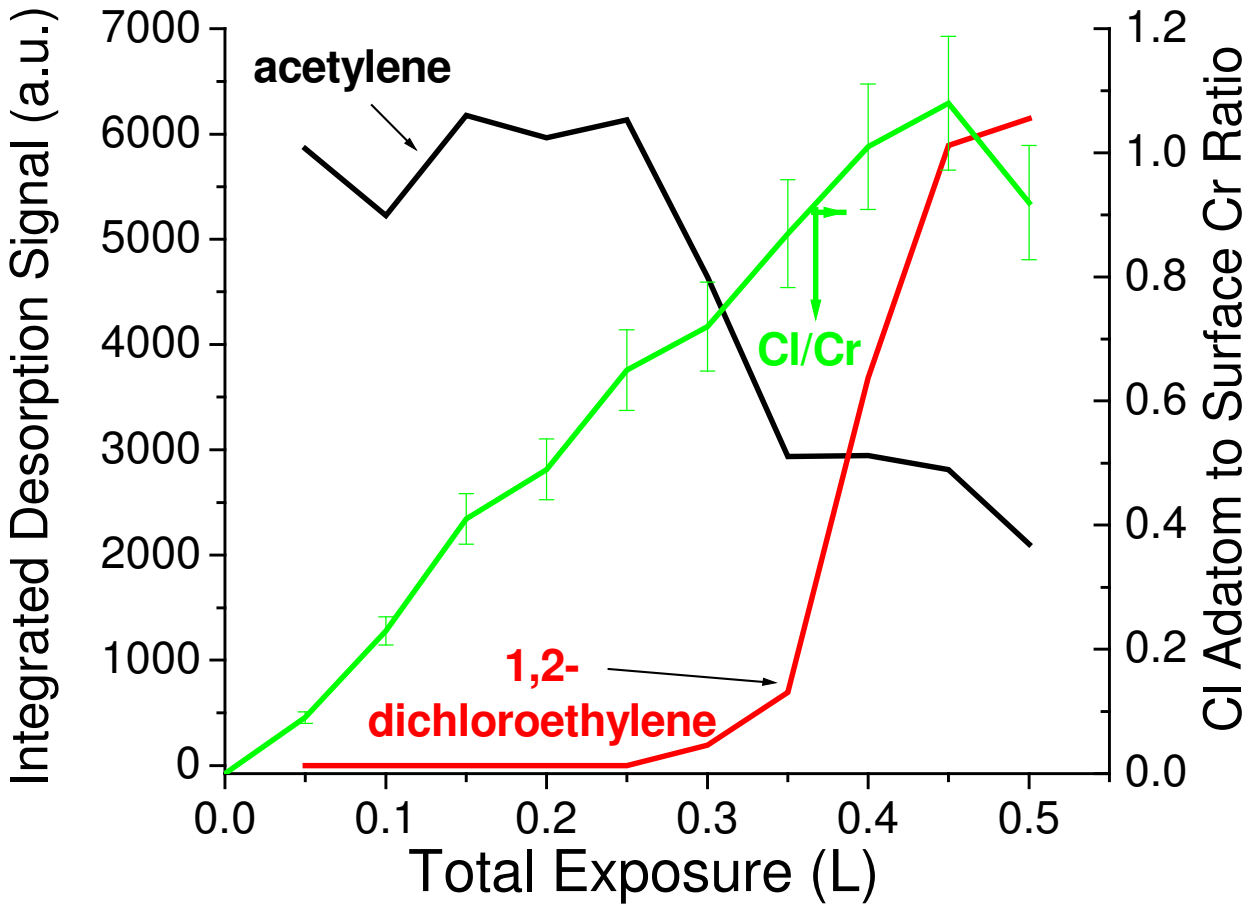

Figure 27. The desorption signal (left-hand axis) and surface chlorine coverage (right-hand axis) change as a function of exposure to trans-DCE. After a total trans-DCE exposure of 0.25 L acetylene production decreases and 1,2-dichloroethylene begins to desorb from the surface.

consecutive dose. No carbon was observed on the surface with AES following the trans-DCE thermal desorption cycles.

In addition to the thermal desorption results discussed above, an interesting occurrence was observed over time with trans-DCE. Figure 28 shows how the acetylene desorption trace changes over time, the traces pictured are those resulting from the 7^{th} consecutive 0.05 L thermal desorption cycle of trans-DCE on an initially clean surface. Over a period of 13 days, acetylene desorption resulting from the reaction of trans-DCE changes from that described in Figure 26 to resemble acetylene desorption from cis-DCE shown in Figure 22. Over time, the high temperature reaction limited feature (550 K) disappears and desorption limited acetylene dominates. While the acetylene desorption traces change as a result of storage time, the desorption temperature of trans-DCE remains at 345 K indicating that trans-DCE was still being adsorbed on the surface. Comparison of the mass spectrometer cracking pattern of trans-DCE for day one and day thirteen reveals that the ratio of mass numbers that characterize acetylene (m/z=26,25,24,12,13) to m/z=61 for trans-DCE are three times larger for day 13 than day one. In fact, the ratio of mass numbers 24 and 25 to the acetylene parent mass (m/z=26) in the cracking fragment of trans-DCE on day 13 is representative of acetylene and not of trans-DCE. The change in the cracking pattern indicates that over time acetylene is produced from trans-DCE in the stainless steel tube fitted with copper gaskets. Subsequent freeze-pump-thaw and flash distillation cycles did not affect the cracking pattern of the old trans-DCE or change the acetylene desorption trace that is pictured for day 13 in Figure 28. The inability to regenerate the original cracking pattern for trans-

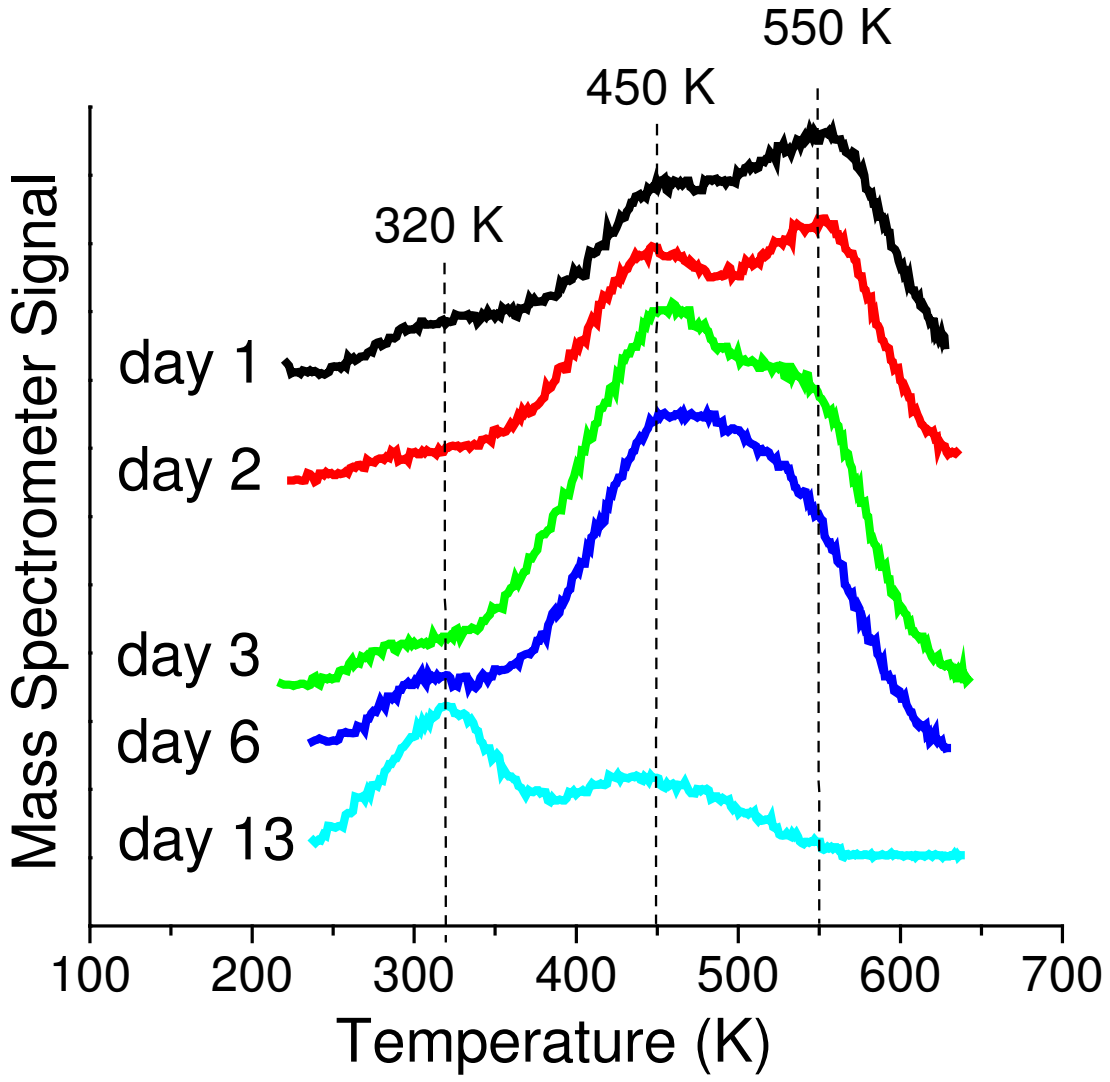

Figure 28. Acetylene production from trans-DCE changes over a period of 13 days indicating that trans-DCE changes as a function of storage time. The spectra collected on day 1 represents acetylene desorbing from the reaction of trans-DCE. The spectra collected on day 13 resembles that of acetylene from cis-DCE (large amount of desorption limited acetylene) and the cracking pattern indicates that molecular acetylene is being adsorbed on the surface.

DCE suggests that freeze-pump-thaw cycles are not an effective method for separating acetylene and DCE. Though trans-DCE is dosed over all 13 days, it is apparent from the large desorption limited acetylene feature (day 13) that molecular acetylene is also dosed inadvertently on the surface.

5.3 spectroscopic characterization

The photoemission (Figure 29) and NEXAFS (Figure 30) spectra shown in this section were collected following an ~200 L dose of trans-DCE at 115 K. Each spectrum represents the species on the surface after the sample was heated to the temperatures labeled in the figures and allowed to cool. The attenuation of the Cr 3p photoemission feature following adsorption (not shown) suggests a multilayer thickness of ~8 Å based on a mean-free-path for the dichloroethylene layer estimated from the NIST Electron Inelastic-Mean-Free-Path Database [75].

The photoemission shown in Figure 29a depicts the C 1s spectra and Figure 29b depicts Cl 2p spectra collected at each temperature. At 115 K the major features for C 1s (285.9 eV) and Cl $2p_{3/2}$ (200.6 eV) indicate that the trans-DCE multilayer present at this temperature is the major contributor to each spectrum, as was seen with cis-DCE in Section 5.2.1.2. Each spectrum also shows a small shoulder at lower binding energy, at ~283 eV for C 1s and ~198 eV for Cl 2p. The shoulders at lower binding energy indicate that upon adsorption some C-Cl bonds break to form non-chlorinated carbon and Cl adatoms. The contribution of chlorovinyl groups to the overall signal is small in comparison to the contribution of the molecularly intact species present in the multilayer at this temperature. Heating to 160 K results in a decrease in intensity of the high binding

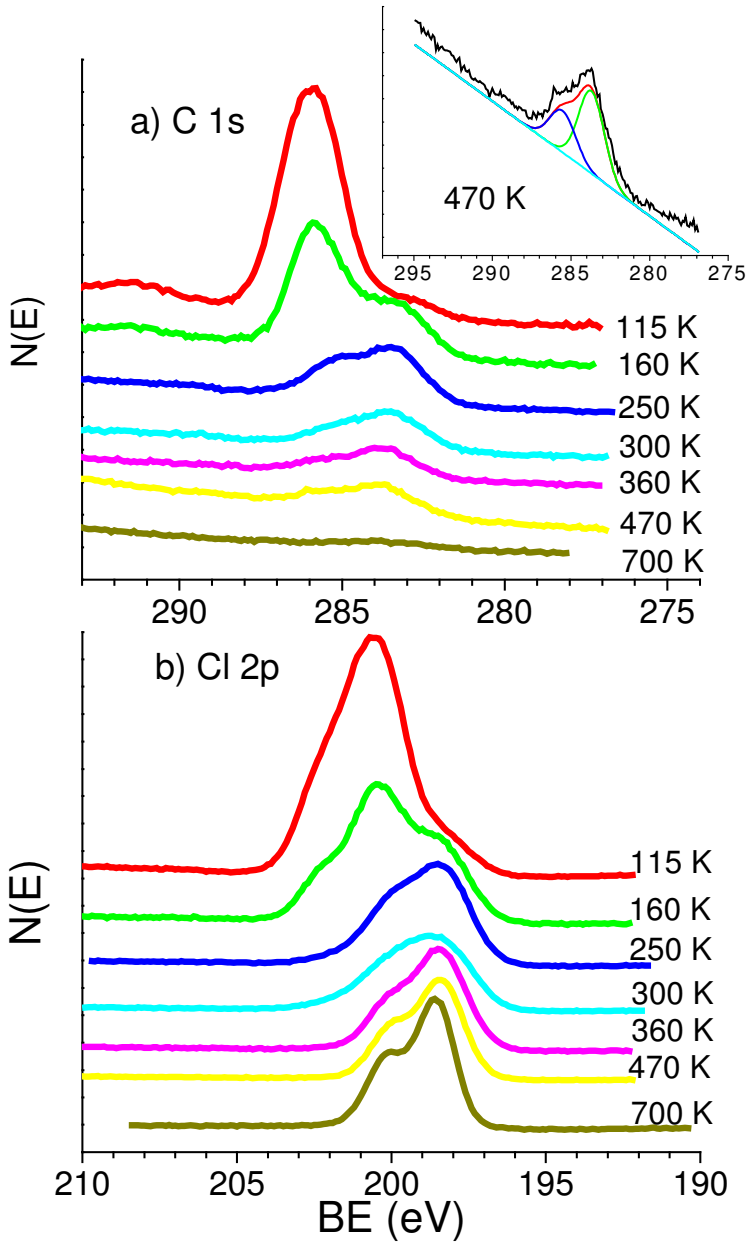

Figure 29. The C 1s (a) and Cl 2p (b) spectra resulting from adsorption of ~200 L of trans-DCE at 115 K on an initially clean surface closely resemble that of cis-DCE. The C 1s spectra show the presence of multiple carbon species at 470 K with the contribution from chlorinated carbon (284.4 eV) representing approximately 35% of the carbonaceous surface species.

energy features, and shift in the C 1s binding energy from 285.9 to 285.5 eV. After heating to 160 K the low binding energy shoulder emerges as an identifiable peak for both C 1s (283.5 eV) and Cl 2p (Cl $2p_{3/2}$=198.5 eV). The change in features with heating is consistent with both desorption of the multilayer and C-Cl bond scission.

The inset in Figure 29a shows that the C 1s spectrum collected at 470 K is fit well with two peaks (FWHM=1.9 eV) separated by 1.8 eV [42]. The two carbon chemical states are associated with singly-chlorinated (285.5 eV) and nonchlorinated (283.7 eV) carbon, Chapters 2 and 3. Comparison of the peak areas for singly-chlorinated carbon (chlorovinyl groups) and non-chlorinated carbon indicate the ratio of chlorovinyl groups to non-chlorinated C2 adsorbates is roughly 2.3:1.0. The Cl 2p spectra collected after heating to 470 K show a single doublet (Cl $2p_{3/2}$ =198.5 eV) characteristic of metal chlorides [41,57] assigned to Cl adatoms bound at surface Cr sites. The relative amount of chlorine adatoms to chlorovinyl groups above 470 K is large and a contribution from C-Cl bonds is likely too small to be seen in the Cl 2p spectrum. Heating the surface to 700 K does not remove the chlorine adatoms, and the remaining carbon is negligible compared to trace carbon seen on the initially clean surface.

Figure 30 shows the trans-DCE NEXAFS spectra collected with grazing incidence light. The carbon K-edge spectra show similar trends to the spectra collected following the adsorption of cis-DCE on this surface. Upon adsorption (115 K) there are two C1s features characteristic of the multilayer with the low photon energy feature at 285.9 eV (FWHM=0.6 eV) associated with a C1s$\rightarrow\pi^*_{(C\text{-}Cl)}$ transition and the higher photon energy shoulder at 287.0 eV associated with a C1s$\rightarrow\sigma^*_{(C\text{-}Cl)}$ transition [39]. Heating to 160 and then to 250 K results in a decrease in intensity for both C1s

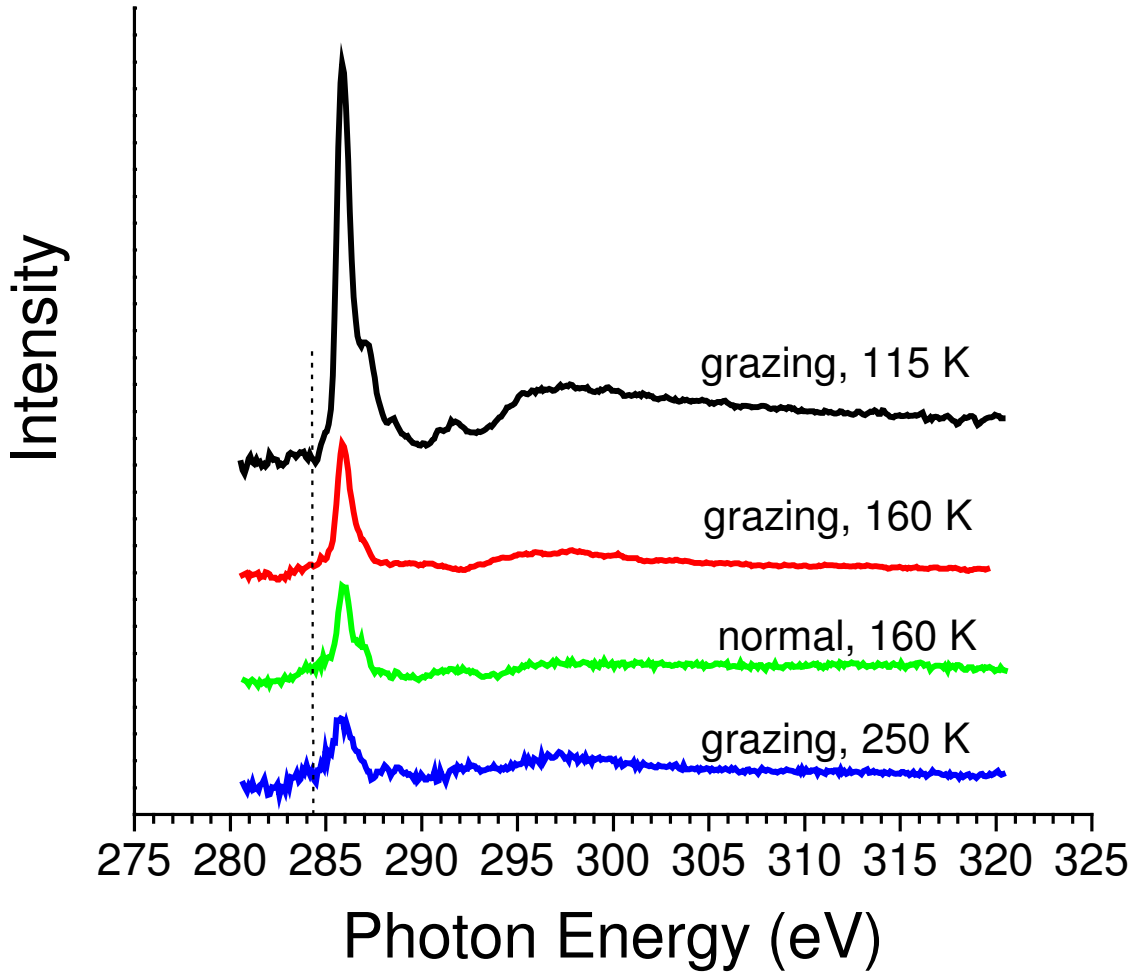

Figure 30. **The NEXAFS spectra resulting from adsorption of ~200 L of trans-DCE at 115 K strongly resemble those seen for cis-DCE adsorption. At 115 K there are two features associated with molecularly intact trans-DCE, and heating to 250 K indicates intact π-systems remain on the surface.**

transitions indicating trans-DCE desorption and C-Cl bond cleavage. The remaining feature observed at 250 K is broader (FWHM=1.3 eV) than that observed upon adsorption at 115 K (FWHM=0.6 eV), and this feature likely contains contributions from chlorovinyl and adsorbed acetylene (Section 3.2.2). As with cis-DCE, the spectra show a shoulder around 284.4 eV, as shown for 160 K at both incidence light angles in Figure 30, indicative of a C1s→π* transition for non-chlorinated carbon in vinyl-like surface groups, Section 2.2.3. The retention of the C1s→π* transition indicates intact π-systems remain on the surface after heating to 250 K.

5.4 Discussion

The reactions of cis-DCE and trans-DCE result in the formation of acetylene as the only gas phase product. However, there are few similarities in the thermal desorption data. The multiple kinetic pathways for acetylene desorption in both reactions are associated with desorption (low temperature) and reaction (high temperature) limited pathways. The desorption limited acetylene which evolves at ~385 K (1^{st} 0.05 L dose) from both reactants is characteristic of an apparent first order activation energy of desorption of 100 kJ/mol, as estimated by the Redhead method assuming a normal first order pre-exponential factor of 10^{13} s^{-1} [54]. The activation energy for desorption limited acetylene is consistent with that for desorption of molecularly adsorbed acetylene on a clean α-Cr_2O_3 ($10\bar{1}2$) surface, Section 3.2.1 and for desorption limited acetylene from the reactions of 1,1-dichloroethylene (Section 4.2.1) and 1-chloro-1-flouroethylene [1].

A factor that might be important to the formation of desorption limited acetylene is the reactant adsorption geometry. Trans-1,2-dichloroethylene reportedly adsorbs parallel to the surface in a molecularly intact configuration at ~85 K on Cu(110) and to

undergo concurrent C-Cl bond cleavage to form adsorbed acetylene [40]. NEXAFS studies of all isomers of dichloroethylene adsorbed on Pt(111) at 95 K indicate that the molecularly intact species adsorb with the molecular plane parallel to the surface, and heating results in desorption of the molecularly intact species without forming more strongly bound adsorbates through C-Cl bond cleavage [77]. Examination of the relationship between molecular structure of the isomers and the α-Cr_2O_3 $(10\bar{1}2)$ surface reveals possible effects that different reactant geometries may have on surface reactivity.

Possible molecular adsorption geometries for the 1,2-dichloroethylenes within the $[02\bar{2}1]$ troughs on the α-Cr_2O_3 $(10\bar{1}2)$ surface are shown in Figure 31. Figure 31a shows a possible configuration for trans-DCE with both Cl atoms directed toward open (coordinately unsaturated) Cr sites. The configuration in Figure 31a could promote the concerted decomposition of both C-Cl bonds on a surface with low Cl adatom coverage. At higher Cl adatom coverages, the close approach of carbon atoms to surface Cr sites could also promote the formation of surface trans-β-chlorovinyl by elimination of a single Cl atom. Figure 31b shows an alternate geometry for trans-DCE that provides close approach of a single molecular Cl atom to an open Cr site, with the second Cl blocked from a Cr site by the zig-zag row of top layer surface oxygen anions. The geometry in Figure 31b also provides a close approach for both carbon atoms to a surface Cr site, providing for a π-bonding stabilization in this geometry. As with 31a, elimination of a single Cl atom could readily lead to the formation of trans-β-chlorovinyl. A favorable geometry appears possible for cis-DCE, shown in Figure 31c, with both Cl atoms directed towards neighboring Cr sites, and a π-bonding interaction between the C=C double bond and an open Cr site. The intact cis-DCE adsorption geometry could allow

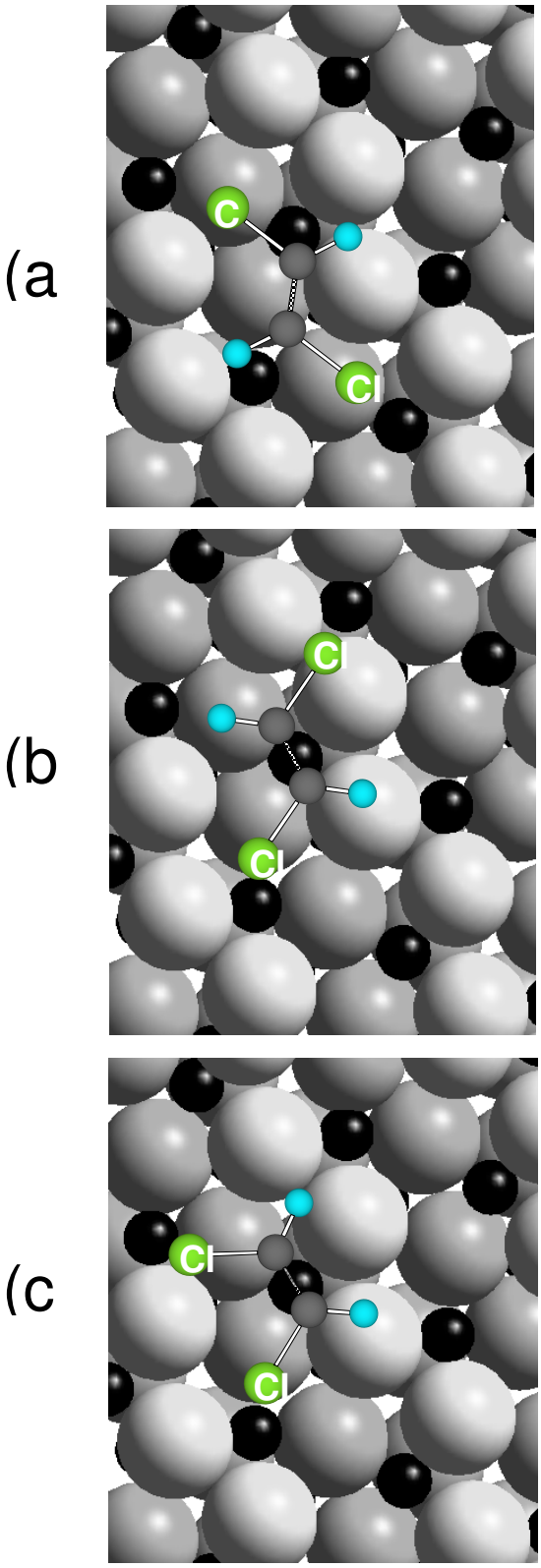

Figure 31. Top view of possible molecularly intact adsorption geometries for cis- (a) and trans-DCE (b and c).

for concurrent C-Cl bond cleavage at low temperature resulting in the large amount of desorption limited acetylene from cis-DCE. Molecular adsorption of trans-DCE does not appear to allow as many stabilizing adsorption points as cis-DCE. These simple geometric considerations suggest that the larger desorption limited feature for acetylene from cis-DCE on a nominally clean surface might be the result of concurrent C-Cl bond cleavage facilitated by a π-bonding interaction that is not as likely for trans-DCE. First principles studies of these reactions are recommended.

Examination of reaction limited acetylene desorption (above 400 K) from the two isomers yields a general picture of the surface intermediates and possible reactions that form acetylene. It can be imagined that the surface intermediates in the reactions of cis- and trans-DCE are "cis"-β-chlorovinyl and "trans"-β-chlorovinyl as pictured in Figure 21. Reaction limited acetylene from both β-chlorovinyl groups is thought to proceed through β-chlorine elimination. Acetylene formation from dichlorinated ethylenes on well-defined metal surfaces show no kinetic dependence on the placement of Cl atoms in the molecule [38,39,81]. In this study, for low Cl coverages, reaction limited acetylene desorbs at approximately the same temperature (~460 K) from both reactants indicating little kinetic differences for β-chlorine elimination from both β-chlorovinyl groups for low Cl coverages.

Figure 32 shows possible binding configurations for β-chlorovinyl groups. For cis-β-chlorovinyl the remaining Cl atom may interact with the surface through an open Cr site (Figure 32a), while for trans-β-chlorovinyl the remaining Cl atom can be imagined to point directly away from the surface, Figure 32b. Additionally, thermal

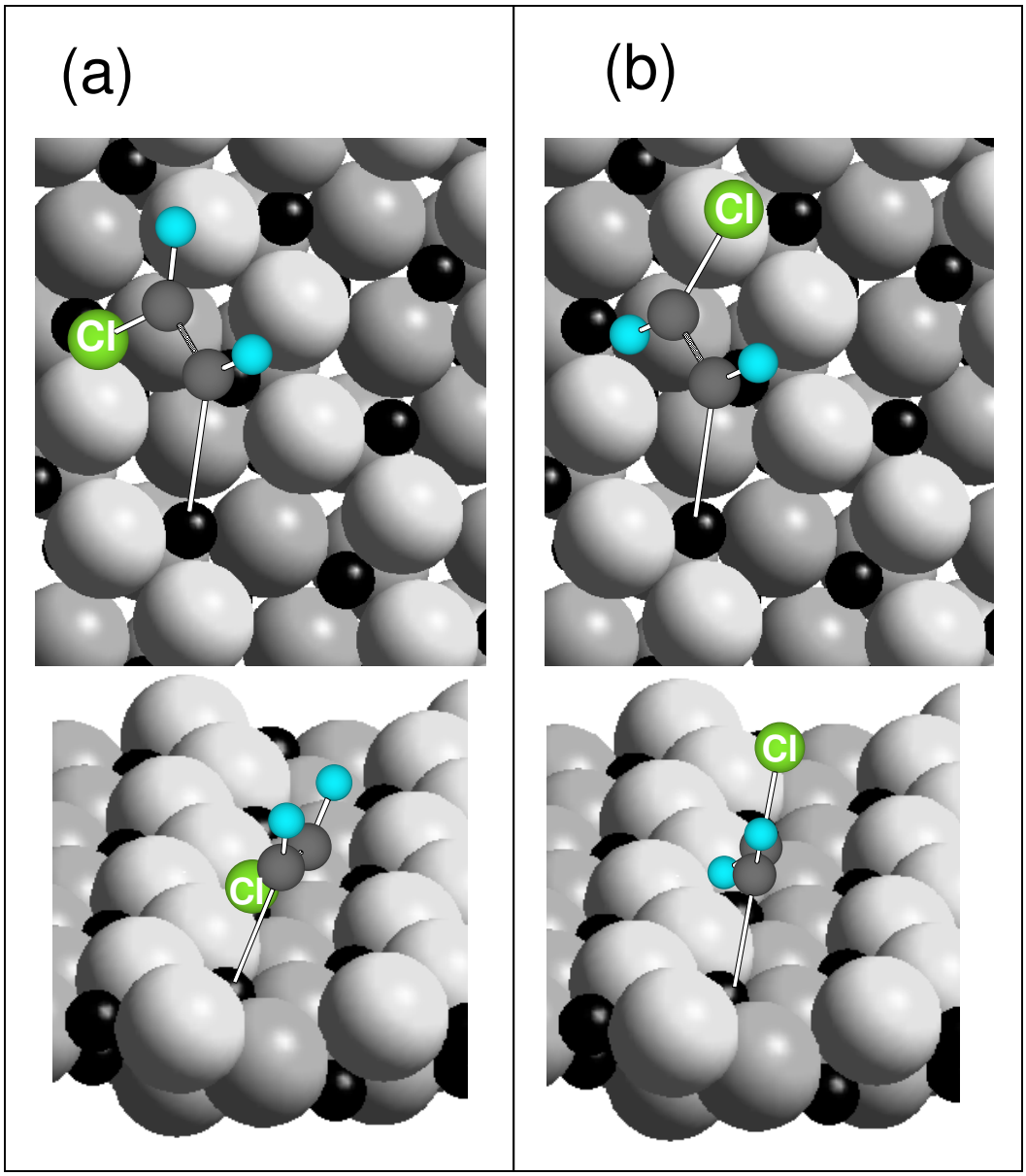

Figure 32. Possible geometries for cis- and trans-β-chlorovinyl groups following a single C-Cl bond cleavage. Cis-β-chlorovinyl (a) and trans-β-chlorovinyl (b) are shown with both top and side views with the remaining Cl is oriented toward or away from available Cr sites for cis- and trans-β-chlorovinyl groups, respectively.

desorption indicates that Cl deposition on the surface lowers the activation barrier (or destabilizes the intermediate) to forming acetylene from cis-DCE resulting in desorption limited acetylene being the dominant pathway. The increase in temperature for the low temperature reaction limited feature from trans-DCE is perhaps caused by an increase in steric hindrance for trans-β-Cl elimination introduced by an increase in the number of surface Cl adatoms.

Another difference seen in acetylene desorption from the two reactants is the formation of a second high temperature feature (~550 K) for the reactions of trans-DCE. The highest temperature feature for acetylene from trans-β-chlorovinyl grows in as the surface is chlorinated and desorption limited acetylene makes up only a very small percentage of desorbing acetylene. It is believed that the high temperature feature appears as a result of a surface ensemble effect created when neighboring Cr atoms are chlorinated. The chlorinated areas may cause stabilization of trans-β-chlorovinyl groups to a point where thermal activation of the remaining C-Cl bond is achieved without the need for a nearby open Cr site, or perhaps a lower energy pathway is prevented by the presence of surface Cl. The evolution of acetylene (from trans-DCE) through the highest temperature pathway involves a rate limiting surface reaction step with an apparent 1^{st} order activation barrier of 140 kJ/mol for desorption versus 125 kJ/mol for reaction limited acetylene from cis-DCE, as estimated by the Redhead method [54].

The reactivity of the 1,2-dichloroethylenes, and other halogenated ethylenes (Chapters 2 and 4) [1], indicate that this surface is highly selective to acetylene production. These studies also show that the placement and the strength of the C-substituent bonds as well as the surface chlorine coverage impact the activation barrier to

acetylene formation, but do not affect selectivity. While the relationship between the effect of Cl coverage on the kinetics and intermediate geometry is not fully understood, it is noted that the halogen coverage dependence of acetylene desorption from cis-DCE is similar to acetylene from 1,1-DCE (Chapter 4) and 1-chloro-1-flouroethylene [1]. The acetylene from trans-DCE resembles that from vinyl chloride, Chapter 2, with the low temperature reaction limited acetylene desorption temperature increasing with increased chlorine coverage.

The change in acetylene desorption with time in the reaction of trans-DCE suggests an explanation of the persistence of desorbing acetylene from both reactants after the surface is apparently fully chlorinated and should be deactivated [1]. Over time, acetylene desorption from trans-DCE resembles that from cis-DCE, and it appears that trans-DCE is converted to acetylene while in storage. The similarities in acetylene desorption trends for aged trans-DCE and new cis-DCE indicate that cis-DCE may also form acetylene in storage even though no clear change over time was observed for cis-DCE. If acetylene is produced in storage of the 1,2-dichlorothylenes, then some of the desorbing acetylene may be a result of inadvertently dosing molecular acetylene with the 1,2-DCE exposures.

The 1,2-DCE desorption temperature is significantly different for the cis- and trans-DCE reactants suggesting a difference in the adsorbates that result in 1,2-DCE desorption. The two isomers have the same mass and atomic composition, and so the difference in desorption energies for the two reactants is likely a result of recombination of surface Cl adatoms with the different chlorovinyl groups discussed above. It appears that the lower temperature for 1,2-dichloroethylene desorption from this surface in the

reaction of trans-DCE when compared to cis-DCE indicates that trans-β-chlorovinyl groups are chlorinated more easily. Additionally, it is possible that the interaction of β-chlorine with the surface that facilitates acetylene production from cis-β-chlorovinyl groups could also increase the activation barrier for recombination and desorption of 1,2-DCE. At this time, there is no definitive experimental proof that 1,2-dichloroetylene desorption in these reactions is a result of recombination, and not simply the desorption of a molecular adsorbed species. It is apparent, however, from thermal desorption trends for 1,2-DCE and acetylene desorption from both reactants that Cl deposition on the surface has an overall stabilizing effect on trans-β-chlorovinyl groups and a destabilizing effect on cis-β-chlorovinyl groups.

The photoemission and NEXAFS spectra collected following adsorption of both 1,2-dichloroethylenes show that both reactants form chemically similar adsorbates; Zhou *et. al.* observed similar photoemission results with the dissociative adsorption of cis- and trans-DCE on Si(100)2×1 [38]. It appears that at 115 K both reactants adsorb primarily in a molecularly intact manner at the multilayer coverages examined. Above the reactant desorption temperatures, adsorbates still exhibit intact π-systems in NEXAFS and some C-Cl bonds; these species can be described as a mixture of chlorovinyl groups and adsorbed acetylene. Zhou *et. al.* also suggest that the non-chlorinated carbon observed following room temperature adsorption of cis- and trans-1,2-dichloroethylene on the Si(100)2×1 surface is contained in a di-σ-bonded acetylene adstructure [38]. NEXAFS spectra collected in this study are consistent with acetylene and β-chlorovinyl groups. At higher temperatures, gaining orientational information about β-chlorovinyl groups from polarization studies is difficult due to the low coverage of carbon containing adsorbates,

inconsistent interference from large background signals, and interference from cylindrically symmetric adsorbed acetylene. Density functional calculations performed for single C-Cl bond cleavage upon adsorption of cis-DCE and trans-DCE on Si(100)2×1, however, show that chlorovinyl groups retain their original configurations as picture in Figure 21 [38].

5.5 Conclusion

The reactions of both trans- and cis-1,2-dichloroethylene result in the formation of chemically similar surface intermediates including chlorovinyl groups and adsorbed acetylene. Thermal desorption, PES, and NEXAFS have shown that while the chemical nature of the intermediates may be similar, the kinetics for acetylene formation from these intermediates are very different. In general for higher Cl coverages, "trans-β-chlorovinyl" groups are shown to be much more stable towards Cl-elimination than the "cis-β-chlorovinyl" groups, as evidenced by differences in activation energies for β-elimination to form acetylene from these intermediates.

Chapter 6

Summary and Recommendations for Future Work

6.1 Summary

The reactions of C2 haloethylenes on the α-Cr_2O_3 $(10\bar{1}2)$ surface are overwhelmingly selective to the formation of acetylene. While all of the reactants outlined in this study form acetylene, the thermal desorption and spectroscopic studies indicate that the acetylene production route is dependent on the reactant. The NEXAFS and XPS studies show that it is possible to control the type of fragment formed on the surface by controlling the position of relatively weak C-X bonds in the reactants. The fragments that were formed in this study were those expected from sequential or concerted C-X bond cleavage, and are consistent with several studies conducted on metals using similar reactants. Regardless of whether vinyl groups (from vinyl chloride), vinylidene (from 1-chloro-1-flouroethylene and 1,1-DCE), or chlorovinyl groups (from 1,2-DCE's) are formed on the surface, acetylene is the dominant product. Binding energies associated with C 1s features for all of the chlorinated ethylene reactants and intermediates formed in these reactions are shown in Table 1.

C 1s Binding Energy (eV)	Carbon Binding Configuration
283.4-284.0	C-Cr bonds, 'chemisorbed' acetylene, methylene, vinyl, and vinylidene carbon
285.5	'Physisorbed' acetylene
285.5-285.8	Singly chlorinated carbon, vinyl chloride or 1,2-DCE
287.1	Doubly chlorinated carbon, molecularly intact 1,1-DCE

Table 1. Table of C 1s binding energies for different adsorbates.

The acetylene product in all of the cases studied in this work is formed by decomposition of surface intermediates. Despite the dominance of the decomposition pathway, none of the surface intermediates that were examined decompose to surface carbon, which is an anomaly in dehydrogenation reactions carried out over supported metals and metal oxides [82-85]. The lack of carbon formation in these studies suggests that either vinyl and vinylidene are not coke forming intermediates, or that the active sites responsible for coke formation on chromia catalysts from vinyl and vinylidene are not present on the well ordered $(10\bar{1}2)$ surface. Alternatively, if a low probability reaction channel to coke from these intermediates exists, then the halogen deposition which prevents multiple turnovers at the Cr^{3+} sites may be responsible for the failure to see these reactions.

Vinylidene isomerization and cis-β-chlorine elimination appear to form acetylene with similar energetics. Vinyl and trans-β-chlorovinyl groups both form acetylene at higher temperatures, with the acetylene desorbing with increasing temperature with Cl coverage from trans-β-chlorovinyl groups just as the acetylene desorption temperature increases with chlorine coverage from vinyl groups.

Vinyl group coupling, Chapter 2, indicates the ease of mobility on the surface for adsorbates with pi-systems, and this phenomenon has been reported before with methylene groups on this surface [29]. The coupling of surface vinyl groups has a lower activation barrier than the decomposition of vinyl groups to acetylene; however, vinylidene groups (Chapter 4) have a lower activation barrier to acetylene formation through vinylidene isomerization than to allene (CH_2=C=C=CH_2) from vinylidene coupling. While methylene [29] and vinyl groups migrate across the surface to form

coupling products, no coupling products were formed from vinylidene groups suggesting that two pi-systems located near the surface result in vinylidene having a lower barrier to isomerization than to migration. It is not known how surface fragment size and/or position of the pi-system in relation to the surface affects the barrier to migration; therefore, a direct comparison between methylene, vinyl, and the possibility of vinylidene migration cannot be made.

Analyzing the reactions of the different dichloroethylene isomers and comparing them to the formation of acetylene from surface vinyl groups indicates that acetylene could easily be made through vinylidene isomerization or breaking of the cis-β-hydrogen bond in vinyl groups. Acetylene formation through a trans-β-hydrogen elimination from surface vinyl groups is not likely the lowest energy reaction pathway, based on the difference in the activation barrier to beta Cl elimination for cis and trans beta chlorovinyl. However, the selectivity to acetylene in all of the reactions studied suggests that breaking any of the C-H bonds in vinyl groups are possible routes to acetylene formation.

It is still not clear if α- or β-hydrogen elimination is the rate limiting step in acetylene formation from surface vinyl groups. However, it has been shown that halogen labeled ethylenes are a viable way to prepare specific surface fragments. It does not seem that the use of halogen labels provides a comprehensive explanation of vinyl group decomposition. For example, halogen adatoms are not expected to interact with surface oxygen (based on the lack of X-O bonds observed in photoemission) which is a step that many argue is a factor in dehydrogenation reactions on oxide surfaces [11,86].

6.2 Suggested Future Work

While much was learned about the likely reaction pathways for unsaturated C2 reactants based on kinetic and spectroscopic studies, first principles studies of the decomposition of surface vinyl groups may identify the hydrogen (α- or β-) that participates in the rate limiting elimination step to acetylene. Additionally, similar studies conducted on other low index surfaces of α-Cr_2O_3, such as the (0001) surface which exposes Cr^{3+} cations with multiple (3) coordination vacancies, would provide a more complete understanding of hydrocarbon reactions on microcrystalline Cr_2O_3 powders by providing insight into the effect of coordination environment of the surface Cr^{3+} cations on reactivity.

Replacing the hydrogen with deuterium in the intermediates also presents a method for isolating the key steps in forming acetylene from vinyl groups. An α-, cis-, or trans-deuterated vinyl group would affect the isotopic product distribution and aid in understanding the reaction of vinyl groups on this surface. For example, if cis-elimination is the rate limiting step for acetylene from vinyl groups then a cis-deuterovinyl group would form primarily HC≡CH and D_2 gas. The formation of deuterated acetylene as a fraction of total acetylene production from cis-deuterovinyl groups would indicate multiple paths to acetylene formation, and the production of exclusively deuterated acetylene would indicate that cis-elimination plays no role in acetylene formation from vinyl groups. Another benefit of using deuterated compounds is the ease of identifying D_2 gas in the vacuum system because m/z=4 does not overlap with gases in the background. Unfortunately, only vinyl chloride-d_3 was commercially

available. It is therefore suggested that synthesis of these compounds be considered so that the above experiments could be carried out.

Since the current study only addresses selectivity issues in ethane dehydrogenation associated with reactions of ethylene, other studies addressing likely intermediates formed from ethane would be interesting. Ethyl, ethylidene, and ethylidyne intermediates could be produced by the same method of C-X substitution to control the types of intermediates formed. All of these studies would help outline the most likely reactions of C2 hydrocarbons on this surface.

The coupling of vinyl groups, described in Chapter 3, presents another interesting possibility for new studies. Chromia, a major element in the Phillips polyethylene catalyst, is well known to promote polymerization of ethylene [87]. Previous studies in our laboratory co-adsorbing iodomethane-d_3 and diiodomethane on the α-Cr_2O_3 $(10\bar{1}2)$ surface show that methylene groups formed on the surface are mobile and create coupling products like ethylene-d_4, doubly deuterated ethylene-d_2, ethylene, and D_2. The coupling products in these experiments indicate that fragments containing a pi-system near the surface tend to be mobile and can even insert into other fragments. Studying higher molecular weight alkenyl surface groups could lend insight into coupling on the surface. For example, using a C3 surface fragment with a pi-system close to the surface (-$CH{=}CH{-}CH_3$) could produce C6 coupling products. A C3 surface fragment could also orient with C-H bonds toward the surface, as was seen with vinyl groups meaning that a second pi-system (-$CH{=}C{=}CH_2$) in a C3 adsorbate may associate with the surface at two points possibly causing decomposition to surface carbon and hydrogen gas. Another possibility for two pi-systems would be the formation of two new surface species

(through C-C bond cleavage) such as acetylide, which could decompose, and methylene groups, which could couple to form ethylene.

An obstacle in this study is related to storage and the changing trans-DCE reactant. The storage container is made of 316 stainless steel containing approximately 60% Fe and up to 20% Cr. It is well known, that both Fe and Cr catalyze dehalogenation reactions possibly resulting in the formation of acetylene before introducing the reactant to the well-ordered surface. A possibility for analyzing the effect of these storage materials would be to use a storage container constructed of glass. While this may retard the formation of acetylene while in storage, the pump manifold is constructed of 316 SS and acetylene could form while on line. The use of glass storage, however, may increase the amount of time that the reactants remain intact without C-Cl bond cleavage.

Finally, the large Cr 2p features from second order light have posed not only an irritating, but also an analysis problem with NEXAFS data. The use of a Cr coated monochrometer to tune synchrotron light might alleviate this problem and make spectral analysis easier, more accurate, and possibly uncover features that are hidden or skewed through background subtraction.

References

[1] S.C. York, D.F. Cox, Journal of Catalysis 214 (2003) 273.

[2] F. Zaera, R.B. Hall, Surface Science 180 (1987) 1.

[3] R.B. Hall, S.J. Bares, A.M. Desantolo, F. Zaera, Journal of Vacuum Science & Technology a-Vacuum Surfaces and Films 4 (1986) 1493.

[4] X.Y. Zhu, M.E. Castro, S. Akhter, J.M. White, J.E. Houston, Surface Science 207 (1988) 1.

[5] A.V. Teplyakov, B.E. Bent, Journal of the Chemical Society-Faraday Transactions 91 (1995) 3645.

[6] X.L. Zhou, J.M. White, Journal of Physical Chemistry 96 (1992) 7703.

[7] J.E. Parmeter, M.M. Hills, W.H. Weinberg, Journal of the American Chemical Society 109 (1987) 72.

[8] M.X. Yang, J. Eng, P.W. Kash, G.W. Flynn, B.E. Bent, M.T. Holbrook, S.R. Bare, J.L. Gland, D.A. Fischer, Journal of Physical Chemistry 100 (1996) 12431.

[9] X.L. Zhou, J.M. White, Journal of Physical Chemistry 95 (1991) 887.

[10] B.E. Bent, Chemical Reviews 96 (1996) 1361.

[11] B.M. Weckhuysen, R.A. Schoonheydt, Catalysis Today 51 (1999) 223.

[12] V.E. Henrich, Reports on Progress in Physics 48 (1985) 1481.

[13] R.N. Pease, Stewart, L., Journal of the American Chemical Society 29 (1927) 2783.

[14] F.E. Frey, W.F. Huppke, Industrial Engineering Chemical 25 (1933) 54.

[15] P.M. Michalakos, M.C. Kung, I. Jahan, H. Kung, Journal of Catalysis 140 (1993) 226.

[16] G. Karamullaoglu, S. Onen, T. Dogu, Chemical Engineering and Processing 41 (2002) 337.

[17] B. Grzybowska, J. Sloczynski, R. Grabowski, K. Wcislo, A. Kozlowska, J. Stoch, E. Serwicka, Polish Journal of Chemistry 72 (1998) 2159.

[18] M. Cherian, M.S. Rao, W.T. Yang, H.M. Jehng, A.M. Hirt, G. Deo, Applied Catalysis a-General 233 (2002) 21.

[19] B.M. Weckhuysen, I.E. Wachs, R.A. Schoonheydt, Chemistry Review 96 (1996) 3327.

[20] P.W. Park, J.S. Ledford, Langmuir 13 (1997) 2726.

[21] D.W. Flick, M.C. Huff, Applied Catalysis a-General 187 (1999) 13.

[22] H.J. Lugo, J.H. Lunsford, Journal of Catalysis 91 (1985) 155.

[23] I. Hemmerich, F. Rohr, O. Seiferth, B. Dillmann, H.J. Freund, Adsorption and reaction of ethene on Cr2O3(0001)/Cr(110), 1997, 31.

[24] B. Grzybowska, J. Sloczynski, R. Grabowski, L. Keromnes, K. Wcislo, T. Bobinska, Applied Catalysis a-General 209 (2001) 279.

[25] S.C. York, D.F. Cox, Journal of Physical Chemistry B 107 (2003) 5182.

[26] S.W. Weller, S.E. Voltz, Journal of the American Chemical Society 76 (1954) 4695.

[27] V.E. Henrich, P.A. Cox, The Surface Science of Metal Oxides, New York, Cambridge University Press, 1994.

[28] D. Scarano, G. Spoto, S. Bordiga, G. Ricchiardi, A. Zecchina, Journal of Electron Spectroscopy and Related Phenomena 64-5 (1993) 307.

[29] C.M. Byrd, PhD Dissertation: Reaction Chemistry of C1 Hydrocarbon Fragments and Oxygenates on Cr_2O_3 (1012), Blacksburg, VA, Virginia Polytechnic Institute & State University, 2003.

[30] P.J. Lawrence, S.C. Parker, P.W. Tasker, Journal of the American Ceramic Society 71 (1988) C.

[31] D. Adler, Solid State Physics 21 (1968) 1.

[32] S.C. York, PhD Dissertation: Halocarbon Reactions on the Cr_2O_3 (1012) Surface, Blacksburg, VA, Virginia Polytechnic Institute & State University, 1999.

[33] P.W. Tasker, Journal of Physics C-Solid State Physics 12 (1979) 4977.

[34] S.C. York, M.W. Abee, D.F. Cox, Surface Science 437 (1999) 386.

[35] H.H. Kung, Transition metal oxides : surface chemistry and catalysis New York, NY, Elsevier, 1989.

[36] M.W. Abee, PhD Dissertation: Interaction of Acid/Base Probe Molecules with Specific Features on Well-Defined Metal Oxide Single-Crystal Surfaces, Blacksburg, VA, Virginia Polytechnic Institute & State University, 2001.

[37] D.J. Titheridge, M.A. Barteau, H. Idriss, Langmuir 17 (2001) 2120.

[38] X.J. Zhou, Z.H. He, K.T. Leung, Surface Science 600 (2006) 468.

[39] M.X. Yang, P.W. Kash, D.H. Sun, G.W. Flynn, B.E. Bent, M.T. Holbrook, S.R. Bare, D.A. Fischer, J.L. Gland, Surface Science 380 (1997) 151.

[40] S. Haq, S.C. Laroze, C. Mitchell, N. Winterton, R. Raval, Surface Science 531 (2003) 145.

[41] J.F. Moulder, W.F. Stickle, P.E. Sobol, K.D. Bomben, Handbook of X-ray Photolelectron Spectroscopy, Edin Prairie, MN, Perkin-Elmer Corporation, 1992.

[42] D.L. Adams, Andersen, J.N., FitXPS 2001.

[43] J. Stohr, NEXAFS Spectroscopy, New York, Springer, 1992.

[44] T.L. Barr, S. Seal, Journal of Vacuum Science & Technology A 13 (1995) 1239.

[45] An ion guage sensitivity was estimated to be 4.6 for vinyl chloride, and 1.7 for dichloroethylenes according to the method by S. George reported in Ref. 46.

[46] R.L. Brainard, R.J. Madix, Journal of the American Chemical Society 111 (1989) 3826.

[47] Intensities for acetylene desorption traces were corrected using an experimentally determined mass spectrometer sensitivity factor of 1.79 for m/z=26, and dichloroethylenes were corrected using a factor of 0.35 for m/z=61. A mass spectrometer sensitivity factor for vinyl chloride (m/z=62) was experimentally determined to be 0.61. Mass spectrometer sensitivity factors of 3.31 for ethylene (m/z=27), and 0.53 for butadiene (m/z=54) were experimentally determined.

[48] H.A. Witcoff, B.G. Reuben, Industrial Organic Chemicals, New York, John Wiley & Sons, Inc., 1996.

[49] U.R. Vaidya, V.M. Nadkarni, Industrial & Engineering Chemistry Research 26 (1987) 194.

[50] M. Sittig, Chemicals from Ethylene, New York, Noyes Development Corporation, 1965.

[51] P. Wiseman, An Introduction to Industrial Organic Chemistry, London, Applied Science Publishers, LTD., 1979.

[52] A.D. Eastman, J.H. Koltz, J.B. Kimble, Novel Production Methods for Ethylene, Light Hydrocarbons, and Aromatics, New York, Marcel Dekker, Inc., 1992.

[53] R.N. Pease, L. Stewart, Journal of the American Chemical Society 49 (1927) 2783.

[54] P.A. Redhead, Vacuum 12 (1962) 203.

[55] L.E. Davis, N.C. MacDonald, P.W. Palmberg, G.E. Riach, R.E. Weber, Handbook of Auger Electron Spectroscopy, MN, Physical Electronics Industries, Inc., 1976.

[56] J.M. Vohs, M.A. Barteau, Surface Science 176 (1986) 91.

[57] C.D. Wagner, W.M. Riggs, L.E. Davis, J.F. Moulder, Handbook of X-Ray Photoelectron Spectroscopy, Eden Prairie, MN, Perkin-Elmer Corporation, 1978.

[58] T. Ramsvik, A. Borg, T. Worren, M. Kildemo, Surface Science 511 (2002) 351.

[59] T. Ramsvik, A. Borg, H.J. Venvik, F. Hansteen, M. Kildemo, T. Worren, Surface Science 499 (2002) 183.

[60] F. Matsui, H.W. Yeom, A. Imanishi, K. Isawa, I. Matsuda, T. Ohta, Surface Science 401 (1998) L413.

[61] A. Pietzsch, F. Hennies, A. Fohlisch, W. Wurth, M. Nagasono, N. Witkowski, M.N. Piancastelli, Surface Science 562 (2004) 65.

[62] F. Zaera, R.B. Hall, Journal of Physical Chemistry 91 (1987) 4318.

[63] R.M. Ormerod, R.M. Lambert, H. Hoffmann, F. Zaera, L.P. Wang, D.W. Bennett, W.T. Tysoe, Journal of Physical Chemistry 98 (1994) 2134.

[64] D.P. Woodruff, et al., Surface Science 358 (1996) 19.

[65] L. Triguero, L.G.M. Pettersson, H. Agren, Physical Review B 58 (1998) 8097.

[66] D.B. Kang, A.B. Anderson, Surface Science 155 (1985) 639.

[67] D. Arvanitis, K. Baberschke, L. Wenzel, U. Dobler, Physical Review Letters 57 (1986) 3175.

[68] X.D. Peng, M.A. Barteau, Langmuir 7 (1991) 1426.

[69] J.B. Nicholas, A.A. Kheir, T. Xu, T.R. Krawietz, J.F. Haw, Journal of the American Chemical Society 120 (1998) 10471.

[70] J.M. Vohs, M.A. Barteau, Journal of Physical Chemistry 94 (1990) 882.

[71] A.V. Ivanov, A.E. Koklin, E.B. Uvarova, L.M. Kustov, Physical Chemistry Chemical Physics 5 (2003) 4718.

[72] A.P. Hitchcock, C.E. Brion, Journal of Electron Spectroscopy and Related Phenomena 10 (1977) 317.

[73] R. Mclaren, S.A.C. Clark, I. Ishii, A.P. Hitchcock, Physical Review A 36 (1987) 1683.

[74] R. Masel, Principles of Adsorption and Reaction on Solid Surfaces, New York, J. Wiley, 1996.

[75] C.J. Powell, A. Jablonski, NIST Electron Inelastic-Mean-Free-Path Database, Gaithersburg, MD, U.S. Department of Commerce, 2000.

[76] E. Papirer, R. Lacroix, J.B. Donnet, G. Nanse, P. Fioux, Carbon 33 (1995) 63.

[77] A. Cassuto, M.B. Hugenschmidt, P. Parent, C. Laffon, H.G. Tourillon, Surface Science 310 (1994) 390.

[78] M.A. Minton, Q. Ma, D.R. Mullins, Q. Ge, M. Neurock, D.F. Cox, (In Preparation).

[79] Y.G. Lei, K.M. Ng, L.T. Weng, C.M. Chan, L. Li, Surface and Interface Analysis 35 (2003) 852.

[80] F. Zaera, N. Bernstein, Journal of the American Chemical Society 116 (1994) 4881.

[81] Z.H. He, X. Yang, X.J. Zhou, K.T. Leung, Surface Science 547 (2003) L840.

[82] S.M.K. Airaksinen, M.A. Banares, A.O.I. Krause, Journal of Catalysis 230 (2005) 507.

[83] K. Kumbilieva, N.A. Gaidai, N.V. Nekrasov, L. Petrov, A.L. Lapidus, Chemical Engineering Journal 120 (2006) 25.

[84] S.A. Bocanegra, A.A. Castro, A. Guerrero-Ruiz, O.A. Scelza, S.R. de Miguel, Chemical Engineering Journal 118 (2006) 161.

[85] E. Heracleous, A.A. Lemonidou, Catalysis Today 112 (2006) 23.

[86] M.D. Argyle, K.D. Chen, A.T. Bell, E. Iglesia, Journal of Physical Chemistry B 106 (2002) 5421.

[87] J.P. Hogan, D.R. Witt, OLEFIN POLYMERIZATION WITH CHROMIUM AND TITANIUM-CONTAINING COMPOUNDS, United States, Phillips Petroleum Company (Bartlesville, OK) 1971.